THE INFLUENCE OF COWS' NUTRITION DURING PREGNANCY ON THE DEVELOPMENT OF THE DISTAL VAGUS NERVE (*GANLION DISTALE NERVI VAGI*) IN NEWBORN CALVES

Adamski M[1], Pospieszny N[2], Kuropka P[2]

[1]*Institute of Animal Breeding, Faculty of Biology and Animal Breeding, University of Environmental and Life Sciences, Wrocław, Poland*
[2]*Department of Anatomy and Histology, Faculty of Veterinary Medicine, University of Environmental and Life Sciences, Wrocław, Poland*

In the literature available, there is a lack of morphological-breeding works concerning the influence of nutrition of pregnant cows on the development of distal ganglion of the vagus nerve. Animals are fed with fodders of known qualitative-quantitative composition. The data of chemical and mineral-vitamin content of the fodder are given in the ingredients list.

This research was conducted on 12 newborn calves of h-fbreed. The calves had not taken the food from their mother, so there were no qualitative or quantitative changes of nurture. The animals were kept in the same husbandry conditions (nourishment, boxes, veterinary care). Both distal ganglions of the vagus nerve were morphologically assessed for their components and derivatives such as: laryngeal cranial nerve (n. laryngeus cranialis) the path of the heart aorta nerve (n. depressor cordis) exit. Both ganglions were subject to morphometry, skeletopy, holotopy and syntopy that was of significance while determining the symmetry and asymmetry. The analyzed ganglions were also subject to X-ray microanalysis using a LEO V435 microscope. Surface analysis of the whole of the ganglions and point analysis of single nerve insets were conducted. The material was dusted with gold and analyzed using a scanning electron microscope (SEM) LEO V435 with accelerating voltage of 20,000 eV.

The analyzed distal left ganglions of the vagus nerve were morphometrically bigger than on the right side of the preparations. Their mean value on the left side was 4.5 mm, while on the right side it was 3.1 mm. In standardized fodder (nutritional standards) elements like sodium, magnesium, zinc, selenium, cobalt, calcium, copper and the whole range of vitamins (A, E, D3, K3, B1, B2, B6, B12, nicotinic and folic acid) were also found. As a result of the conducted qualitative analysis of ganglions using the histological methods mentioned above, it was demonstrated that the characteristic for the left ganglion is a higher level of nerve fibre organization. The fibres are tightly bound creating bunches running towards the circumference and towards the spinal cord. They are surrounded by collagen fibres forming the perineurium. X-ray analysis showed an irregular distribution and the occurrence of chemical elements in the developing ganglion area. Among trace elements, there were aluminium, silicon and molybdenum. However, in point analysis, a significantly higher concentration of silicon was noted.

This is one of the very first attempts of proving the influence of the mother's nutrition during pregnancy on the developing embryo and then the foetus.

THE INTERCELLULAR JUNCTIONS IN DENTAL PULP

Alwas-Danowska HM, Danowska-Klonowska D

Department of General Dentistry, Department of Histology and Embryology, Medical University of Łódź, Łódź, Poland

Recognition of the structures conducting the impulses from the enamel is a very important problem because it enables a better understanding of many physiological processes.

Teeth (extracted with the use of local anaesthesia) were cut and their pulp was fixed in 2% glutardialdehyde in a cacodylate buffer and then in 1% osmium tetroxide, dehydrated and embedded in EPON 812. Just after extraction, some of the teeth were treated with small charges of electric current. Hemithin sections were taken with the use of a Tesla BS 480 ultramicrotome and stained with buffered 1% toluidine blue. Ultra thin sections were cut with an MTI ultramicrotome and contrasted with uranyl acetate and lead citrate. They were investigated and photographed using a JEOL electron microscope.

In the electron microscopic pictures of the lateral surfaces of the cells (between the odontoblasts, odontoblasts and nerve fibres, odontoblasts — leucocytes as well as in the blood vessel walls), the junctions are visible as short callosities of plasmolemma. Such junctions between the cells enable a so-called junctional transfer — a free flow of ions, so they act as electric synapses. The junctional complex is formed by gap junctions, desmosomes and tight junctions. Hemidesmosomes were also present. Belt desmosomes provide strong bonds between the cells. Small spot desmosomes are also present between the odontoblasts. Tight junctions do not completely encircle the cells because of the presence of small openings, for instance in the interodontoblastic spaces.

The pictures of intercellular junctions were very distinct in the teeth treated with small charges of electric current.

THE INFLUENCE OF LONG-TERM THERAPY OF HYDROCORTISONE, CALCIUM AND BOVINE WHEY ON THE STRUCTURE OF THE FEMUR OF RATS

Anasiewicz A[1], Golan J[1], Czabak-Garbacz R[2], Bogacz A[3], Wróblewska K[4], Anasiewicz M[4], Korzan J[4], Korzan M[4], Jagnicki J[4]

[1]*Department of Human Anatomy, Medical University of Lublin, Lublin, Poland*
[2]*Department of Human Physiology, Medical University of Lublin, Lublin, Poland*
[3]*Department of Orthopaedics and Traumatology, Medical University of Lublin, Lublin, Poland*
[4]*Student of Scientific Association, Department of Human Anatomy, Medical University of Lublin, Lublin, Poland*

The aim of the study was to investigate the influence of long-term therapy of hydrocortisone on the structure of femur through simultaneous administration of bovine whey.

The research material consisted of eight groups of female Wistar strain rats, 200–220 g body weight (on the first day of the experiment):

1. untreated control;
2. treated control, physiological saline i.p. 0.5 ml/kg b.w. every day;
3. hydrocortisone (Hydrocortisonum hemisuccinatum, Polfa, Poland), i.p. 22.5 mg/kg b.w. 2 × day;
4. 10% solution of calcium i.p., 15.0 mg/kg b.w. 2 × day and 200 j.m. vit. A with 100 j.m. vit. D3 (Vitaminum A + D3, Terpol, Poland), every day;
5. hydrocortisone, calcium, vit. A + D3 identical dose and means of administration;
6. bovine whey, by gavage 0.25 mg/kg b.w. 2 × day;
7. hydrocortisone and bovine whey, identical dose, means and time of administration;
8. Vitaminum A + D3, identical dose, means and time of administration.

The rats were euthanized on the 56th day of the experiment. The femur were taken out for histological studies and mechanical strength examinations. The strength properties of the femur were determined using an Instron 4 302 machine. The femur in the horizontal position was supported in two points and was loaded in the centre until the moment of fracture.

On the basis of these histological studies of the structure of the femur, it was observed that the administered hydrocortisone caused considerable damage. The mechanical strength of the femur was observed to have been made considerably weaker by the administered hydrocortisone. The destructive effect of hydrocortisone can be considerably reduced by simultaneous administration of calcium with vit. A + D3 or bovine whey.

EVALUATION OF THE INFLUENCE OF LEAD ACETATE AND BOVINE WHEY ON THE MANDIBULA STRUCTURE OF YOUNG FEMALE RATS

Anasiewicz A[1], Szyszkowska A[2], Wysokińska-Miszczuk J[2], Święs Z[3], Klatka M[4], Koliński P[2], Buczarska B[5], Szkutnik M[5], Miszczuk S[5]

[1]*Department of Human Anatomy, Medical University of Lublin, Lublin, Poland*
[2]*Department of Dentistry, Medical University of Lublin, Lublin, Poland*
[3]*Department of Hygiene, Medical University of Lublin, Lublin, Poland*
[4]*Department of Paediatric Endocrinology and Neurology, Medical University of Lublin, Lublin, Poland*
[5]*Student of Scientific Association of Department of Human Anatomy, Medical University of Lublin, Lublin, Poland*

The aim of this experiment was to investigate the influence of lead acetate solution and the influence of bovine whey on the structure of the mandibula of young female Wistar rats (130–140 g body weight on the first day of the experiment).
The solution of lead acetate was administered by gavage daily to rats in dose 1/100 LD_{50} per 1 kg of body weight. The bovine whey was administered by gavage daily in dose 0.25 mg per 1 kg of body weight. The treated control groups were given water to drink by gavage once per day in dose 0.25 ml per 1 kg of body weight. One group of rats received the solution of lead acetate and the bovine whey in identical doses once per day. The last group of rats was an untreated control group.
The rats were euthanized on day 60th of experiment. The mandibula were taken out for histological and densitometrical examinations DPX-A, Manual Analysis with Bone Mineral Density and Bone Mineral Content.
On the basis of this experiment it has been found that harmful effect of lead acetate may be reduced by a concomitant administration of the bovine whey.

ANATOMY OF THE PERFORATING BRANCHES AROUND THE CIRCLE OF WILLIS

Andrzejczak A[1,2], Ciszek B[1,3], Ungier E[1], Krajewski P[4]

[1]*Department of Anatomy, Centre of Biostructure Research, Medical University of Warsaw, Warsaw, Poland*
[2]*Department of Neurology, II Medical Faculty, Medical University of Warsaw, Warsaw, Poland*
[3]*Department of Neurosurgery, Bogdanowicz Pediatric Hospital, Warsaw, Poland*
[4]*Department of Forensic Medicine, Medical University of Warsaw, Warsaw, Poland*

The imaging of the circle of Willis is a well-established standard, but many vascular diseases are related to a different pathology of perforating branches. Amongst these, the ischemic and haemorrhagic foci of the basal nuclei and internal capsule present the greatest frequency.
Modern imaging methods of the cerebrovascular system like spiral angio-CT or MRI step by step are closer to the level of perforating branches. However, the complete visualisation of the anatomy of these vessels by means of imaging is still a matter of technical effort.
The anatomy of the perforating branches has been analysed by many authors. Most of these studies were limited to the perforators of one of the intracranial arteries or its part only.
The aim of the present study is to analyse the anatomy of all perforating branches of the circle of Willis as a support for holistic diagnostic analysis of the intracranial vasculature.
The number and morphometry of the perforating branches of the circle of Willis obtained from 50 brains were analysed by microanatomical investigation. This information was correlated with the variability of the circle e.g. hypoplasia or hypertrophy of the arterial segments. The number and diameter of the perforating branches were related to the thickness of the parent artery. This information has a predictive value for radiological evaluation of the circle of Willis.

EXPRESSION OF NEURONAL NOS IN INTRAPANCREATIC GANGLIA OF SHEEP

Arciszewski MB

Department of Animal Anatomy and Histology, Agricultural University of Lublin, Lublin, Poland

Since the physiology of pancreas of ruminants differs substantially from that of monogastric animals, it is of interest to explain whether this phenomenon has any neuroanatomical background. In numerous mammals, nitric oxide (NO) influences the activity of the exocrine and endocrine pancreas. In the present study, immunocytochemistry was applied to investigate the expression of neuronal nitric oxide synthase (nNOS) in intrapancreatic ganglia of sheep. Mouse antibodies against HuC/D were used as pan-neuronal markers and mixed with rabbit antisera raised against nNOS. Immunolabeled sections were examined under a spinning disk confocal microscope. The frequency of nNOS-immunoreactive (IR) intrapancreatic neurons was presented as a percentage relative to the total number of Hu-positive neurons analyzed. Based on its size, Hu/nNOS-IR intrapancreatic neurons were categorized as small (length up to 25 μm), medium (25–50 μm) or large (above 50 μm).
Among Hu-IR intrapancreatic neurons only 9.6 $\pm$ 1.3% (n = 5) were found to express nNOS whereas the significantly greater subpopulation constituted of perikarya lacking nNOS (90.4 $\pm$ 1.3%; n = 5, $p < 0.05$, ANOVA). Single Hu/nNOS-IR neurons were surrounded (in general only partially) by nNOS-containing nerve terminals. The vast majority of Hu/nNOS-IR neurons were round and oval in shape. A group of Hu/nNOS-IR intrapancreatic neurons classified as middle-sized was statistically greater as compared to the subpopulation of Hu/nNOS-IR neurons considered as small (83.3 $\pm$ 2.6% and 16.7 $\pm$ 2.6% respectively; n = 5, $p < 0.05$). The mean length of small-sized intrapancreatic neurons was 21.3 $\pm$ 0.5 μm (n = 5), whereas the average diameter of neurons from the middle group was 34.5 $\pm$ 1.2 μm (n = 5). None of the Hu/nNOS-IR neurons (n = 5) belonged to the large group (with a long axis more than 50 μm).
The comparison with other mammals suggests that nitrergic innervation of the ovine pancreas is species-determined and may be a reflection of the digestion specificity of ruminants.

EFFECTS OF CAFFEINE INJECTION ON HISTOLOGICAL CHANGES IN MOUSE OVARIES

Balcerzak A, Bartel H

Department of Histology and Tissue Ultrastructure, Medical University of Łódź, Łódź, Poland

Long-term studies of the effect of caffeine (1, 3, 7-trimethylxanthine) on the embryos of the rodents have demonstrated that it is a factor causing teratological changes during development. On the other hand, during the past decade, several studies have failed to demonstrate the role of caffeine as a factor causing alterations in the ovaries and disturbances in the function of the female reproductive system. Wilcox et al. were the first to indicate the effect of caffeine on human fertility.
A great number of ovarian follicles start to develop but a lot of them, after the formation of antrum, undergo atresia, and the molecular mechanism underlying this process is apoptosis. There exists bidirectional communication between oocytes and granulosa cells (GCs) formed as microvilli, which is important for folliculogenesis. Viability of GCs is essential for ovarian function. Contact between GCs is due to the presence of adhesion-type junctions resulting from haemophilic binding of N-cadherin. It is assumed that cAMP in GCs can induce apoptosis and has been shown to decrease N-cadherin in a dose-dependent manner.

The aim of this study was to characterize the morphological structure of the ovaries after applying caffeine. The material consisted of mouse ovaries obtained from Balb/c mice. Adult female Balb/c mice were divided into three groups and injected three days a week for four weeks subcutaneously with caffeine solutions of 50 mg/kg; 100 mg/kg and 150 mg/kg, respectively. The mice from the control group were injected subcutaneously with saline alone. The animals were killed by dislocation of the spinal cord and then the ovaries were collected and prepared for optical and electron microscope examination.

Under the optical microscope, we observed specific histological changes in the granulosa cells of follicles in advanced stages of atresia including: detachment from the basement membrane; the presence of pycnotic nuclei and a massive reduction in the number of granulosa cells. The theca interna was hypertrophied; only a few granulose cells were left. Pycnotic nuclei were present in the granulosa cells, and the follicular fluid contained cell debris.

Morphological analysis of the ovaries made under an electron microscope revealed the presence of many degenerating, morphological signs of atresia in ovarian follicles from experimental groups I and II. For granulosa cells, the following characteristics were estimated in comparison with those of the controls: reduction in size and high condensation of chromatin in the nucleus; irregular shape and ruptures of membranes of mitochondria; dilation of vesicles and tubules and dissociation from mitochondria of the SER; decreased number of microvilli through zona pellucida and an increased number of varying size cytoplasmic vacuoles.

Studies from the control group revealed well-defined cell-cell contacts: the nuclei and cell organelles were intact. Numerous mitochondria exhibited intact internal membranes.

The question remains concerning the possible molecular mechanism injuring follicular cells by caffeine. It may be associated with increasing intracellular level of cAMP through inhibition of phosphodiesterase that causing caffeine significant factor promoting apoptosis in GCs. Therefore, the aim of further studies by us will be to characterize the localization and expression of N-cadherin in ovarian follicles in comparison of different doses of caffeine utilizing the avidin-biotin peroxidase staining complex (ABC).

CORONARY ARTERY TRUNKS OF DOMESTIC CHICKENS (*GALLUS GALLUS F. DOMESTICA*) AND TURKEYS (*MELEAGRIS GALLOPAVO*)

Bartyzel BJ[1], Kobryń H[1] , Szmidt M[1], Bartyzel I[2]

[1]*Department of Morphological Sciences, Faculty of Veterinary Medicine, Warsaw Life Science University — SGGW, Warsaw, Poland*
[2]*Solec Medical Hospital, Warsaw Medical University, II Medical Department, III Clinic of Internal Diseases and Cardiology, Warsaw, Poland*

The aim of the work was to describe the heart left coronary artery trunk of these birds, especially in terms of branches which start directly from the aortic sinus. The second aim was to determine the types of branches and perform a comparison of investigated features between and among the species. This type of the research may provide new standards in non-invasive methods for the evaluation of coronary arteries in Aves.

The experiments were conducted on 110 hearts from two species: domestic chicken (n = 74) and turkey (n = 36). Both species belong to *Galliformes*. The birds were obtained from private farmers between the year of 2005 and 2006. The hearts were flushed and dried. Afterwards, acrylic material was injected directly into the initial coronary artery ostiums. Then the hearts underwent thermal and enzymatic processes in order to obtain corrosion specimens of the examined structures. Corrosion specimens were described with the assistance of a digital camcorder connected to an MST-130 microscope.

There are two ways in which the left coronary artery of chickens starts from aorta: I — with the single ostium (52%), and II — with the double ostium which includes the left coronary artery and its interatrial branch. This branch goes directly from the aortic sinus towards the mitral valve, excluding the left coronary artery trunk. However, in the case of turkeys we found only the first type. The research needs to be continued on a larger number of animals from different species. It would allow the colligation of the anatomy of blood systems with an animal lifestyle.

THE POSITION OF DOMESTIC CHICKEN (*GALLUS GALLUS F. DOMESTICA*) AORTIC CORONARY ARTERY OSTIUM

Bartyzel BJ[1], Kobryń H[1], Szmidt M[1], Bartyzel I[2], Dzierzęcka M[1]

[1]*Department of Morphological Sciences, Faculty of Veterinary Medicine, Warsaw Life Science University — SGGW, Warsaw, Poland*
[2]*Solec Medical Hospital, Warsaw Medical University, II Medical Department, III Clinic of Internal Diseases and Cardiology, Warsaw, Poland*

The aim of the work was to describe the location of the beginning part of the coronary arteries in relation to the aortic valve cusp as well as to perform a comparison of the investigated elements among the species.

The research was conducted on 80 hearts prepared from dead birds of meat stock. The birds were obtained from private chicken farmers from the province of Mazowieckie between the years 2003 and 2006. The hearts were flushed of blood, dried with paper towels and fixed in 10% formalin with the addition of ethanol. After at least 6 weeks, the aortic valves were prepared from the hearts. Subsequently, the position of the aortic coronary arteries ostium was evaluated and the description of the valves was performed with the assistance of an MST-130 microscope.

Three main types of initial coronary artery ostium locations were determined: 1. on the level of the cusp free edge; 2. below the cusp free edge in the aortic sinus; 3. above the cusp free edge.

Single type 2 coronary artery initial ostiums of the right dorsal aortic valve were found in 8 cases during the analysis of the location of the coronary arteries initial ostiums. We are not aware of any other publications describing this kind of artery. There are many precise descriptions of other coronary arteries (left or right). This is why the authors suggest naming this aorta as the median coronary artery — *a. coronaria mediana*.

DOMESTIC CHICKEN (*GALLUS GALLUS F. DOMESTICA*) AORTIC VALVE MORPHOLOGY

Bartyzel BJ[1], Szmidt M[1], Bartyzel I[2], Kobryń H[1]

[1]*Department of Morphological Sciences, Faculty of Veterinary Medicine, Warsaw Life Science University — SGGW, Warsaw, Poland*
[2]*Solec Medical Hospital, Warsaw Medical University, II Medical Department, III Clinic of Internal Diseases and Cardiology, Warsaw, Poland*

The aim of the work was to evaluate a number of domestic chicken aortic valves. Performed observations may allow us to precisely determine the structure of bird hearts and highlight some of the morphological types, which is helpful in image investigations.

The research was conducted on 162 hearts prepared from dead birds (72 females and 90 males) of meat stock. The birds were obtained from private chicken farmers from three Polish regions (Mazowieckie, Lubelskie and Podlaskie) between February and September of 2006. The hearts were flushed with NaCl solution with the addition of surfactants and ethanol at 42°C. Then the tissue was dried with paper towels and a water pump. The hearts were divided in two groups. The first included hearts (36 females, 45 males) fixed in 10% formaldehyde for 6 weeks (checked by MST-130 microscope). The second group included hearts (36 females,

45 males) injected with a solution which hardens after high temperature polymerization (unpublished corrosion method by B J Bartyzel) in order to obtain corrosion specimens of the aortic valves.
The experiments revealed two types of domestic chicken aortic valves. Type I includes 3 cusps: semilunar left, dorsal right and ventral right. Type II includes 4 cusps: semilunar left, accessory left, dorsal right and ventral right. This type of valve structure appeared only in one case among the corrosion specimens. The general hypothesis about the existence of 3 cusps in domestic chicken aortic valves was not confirmed. There is a need for further investigation and additional experiments regarding animals from *Aves* and *Galliformes*.

MORPHOLOGY AND DEVELOPMENT OF CRANIAL LARYNGEAL NERVES OF PIGS IN PRENATAL PERIOD

Bąkowska J[1], Pospieszny N[1], Pospieszna J[2], Rodek E[1]

[1]*Department of Anatomy and Histology, Faculty of Veterinary Medicine, University of Environmental and Life Sciences, Wrocław, Poland*
[2]*Institute of Basic Electrotechnic and Technology, University of Technology, Wrocław, Poland*

Because of the wide range of possibilities of using domestic pigs as laboratory animals and of using it in embryological, transplant and biotechnological tests, it would seem to be useful to get to know the prenatal period processes including the cranial laryngeal nerve. The issue is not precisely presented in available academic literature.
The research was carried out on 197 foetuses of 20 wombs. 100 foetuses were from left uterine horn (50.5%) and 97 from right uterine horn (49.5%). In the whole research work there were 105 females (53%) and 92 males (47%). The research material was from one farm with the same conditions. Sowes (wbp x pbz) were inseminated by Duroc and Hampshire boar or by Pietrain crossbreed. This led to the detailed statistical and morphological analysis and proper analysis of the received results. The age was estimated according to Marrable, and we used the extract from farm books. Statistical, macro- and micro-anatomical methods were used; the morphology of the researched nerve was analyzed with regard to biokinetic matter.
The cranial laryngeal nerve shows low developmental stabilization during the whole foetal period with reference to the place where the distal ganglion vagus nerve exits. In principle, this place is found along the whole edge of the ganglion. To systematize the issue we can say that, approximately, the location is found in the upper part of the distal ganglion in the foetus in 10–11 weeks of pregnancy, and after the 12th week of prenatal life it is a bit lower or in the middle of the researched distal ganglion vagus nerve. As the location of the ganglion lowers, we can notice very clearly the change of the value of angle between the divine nerve and the edge of the distal ganglion vagus nerve; the value of the angle is between 35 and 95 degrees. The above data concerns the path and quality of the cranial laryngeal nerve to the researched ganglion. Its further behaviour in individual age brackets is mainly connected with the appearance of secondary divisions among the nerve and with the means of supplying the larynx interior by the cranial laryngeal nerve. The following nerves and branches go from that nerve: aortic nerve, external and internal branch. The Aortic nerve (n. depressor) goes directly from the cranial laryngeal nerve or to the distal ganglion vagus nerve if it has a smaller number of preparations. It goes to the base of heart where it supplies the aortic arch and the very heart and ductus arteriousus. The external branch (*ramus externus*) is very strong and developed very well. It supplies the cricotrachealis (*m. cricothyroideus*). The internal branch (*ramus internus*) is also very well developed. It is single in the youngest foetuses and shows a tendency for secondary multiple divisions supplying the larynx interior as the foetus develops.

DISTRIBUTION OF COCAINE- AND AMPHETAMINE-REGULATED TRANSCRIPT (CART) IMMUNOREACTIVITY IN THE PREOPTIC AREA OF PIGS

Bogus-Nowakowska K[1], Robak A[1], Równiak M[1], Wasilewska B[1], Bossowska A[2], Wojtkiewicz J[2], Skobowiat C[2], Majewski M[2]

[1]*Department of Comparative Anatomy, University of Warmia and Mazuria, Olsztyn, Poland*
[2]*Department of Functional Morphology, Division of Clinical Physiology, Department of Comparative Anatomy, University of Warmia and Mazuria, Olsztyn, Poland*

Cocaine- and amphetamine-regulated transcript (CART) is a novel neuropeptide involved in multiple physiological functions including feeding, body weight regulation and mediation of stress response. Although most studies concerning CART action in the brain areas have related to feeding behaviour, recent investigations have suggested that CART may play a role in the regulation of gonadotropin release as well as in the induction of maternal behaviour. In view of the crucial role of the preoptic area (POA) in a variety of reproductive functions, the aim of the present study was to investigate the distribution of CART-immunoreactivity in the POA of juvenile pigs.
The animals used in our study were transcardially perfused with 4% paraformaldehyde and their brains, after removing from the skull, were post-fixed for 1 hour. Then the material was washed in 0.1 M phosphate buffer and cryoprotected in sucrose until they sank. 10 or 20 μm cryostat sections were processed for immunohistochemical staining with an antiserum directed against the CART peptide fragment 61–102.
Immunohistochemistry revealed that all the POA parts contained CART-immunoreactive fibres. The highest density of staining fibres was found in the periventricular region of the POA, and high to moderate in the medial preoptic area (MPA). The lateral preoptic area displays a less dense concentration of CART-immunoreactive fibres than MPA. A moderate to low expression of staining fibres was observed in the median preoptic nucleus. The CART-immunoreactive fibres were segregated into two types: the first with large varicosities and the second with small varicosities. Both the fibre types displayed immunoreactivity in all POA parts; however, the highest density of fibres with large varicosities was found mainly in the MPA and the periventricular region. The fibres were observed to surround nonimmunoreactive cell bodies and often dendrites, forming pericellular arrays or baskets. The POA exhibited a low density of immunoreactive cells and single CART-positive cell bodies were located in the MPA and the periventricular region of the POA.

REVERSAL OF P-GLYCOPROTEIN-DEPENDENT ANTHRACYCLINE RESISTANCE BY QUERCETIN

Borska S[1], Drąg-Zalesińska M[1], Wysocka T[1], Gębarowski T[2], Zabel M[1,3], Dzięgiel P[1]

[1]*Department of Histology and Embryology, Medical University, Wrocław, Poland*
[2]*Department of Basic Medical Sciences, Medical University, Wrocław, Poland*
[3]*Department of Histology and Embryology, Medical University, Poznań, Poland*

Daunorubicin (DB) is one of the most effective chemotherapeutic agents of the anthracycline family. However, its use is seriously limited by chronic toxic effects and a phenomenon called multidrug resistance (MDR), which is a significant obstacle to providing effective chemotherapy to many patients. Multi-factorial in etiology, classic MDR is associated with the over-expression of P-glycoprotein (P-gp), ATP-dependent membrane transporter encoded by the *MDR1* gene. This results in an increased efflux of chemotherapeutic drugs from cancer cells. Inhibiting P-gp as

a way of reversing MDR has been extensively studied for the last three decades. Many agents that modulate P-gp function have been identified but most of them have been associated with unacceptable side effects. Biopolyphenols, including quercetin, are known as agents of anti-cancerogenic properties due to their anti-proliferative and pro-apoptotic activity. It has been recently reported that some of them may also act as selective and safe modulators of P-gp function.

The first aim of these studies was to determine if quercetin exerts a significant influence on the proliferation and apoptotic process in selected tumour cell lines. In our experiments, we also attempted to define if quercetin can modulate the expression of P-gp in daunorubicin-resistant cancer cell lines. The studies were performed *in vitro* on two tumour cell lines: daunorubicin-resistant pancreatic cell line EPP85-181RDB and its sensitive variant EPP85-181P as a control. Cytotoxicity analysis was performed after drug exposure (quercetin and DB) using cytocolorimetric SRB assay. Apoptosis was detected by neutral comet technique and TUNEL. P-gp expression was analyzed by immunocytochemical and immunofluorescent (calcein M efflux) methods. Data were confirmed by real-time PCR analysis of MDR1 expression.

Quercetin was found to exert an anti-proliferative and pro-apoptotic effect on the cells of the studied sensitive and resistant pancreatic cancer lines. Moreover, in particular doses, it inhibited P-gp expression in resistant cells. Additionally, the studies have proved augmentation of the EPP85-181P cell sensitivity to DB.

NEUROCHEMICAL CHARACTERIZATION AND PLASTICITY OF INFERIOR MESENTERIC GANGLION (IMG) NEURONS SUPPLYING THE PORCINE URINARY BLADDER AFTER TETRODOTOXIN (TTX) TREATMENT

Bossowska A, Zapart A, Iwańczyk B, Radczak A, Gonkowski S, Wojtkiewicz J, Majewski M

Division of Clinical Physiology, Faculty of Veterinary Medicine, University of Warmia and Mazury, Olsztyn, Poland

While the distribution pattern and chemical coding of IMG neurons projecting to the urinary bladder of animals from different species is relatively well documented, data on the distribution and chemical characterization of sympathetic neurons located in the IMG and supplying the porcine urinary bladder are still fragmentary. Moreover, neurotoxins such as resiniferatoxin or botulinum toxin are now used to "reconstruct" the physiological pattern of pathologically changed bladder innervation. Therefore, this study aimed at disclosing the origin, neurochemical phenotypes and changes in the expression pattern of neurotransmitters in IMG neurons projecting to the urinary bladder after intravesical TTX treatment. The urinary bladder wall was injected with retrograde tracer Fast Blue (FB) in twelve juvenile female pigs and an intravesical instillation of TTX (12 μg in 60 ml of buffer per animal) was performed three weeks later in six of them. After a week, the right and left IMGs were collected from all animals and processed for single and double-immunofluorescence labelling on 10 μm-thick cryostat sections using combinations of primary antisera raised in different species and directed towards tyrosine hydroxylase (TH), neuropeptide Y (NPY), vasoactive intestinal polypeptide (VIP), galanin (GAL), pituitary adenylate activating polypeptide (PACAP), somatostatin (SOM), calbindin (CB) and nitric oxide synthase (NOS). In the control animals, the vast majority of FB^+ neurons contained TH and/or NPY (95% and 85%, respectively). Only a few of them were immunolabelled for SOM, VIP, CB or GAL (2.2%, 2%, 1.7% and 1.2%, respectively). NOS and PACAP were absent from urinary bladder-supplying IMG neurons. After TTX treatment, a significant increase in the number of FB^+ neurons containing SOM, CB and GAL was observed (53%, 14% and 12%, respectively), while the number of NPY-IR IMG cells projecting to the urinary bladder dramatically decreased (to 7.5%). PACAP, NOS and VIP were absent in FB^+ cells. Thus, the urinary bladder instillation with TTX is able to change profoundly the neurochemical architecture of sympathetic limbs of peripheral micturition reflexes.

ANATOMY OF THE RECTUS FEMORIS MUSCLE

Braun W, Falęcki WJ, Deszczyński JM, Gadomski Ł, Szaro P, Witkowski G, Ciszek B

Department of Anatomy, Centre of Biostructure Research, Medical University of Warsaw, Warsaw, Poland

The gross anatomical description of the skeletal muscle seems well established. However, recent insights from imaging have changed this classic approach. As an example of this approach, we present an analysis of the structure of the rectus femoris muscle. The structure of the rectus femoris muscle was analyzed on the base of dissection of the 20 fixed specimens. In all specimens, we have confirmed that the real insertion of the muscle fibres are the wide aponeuroses. The superior one partly enters the mass of the muscle. The length of fibres on different levels of the rectus femoris muscle was similar. The surfaces of the insertions were comparable and were very similar to the surface of the cross section through all muscle fibres. These values ranged from 50 to 80 cm^2. It is more than 4 times greater than standard value of cross section of this muscle reported in other works.

The presented approach changes the understanding of muscular anatomy and physiology and has an important influence on the surgical reinsertion of so-called broken muscles.

TOPOGRAPHICAL RELATIONSHIPS IN PROJECTION FROM THE CUNEATE AND GRACILE NUCLEI TO THE CAUDAL VERMIS

Bukowska D[1], Zguczyński L[2], Mierzejewska-Krzyżowska B[2], Kaluga E[3]

[1]*Department of Neurobiology, University School of Physical Education, Poznań, Poland*

[2]*Department of Anatomy, University School of Physical Education, Gorzów, Poland*

[3]*Department of Biology, University School of Physical Education, Poznań, Poland*

The cuneate (Cu) and gracile (Gr) nuclei, which compose the dorsal column nuclei (DCN), are the first relay station in the somatosensory system. Cu and Gr receive afferents from peripheral receptors in the forelimbs and upper trunk, and hind limbs and lower trunk, respectively. Their projection is directed mainly to the thalamus but connections to other structures, including the cerebellum, also exist. The aim of this study was to demonstrate DCN projection patterns to the cerebellar caudal vermis, employing a retrograde double tracing technique in eight rabbits. Two fluorescent tracers, Fast Blue and Diamidino Yellow, were microinjected into the pyramis (with input from the spinal cord) and uvula (cooperates with the vestibular system) resulted in labelled neurons ($n = 14868$) in certain regions of DCN. These neurons are parent for the DCN-caudal vermis projection. The findings show that projection is bilateral, with four-times ipsilateral preponderance, and one and a half greater to the uvula than to pyramis. The strongest projections arise from the lateral cuneate nucleus (CuL; $n = 11677$) and these from the complex of gracile and medial cuneate nucleus (Gr + CuM; $n = 3010$) are relatively weak. A small number of fibres originate from CuM ($n = 124$) and Gr ($n = 57$). It may be emphasized that no connections from the contralateral CuM reach the pyramis, and connections from Gr to the uvula are nonexistent. The distribution pattern of labelled neurons shows that projection is topographically organized. In CuL, neurons projecting to the pyramis are present mainly in the ventrolateral region, but these project to the uvula — in the ventromedial region. The interface region shares connections among the pyramis and uvula. Projections from the dorsolateral Gr + CuM and lateral CuM to both pyramis and uvula are common to a great extent. The dorsal and

dorsolateral Gr supply exclusively the pyramis. The above findings indicate that projections to the pyramis and uvula originate from restricted DCN regions and differ in number of connections from individual nuclei. This may be because of the different roles that are played by the two cerebellar targets.

THE PINEAL GLAND OF THE EUROPEAN BEAVER — PRELIMINARY ANATOMICAL AND HISTOLOGICAL STUDIES

Bulc M, Lewczuk B

Division of Histology and Embryology, Department of Functional Morphology, Faculty of Veterinary Medicine, University of Warmia and Mazury, Olsztyn, Poland

The aim of this study was to describe the basic morphological features of the pineal gland of the European Beaver (*Castor fiber*).
The study was performed on female European beavers captured in their natural habitat in North-Eastern Poland (intervention captures commissioned by the local Environmental Conservator) or obtained from the experimental beaver farm of the Polish Academy of Sciences in Popielno. The animals were killed by exsanguination performed under deep anaesthesia induced by administration (i.m.) of ketamine and xylazine (procedure accepted by the local Ethical Commission and the local Environmental Conservator). The pineal glands with adjacent parts of the diencephalon were removed. For histological studies, the tissues were fixed in 4% paraformaldehyde or in Solcia's solution, dehydrated in alcohol and embedded in paraffin. Serial sections with a thickness of 8 μm were cut in the sagittal plane and stained in turn with one of two methods: HE or Mallory's method.
At a macroscopic level, the pineal gland of the European beaver has been described as a small, cone-shaped or oval organ, located between the habenular and posterior commissures, and corresponding to type A of Vollrath's classification. Histological studies have revealed many specific features of the beaver pineal, which were not described in any hitherto studied mammals. The pineal contained very deep recessus of the III ventricle, reaching the apical pool of the gland. The parenchyma was asymmetrically distributed around the pineal recessus. A thick layer of parenchyma surrounded it at the caudo-dorsal side, and a very thin layer at the cranio-abdominal side. Another specific feature of the beaver pineal is the presence of numerous tubes and cysts, which were limited by cubic or flat cells. It is reasonable to suspect that these spaces are connected and open into the third ventricle. A large cluster of irregularly placed cells was found inside the third ventricle at the abdomen surface of the posterior commissure. It took the shape of a strand, which was thick in the vicinity of the abdomen part of the commissure and very thin and discontinuous at the dorsal part. The histological appearance of this cell cluster closely resembled the pineal parenchyma structure. Further studies are necessary to establish if this cluster of cells is part of the pineal gland.

PRENATAL AND POSTNATAL DEVELOPMENT OF RATS EXPOSED IN-UTERO TO IBUPROFEN

Burdan F[1], Belzek A[1], Szumilo J[2], Belzek M[1], Dudka J[2], Klepacz R[2]

[1]*Experimental Teratology Unit of the Human Anatomy Department, Medical University of Lublin, Lublin, Poland*
[2]*Clinical Pathomorphology Department, Medical University of Lublin, Lublin, Poland*

Two-generation studies are obligatory for regulatory evaluation of xenobiotic tolerability. The aim of the experiment was to evaluate developmental toxicity of ibuprofen — a popular cyclooxygenase inhibitor — using the traditional two-generation protocol. The drug was administered to pregnant Wistar rats on gestational days 8–17 in doses 5.7–171.0 mg/kg. On gestation day 21, the pregnancy was terminated in half of the dams. Comprehensive developmental measurements, including skeletal double staining, were performed on the foetuses. The remaining dams delivered spontaneously and the offspring were evaluated using traditional teratological methods during the next 90 days. The dams of the first generation were inseminated and their 21-day-old foetuses were examined. It was found that ibuprofen revealed maternal, embryo- and fetotoxicity, as well as decreased fertility of the first generation. A low, insignificant incidence of skeletal malformations and developmental variations was found. The most common localizations of such changes were the skull, vertebrae and sternum. Less frequently, such abnormalities were noted in the appendicular skeleton, in which low or unossified metacarpal and metatarsal bones, as well as phalanges, were the most often affected. A lack of any significant developmental side effects was found in the second generation. It could be concluded that high doses of ibuprofen caused embryo- and fetotoxicity, as well as decreased fertility of the first generation of rat offspring, and had no effect on the second generation. The study did not reveal any teratogenic effect of ibuprofen on either skeletal or visceral organ levels.

MORPHOLOGY OF THE KNEE JOINT AND ADJACENT EPIPHYSEAL CARTILAGES IN 7-DAY-OLD RAT PUPS EXPOSED TO NON-SELECTIVE CYCLOOXYGENASE INHIBITORS DURING PREGNANCY AND LACTATION

Burdan F[1], Szumilo J[2], Solecki M[1], Marzec B[3], Dudka J[2], Klepacz R[2]

[1]*Experimental Teratology Unit of the Human Anatomy Department, Medical University of Lublin, Lublin, Poland*
[2]*Clinical Pathomorphology Department, Medical University of Lublin, Lublin, Poland*
[3]*Medical Genetic Department, Medical University of Lublin, Lublin, Poland*

Chondrotoxicity of non-selective cyclooxygenase (COX) inhibitors has not been studied extensively in foetuses or newborns. The aim of the study was to evaluate the cartilage effect of ibuprofen, piroxicam and tolmetin in rat offspring. The tested drugs were administered intragastrically to pregnant Wistar rats between gestation day 8 and lactation day 7. On postnatal day 7, the offspring were sacrificed and the hind paws were dissected. The epiphyseal cartilages of femur, tibia and fibula were separated. The expression of tumour necrosis factor (TNF) and housekeeping genes was checked by RNase Protection Assay. The TNF protein level was evaluated by ELISA. The localization of the cytokine was immunohistochemically visualized. The knee joint morphology was studied macroscopically using double-staining methods and microscopically after various histological and histochemical staining. Cartilage ultrastructure was examined by transmission electron microscope. It was found that the highest doses of ibuprofen (255 mg/kg/day) and piroxicam (3.0 mg/kg/day) increased the level of TNF in cartilage homogenates. No differences were found in the gene expression and immunostaining for TNF. The morphology of the knee joint and adjacent epiphyseal cartilages was not disturbed. In spite of the normal epiphysis ultrastructure, a small number of dark chondrocytes was detected in both the control and drug-exposed groups. It should be stressed that the tested non-selective COX inhibitors did not affect the joint and cartilage development in rats.

A COMPARISON OF THE DISTRIBUTION AND MORPHOLOGY OF ChAT-, VAChT-IMMUNOREACTIVE AND AChE-POSITIVE NEURONS IN THE THORACOLUMBAR AND SACRAL SPINAL CORDS OF PIGS

Całka J, Załęcki M, Wąsowicz K, Łakomy M

Department of Functional Morphology, Division of Animal Anatomy, Faculty of Veterinary Medicine, University of Warmia and Mazury, Olsztyn, Poland

Present knowledge concerning the organization of cholinergic structures of the spinal cord has been derived primarily from studies on small laboratory animals, while there is a complete lack of information concerning its structure in pigs. In the present study, we employed choline acetyltransferase (ChAT) and vesicular acetylcholine transporter (VAChT) immunocytochemistry and acetylcholinesterase (AChE) histochemistry to identify the cholinergic neuronal population in the thoracolumbar and sacral spinal cords pigs. The distribution of ChAT-, VAChT- and AChE-positive cells was found to be similar. Distinct groups of cholinergic neurons were observed in grey matter of the ventral horn, the intermediolateral nucleus, the intermediomedial nucleus, and individual stained cells were found in the area around the central canal and in the base of the dorsal horn. Double staining confirmed complete co-localization of ChAT with AChE in the ventral horn and intermediolateral nucleus. Although in the intermediomedial nucleus, only 64% of the AChE-positive neurons expressed ChAT-immunoreactivity, indicating unique, region restricted diversity of ChAT and AChE staining. Our results revealed details concerning spatial distribution and morphological features of the cholinergic neurons in the thoracolumbar and sacral spinal cord of pigs. We also found that the pattern of distribution of cholinergic neurons in the porcine spinal cord shows great similarity to the organization of the cholinergic system in other studied mammalian species.

PARTICIPATION OF ANTLEROGENIC CELLS IN THE REGENERATION OF CARTILAGE AND BONE DEFECTS IN RABBITS

Cegielski M[1], Dzięgiel P[1], Gębarowski T[2], Podhorska-Okołów M[1], Bochnia M[3], Zabel M[1,4], Baliński S[5]

[1]*Chair and Department of Histology and Embryology, University School of Medicine, Wrocław, Poland*
[2]*Chair and Department of the Basis of Medical Sciences, University School of Medicine, Wrocław, Poland*
[3]*Department of Otolaryngology, University School of Medicine, Wrocław, Poland*
[4]*Chair and Department of Histology and Embryology, Medical University, Poznań, Poland*
[5]*Dental Practice in Świdnica, Świdnica, Poland*

The shedding of antlers and their reconstruction in the course of stag's life takes place cyclically, year after year. Thus, the process provides a unique model for studying mechanisms conditioning tissue regeneration in mammals. In initiation and continuation of antler growth, an important role is played by stem cells.
Examination of the involvement of antlerogenic cells in xenogeneic grafts was performed in order to regenerate defects of chondrous and osseous tissue in rabbits.
Stem cells placed in a carrier were grafted to defects in cartilage and bone, which had been made earlier, in six experimental rabbits. After four weeks, in the sites of grafting, the regeneration process was checked. The sampled experimental material was subjected to histological, immunocytochemical and ultrastructural evaluation. Serum protein electrophoresis was also performed. Immune response, confirmed by electrophoretic examination of serum proteins was poorly expressed and accompanied by no graft rejection reaction. Histological, immunohistochemical and ultrastructural analysis performed 4 weeks after grafting pointed to the involvement of xenogeneic proteins in the regeneration processes. The results permitted the suggestion that the antlerogenic cells might also find application in the reconstruction of chondrous and osseous tissues in other species.

ANATOMY OF THE MENISCOFEMORAL LIGAMENTS IN HUMAN FOETUSES

Chwaluk A[1], Ciszek B[2]

[1]*Department of Anatomy, Academy of Physical Education, Warsaw, Faculty Biała Podlaska, Poland*
[2]*Department of Anatomy, Medical University, Warsaw, Poland*

The meniscofemoral ligaments (MFLs) are the structures of knee joint connecting the lateral meniscus to the medial femoral condyle. The anterior meniscofemoral ligament (AMFL) and posterior meniscofemoral ligament (PMFL) have been distinguished.
There are some divergences according to exact incidence of MFLs. Sometimes both ligaments are found together in the same joint, or only one of them (anterior or posterior) or neither, and it may vary in each knee joint of an individual. There is a hypothesis that they might degenerate with age. Occasionally, accessory ligaments attached to the other corners of the menisci are found.
Previous studies have paid attention to the incidence and typical morphology of MFLs in adults but there is lack of investigation of these ligaments in foetal material.
The aim of this study was to asses the incidence, distribution and anatomical variances of MFLs in foetuses.
The study covered 50 foetal knee joints from both genders from 25 foetuses 14–21 hbd fixed in formaldehyde from the collection of the Department of Anatomy of the Medical University in Warsaw. Dissections were carried out with microsurgical instruments and surgical microscopes.
Meniscofemoral ligaments were found in 92% of foetal knees. AMFLs were found in 64%, as PMFLs. The incidence of these ligaments in left and right knees was 88% and 96%, respectively, without significant variation. The incidence of MFLs in female foetal knees (95.5%) does not differ with the incidence in male foetal knees (89%). Only the incidence of anterior meniscofemoral ligaments varied depending on sex, and in female foetal joints was greater than in male foetal joints. Among the knees with one ligament, the posterior meniscofemoral ligament was found more frequently in male than in female knee joints. In the foetuses, 94% of anterior and 75% of posterior meniscofemoral ligaments presented typical morphology. There was no accessory meniscofemoral ligament found in any of the dissected knee joints.

THE DEVELOPMENT OF THE HUMAN PELVIS DURING PRENATAL LIFE

Cieściński J[1], Siedlecki Z[1], Szpinda M[1], Lisewski P[1], Stachowicz A[2], Szostak M[2], Woźniak K[2]

[1]*Department of Normal Anatomy, Collegium Medicum in Bydgoszcz of Nicolaus Copernicus University, Toruń, Poland*
[2]*Student's Scientific Society of Normal and Clinical Anatomy, Collegium Medicum in Bydgoszcz of Nicolaus Copernicus University, Toruń, Poland*

The human pelvis presents sexual dimorphism which is associated with its function. In both sexes, the pelvis is the girdle of inferior extremities and provides protection for the rectum, anus, bladder and sexual organs. In females, the pelvis also a birth canal and its diameters are of great clinical relevance to obstetrics and gynaecology.

The aim of the study was to analyse the pelvic diameters of human foetuses and calculate gender differences. The examinations were carried out on 57 human foetuses of both sexes (29 female, 28 male) between the 16th and 25th weeks of gestation. Foetal age was determined by crown-rump (CR) measurement on the basis of Iffy tables. For each foetus, the following linear distances were measured: 1. interspinous diameter, 2. intercristal diameter, 3. intertrochanteric diameter, and 4. external conjugate. The correlation coefficient was calculated between each pelvic diameter and foetal age in both sexes. The size of the foetal pelvis increased according to a linear function and showed high correlation with foetal age ($p < 0.05$). The material examined revealed gender differences in intertrochanteric diameter. Sex dimorphism was observed from the 22nd week of intrauterine life. The lengths of the intertrochanteric diameters were statistically significant longer in female foetuses ($p < 0.05$).

THE ANATOMY OF UNRUPTURED INTRACRANIAL ANEURYSMS

Ciszek B[1, 3], Andrzejczak A[1, 2], Ungier E[1], Krajewski P[4]

[1]Department of Anatomy, Centre of Biostructure Research, Medical University of Warsaw, Warsaw, Poland
[2]Department of Neurology, II Medical Faculty, Medical University of Warsaw, Warsaw, Poland
[3]Department of Neurosurgery, Bogdanowicz Paediatric Hospital, Warsaw, Poland
[4]Department of Forensic Medicine, Medical University of Warsaw, Poland

The problem of unruptured intracranial aneurysms is a very important topic from the point of view of epidemiology, pathology, neurology, neurosurgery and forensic medicine.
The real frequency of such silent unruptured intracranial aneurysms is unknown. Therefore, the risk of rupture of such aneurysm is an enigma in the case of incidental discovery. Only a few papers have been devoted to the search for these silent aneurysms. In many other papers, the figure of 5% is continually repeated.
We undertook a preliminary study of the frequency of unruptured aneurysms based on 100 consecutive autopsies without features of fresh or old intracranial bleeding and non-neurological death. Fifteen unruptured aneurysms in different locations, such as the middle cerebral artery, anterior communicating artery, basilar artery and internal carotid artery were detected.
This means that even 15% of the population may develop intracranial aneurysms and die from other causes.

CORONARY ARTERIES OF MOUSE HEARTS

Ciszek B[1], Ratajska A[2]

[1]Department of Anatomy, Centre of Biostructure Research, Medical University, Warsaw, Poland
[2]Department of Pathological, Anatomy Centre of Biostructure Research Medical University, Warsaw, Poland

The anatomy of the coronary arteries of the heart in mice presents marked differences in relation to other species, including humans. Forty mice (20 females, 20 males) were perfused and injected with latex by the thoracic aorta. After fixation in formaldehyde and removal of the hearts, observations and documentations were conducted with the aid of a surgical microscope.
The most frequent arrangement of the coronary arteries was branching of the three main trunks. The right coronary artery and separated septal artery started from the right sinus of the aorta. From left sinus of the aorta originated the left coronary artery.
There were some cases with two septal arteries from the right and left sinuses as well. The left coronary artery supplied the auricular surface of the heart and left ventricle. The right coronary artery mainly supplied the right ventricle and atrial surface of the left one.

IMMUNOCYTOCHEMICAL INVESTIGATIONS OF RAT THYROID C CELLS IN EXPERIMENTAL OSTEOPOROSIS

Danowska-Klonowska D[1], Tosik D[2], Brzeziński P[1], Lasota A[2], Bartel H[2]

[1]Chair of Histology and Embryology, Department of Cytophysiology, Histology and Embryology, Medical University of Łódź, Łódź, Poland
[2]Department of Histology and Ultrasctructure of Tissues, Medical University of Łódź, Łódź, Poland

Osteoporosis is a disease of the skeleton, in which there is a grater risk of bone fracture because of the decrease of bone durability. The most common form of the disease is postmenopausal osteoporosis. The most suitable species is the rat and ovariectomy is now recognized and raising-no-doubts procedure leading to osteoporotic changes.
Immunocytochemical estimation of the numbers of thyroid C-cells in the course of experimental osteoporosis.
For the experiment, 70 female white rats were used, divided into two groups (control and ovariectomised, 35 animals each). Calcitonin in the thyroid was detected using the immunocytochemical ABC method. The thyroids for the investigation were removed, fixed in Bouin's fluid and mounted in paraffin, in the same way as in studies with the use of classical methods.
In the slides, in which the immunocytochemical reaction for calcitonin was done, the cells with brown stained cytoplasm can be seen. They are the thyroid C-cells. For the results preparations the volume of immunocytochemical-positive C-cells was compared to the volume of the whole thyroid.
As a consequence of immunocytochemical studies, the differences in the immuno-positive areas of the thyroids were found between control and ovariectomised individuals. In osteoporosis, the immuno-positive area is greater than in control rats.

BETULINIC ACID HAS THE SAME CYTOTOXIC ACTIVITY AGAINST SENSITIVE AND MULTIDRUG--RESISTANT HUMAN CANCER CELL LINES

Drąg-Zalesińska M[1], Jagoda E[1], Drąg M[2], Oleksyszyn J[2], Surowiak P[1, 3]

[1]Department of Histology and Embryology, University School of Medicine, Wrocław, Poland
[2]Department of Chemistry, Division of Medicinal Chemistry and Microbiology, Wrocław University of Technology, Wrocław, Poland
[3]Lower Silesian Centre of Oncology, Wrocław, Poland

Betulinic acid (3β-hydroxy-lup-20(29)-en-28-oic acid), pentacyclic lupane triptene, is a known natural compound with various biological effects. Cytotoxic activity against malignant cells belongs to the most intensively studied effects of these compounds. The aim of the study was to investigate cytotoxic activity of betulinic acid against sensitive and multidrug-resistant human cancer cell lines. The study was performed on human pancreas carcinoma cell line EPP 181/85P and its multidrug-resistant derivates: EPP 181/85RDB and EPP 181/85RNOV, as well as on human gastric carcinoma cell line EPG 257/85P and its multidrug-resistant derivates: EPG 257/85RDB and EPG 257/85RNOV. For each studied cell line, we performed cytotoxicity tests three times using the SRB-staining method to evaluate IC50 for betulinic acid. The performed studies showed that there are no significant differences between betulinic acid sensitivity of drug-sensitive and drug-resistant human cancer cells.
The study showed that betulinic acid is a promising anticancer agent with activity against cytostatic drug-sensitive and drug-resistant tumours.

FALSE *CHORDAE TENDINEAE* IN THE LIGHT OF TOPOGRAPHY OF THE CONDUCTION SYSTEM IN THE RIGHT VENTRICLE OF ADULT HUMANS

Dubaniewicz A[1], Kosiński A[1], Grzybiak M[1], Kozłowski D[2], Piwko G[1], Nowicka E[1]

[1]*Department of Clinical Anatomy, Medical University of Gdańsk, Gdańsk, Poland*
[2]*Second Department of Cardiology, Medical University of Gdańsk, Gdańsk, Poland*

False *chordae tendineae* are described as fibro-muscular cords within the light of the ventricle that, contrary to the "real" *chordae*, do not attach to the atrio-ventricular valves, and thus are not elements of the valvular apparatus. There are numerous publications suggesting their influence on electromechanical processes in the heart (modification of the systolic function of the right ventricle, generation of some acoustic phenomena such as heart murmurs, some significance in pulmonary embolism incidents or dysrhythmias). Many controversies around their morphology, as well as some significant clinical implications of their presence, motivate detailed analysis of the problem. The histological evaluation of the false *chordae tendineae* in the right ventricle, including the elements of the conduction system, was the main goal of the study. The material consisted of 25 hearts of adult humans, aged 18–59 years, without any pathological or developmental changes, who died of non-cardiological causes. Histological specimens were taken from different types of false *chordae tendineae*. In total, 62 *chordae* were analysed. The specimens were stained with Masson's method with Goldner's modification. The placement of muscle tissue — especially the elements of the conduction system, fibrous tissue and blond vessels — was analyzed. The evaluation of the false *chordae* revealed that these are mainly made of muscle tissue, grouped in one or few bands divided with connective tissue and surrounded by endocardium. Vascular supply was also well developed — with the muscular bands, the vessels were present alongside their whole run. There was no direct evidence of the right branch of His bundle branches; however, there were some solitary muscle fibres with morphology that could correspond with distal parts of conduction system — the Purkinje fibres.

DIFFERENCES IN THE APPEARANCE OF PRIMARY OSSIFICATION CENTRES OF THE PETROUS PART OF THE TEMPORAL BONE IN RADIOLOGICAL AND HISTOLOGICAL STUDIES

Dzięciołowska-Baran E, Sławiński G, Czerwiński F, Teul I, Gawlikowska-Sroka A

Chair and Department of Human Anatomy, Pomeranian Medical University, Szczecin, Poland

The aim of the work was to compare the time of appearance of the primary ossification nuclei in the petrous part of the temporal bone in radiological and histological examinations.
The temporal bones of 76 foetuses aged between 9–32 weeks of foetal life were separated. X-ray images of each bone were performed in projection on the anterior and posterior wall of the pyramid of the temporal bone. One bone of each pair was used as a histological specimen. It was decalcified, dehydrated and after stabilization cut along the longitudinal axis or perpendicular to it (randomly) into 3–4 μm wide specimens and dyed. Then it was observed under a lumen microscope with 5 ×, 10 × and 20 × magnification.
The time of appearance of the primary ossification nuclei was estimated both in radiological and histological images. Usually the ossification nuclei was seen about one week earlier in histological than radiological studies in foetuses between 15–20 weeks of gestational life. Only five primary ossification nuclei were always confirmed in histological examinations. Most of the seemingly primary nuclei which appeared after the 20th week of foetal life were not confirmed in histological examinations. Some of them were seen in the specimen as a continuation of earlier existing primary nuclei. Another group of seemingly present primary ossification centres in x-ray images were absent in histological specimens and their presence in x-ray images can be explained as total X-ray absorption on different levels of the petrous part of the temporal bone giving a false result.
All primary ossification nuclei observed in X-ray images should be verified in histological studies.

MELATONIN: ADJUVANT THERAPY OF MALIGNANT TUMOURS

Dzięgiel P

Department of Histology and Embryology, Medical University of Wrocław, Wrocław, Poland

In the literature, the most important data have been presented on intense studies carried out in recent decades on the potential for employing melatonin in adjuvant treatment of tumours. Results of clinical studies were preceded by descriptions of experiments conducted on neoplastic cell lines and on laboratory animals. Most of the reports unequivocally confirmed anti-oxidant and immunostimulatory action of the pineal hormone, both in *in vitro* and *in vivo* experiments. Results of studies on cell lines of various tumours showed that the anti-proliferative effect of melatonin might involve a receptor-mediated mechanism. In experiments on animals, the cardio-, nephro-and myeloprotective action of melatonin was confirmed in the course of the application of various cytostatic drugs. Metaanalysis of clinical studies in which melatonin was applied as an adjuvant drug in therapy of various tumours pointed to some effects of its administration and offers hope for the future in anti-neoplastic use of the pineal hormone.

THE EFFECT OF MELATONIN ON THE PROLIFERATION OF COLON CARCINOMA CELLS — SENSITIVE (LoVo) AND RESISTANT (LoVo$_{DX}$) TO DOXORUBICIN IN *IN VITRO* TESTS

Fic M[1], Podhorska-Okołów M[1], Drąg-Zalesińska M[1], Wysocka T[1], Dzięgiel P[1], Zabel M[1,2]

[1]*Department of Histology and Embryology, University School of Medicine, Wrocław, Poland*
[2]*Department of Histology and Embryology, Medical University of Poznań, Poznań, Poland*

Melatonin (MLT) is a pineal hormone affecting the proliferation of neoplastic cells *in vitro*. The mechanism of its action has not been fully recognized. It is known to inactivate free radicals in a direct and an indirect way, which are generated in the body in substantial amounts, i.e. during turnover of anthracyclines (e.g., doxo- and daunorubicin). In addition, it has been found that MLT does not alleviate the toxic action of the cytotoxic drugs exerted to neoplastic cells. It seems that there exists a potential for overcoming, by MLT, the multi-drug resistance (MDR) of neoplastic cells to doxorubicin (DOX).
This study aimed at the evaluation of the *in vitro* effects of MLT on the proliferation of cells originating from colon carcinoma, sensitive (LoVo) and resistant (LoVo$_{DX}$) to DOX.
The experiments were conducted in in vitro conditions on LoVo and LoVo$_{DX}$ cells. The cells were exposed to MLT in concentrations of 0.1 mM and 1.0 mM and to DOX in concentrations of 0.005 μg/ml (K3), 0.05 μg/ml (K2) or 0.5 μg/ml (K1). The extent of proliferation inhibition in cell cultures was evaluated using staining with sulforhodamine B (SRB

technique) and optical density readout from an automatic microplate densitometer (Elx 800). The types of lesions developing in cell nuclei was estimated by comet test. The results were subjected to statistical analysis using Mann-Whitney's test and Statistica 7.1 software.
In both cell lines, the inhibition of tumour cell proliferation (%) clearly increased in parallel to growing DOX concentration, but the resistant cell line proved to be definitely less sensitive. MLT also significantly inhibited cell proliferation of LoVo and $LoVo_{DX}$ cells, but an increase in MLT concentration did not intensify the cytotoxic effect. However, in the case of LoVo cells, MLT intensified cytotoxicity of DOX at the concentration of K3. In parallel, MLT significantly overcame resistance to DOX of $LoVo_{DX}$ line cells.
The obtained data confirmed the anti-proliferative effects of MLT on some neoplastic cell lines and its role in overcoming resistance to DOX in resistant cell lines.

ARTERIES OF THE HEAD OF THE REPRESENTATIVE *RHINOCEROTIDAE*

Frąckowiak H

Department of Animal Anatomy, Agricultural University of Poznań, Poznań, Poland

The aim of this study was to conduct the comparative analysis of arteries of the head in the white rhinoceros, a representative of the *Rhinocerotidae* family.
Observations were conducted on a corrosion cast of arteries of the head of a female white rhinoceros aged 3.5 years, which was prepared from post-mortem examination material obtained from the Zoological Garden in Poznań.
Analysis of arteries of the head in the analyzed rhinoceros from the family *Rhinocerotidae* showed certain common features as well as differences in comparison to the vascular pattern described in representatives of the families *Equidae* and *Tapiridae*.
The common carotid artery in the rhinoceros, similarly to *Equidae* and tapirs, undergoes final segmentation into the external carotid artery and the internal carotid artery.
The lingual artery and the facial artery in the rhinoceros, similarly as in the tapir, branch directly off the external carotid artery. In all *Equidae*, the lingual artery and the facial artery branch off the linguofacial trunk, which is a permanent branch of the external carotid artery.
The method of branching of the superficial temporal artery, found in the rhinoceros, is not observed in representatives of other families from the order *Perissodactyla*. Of all *Perissodactyla*, only the internal carotid artery in the rhinoceros bifurcates into numerous vessels even before it enters the cranial cavity and forms the arterial rete mirabile (epidural rostral), from which arteries forming the arterial circle of the brain originate.
The rete mirabile of the carotid artery in the rhinoceros is the only known case of the occurrence of an arterial rete mirabile in the area of the arteries of the head in animals from the order *Perissodactyla*. In contrast to the rostral epidural rete mirabile in *Artiodactyla* in the rhinoceros it communicates with the maxillary artery only through a single thin ramus.
The common characteristic of the arterial pattern of the head in the white rhinoceros and all *Perissodactyla* is the method of final segmentation of the common carotid artery.
In the white rhinoceros, the lingual artery and the facial artery, similarly as in animals from the *Tapiridae* family, branch off separately from the arterial route of the head.
The arterial rete mirabile in the area of the arteries of the head in the rhinoceros is the only such known case in animals from the order *Perissodactyla*, and at the same time a specific distinguishing characteristic of the family *Rhinocerotidae*.

ARTERIES OF THE CRANIAL CAVITY OF THE AUROCHS (*BOS PRIMIGENIUS BOJANUS* 1827) — RECONSTRUCTION ATTEMPT

Frąckowiak H, Godynicki S

Department of Animal Anatomy, Agricultural University of Poznań, Poznań, Poland

The reconstruction attempt of the arteries of the cranial cavity of the extinct aurochs was based on the comparison analysis of the cranial base of the skulls of seven aurochs and modern species of the *Bovinae* subfamily. Moreover, the pattern of the arteries of the brain of modern genera (*Bison, Bos, Boselaphus, Taurotragus* and *Tragelaphus*) was studied. Also, taxonomy analysis of the *Bovinae* subfamily was also made.
A large similarity of the crania skeleton of aurochs and of the modern species of the *Bovinae* subfamily was observed. The Foramen orbitorotundum, the foramen ovale, the jugular foramen and the petrobasal fissure are common for all ruminants and are penetrated by the blood vessels. The hypoglossal nerve canal also participates in cranial cavity drainage via the condylar artery.
In the modern species of the *Bovidae* family, the rostral branches to the rostral epidural rete mirabile pass through the foramen orbitorotundum. Whereas, the caudal branch to the rostral epidural rete mirabile passes through the foramen ovale.
The rostral epidural rete mirabile of the *Bovinae* subfamily species lies on the cranial base, inside the cranial cavity, around the hypophyseal fossa. Additional rostral epidural rete mirabile were observed in banteng, bison, domestic cattle, yak, zebu and European bison (*Bison* and *Bos* genera). The rostral epidural rete mirabile was absent in the *Boselaphus, Tragelaphus* and *Taurotragus* genera.
The internal carotid artery, only in cattle foetuses, is connected with the rostral epidural rete mirabile. The extracranial segment of the internal carotid artery was obliterated in all investigated adult specimens (also probably in the aurochs). The intracranial segment was preserved as the interretial and the over-retial sections. The over-retial section of the internal carotid artery, in all investigated species, was terminally divided into the arteries, which represent the main components of the circle of the brain.
The comparison analysis of the arterial vessels supplied the brain in all investigated species, suggested, the vessels pattern of the aurochs was perhaps similar to the vessels affirmed in the *Bison* and *Bos* species only.

ARTERIAL PATTERN OF THE GIRAFFE BRAIN

Frąckowiak H, Jakubowski H

Department of Animal Anatomy, Agriculture University of Poznań, Poznań, Poland

The aim of the study was to analyze the system of arteries of the brain in the giraffe, including the arterial circle of the brain, its branches and junctions, as well as individual variations of vessels. Analyses were performed on 12 heads of giraffes. Arteries of these heads were injected with latex and vinyl superchloride.
Arteries supplying the brain in the giraffe branch off the arterial circle of the brain, formed as a result of the segmentation of the end intracranial part of the internal carotid artery.
Bilateral rostral cerebral arteries and caudal communicating arteries, together with the basilar artery, form the arterial circle of the brain.
The giraffe brain is supplied by the rostral epidural rete mirabile, which is connected to the maxillary artery. Moreover, a thin condylar artery branching off the occipital artery joins the rete.
Branches to individual brain structures branch off from segments of the arterial circle of the brain. A rostral choroid artery branches off the initial segment of the rostral cerebral artery. The middle cerebral artery is the strongest branch of the central segment of the rostral cerebral artery. The internal ethmoidal artery most frequently branches off the end segment

of the rostral cerebral artery. Bilateral rostral cerebral arteries are anastomosed by the rostral communicating artery.
The caudal communicating artery is characterized by a varied shape and course. The caudal cerebral artery is the strongest branch of the caudal communicating artery. The caudal choroid artery is another branch of the caudal cerebral artery. The rostral cerebellar artery branches off the caudal communicating artery. Near the site of branching of the rostral cerebellar artery, numerous small vessels were found. The bilateral caudal communicating arteries are anastomosed by the communicating branch of the arterial circle of the brain.
The basilar artery is anastomoses rostraly with caudal communicating arteries. The diameter of the basilar artery varies and its lumen decreases caudally. The caudal cerebellar artery and branches to the pons and the medulla oblongata constitute ramifications of the basilar artery. The caudal cerebellar artery is the strongest ramus of the basilar artery. In all specimens asymmetry can be seen in the method of branching off and a slight asymmetry in the diameter.

CORONARY ARTERIES IN SOME MAMMALIAN ORDERS

Frąckowiak H, Jasiczak K

Department of Animal Anatomy, Agricultural University of Poznań, Poznań, Poland

The aim of the study was the classification of the type of the arterial vascularization of the heart in some mammalian orders: *Carnivora* (*Alopex logopus, Nyctereutes procyonides, Vulpes vulpes*), *Perissodactyla* (*Equus Przewalski, Ceratotherium simum*), *Artiodactyla* (*Sus scrofa, Choeropsis liberiensis, Graffa camelopardalis, Capreolus capreolus, Ovis ammon*), *Rodentia* (*Myocastor coypus*). On the basis of observation, coronary artery patterns were classified to the left (with modifications) and symmetrical types of the arterial vascularization of the heart.
Coronary arteries were filled with coloured dental mass Duracryl and latex LBS 3060. The preparations filled with latex were then fixed in a 10% formalin solution and prepared manually in order to uncover the vessel course. Preparations filled with Duracryl after polymerizing were macerated in order to prepare corrosion casts of the vessels.
The left type of arterial vascularization of the heart was observed in animals representing some mammalian orders: *Carnivora, Rodentia* and also in *Artiodactyla* (the giraffe, the roe deer and the Wrzosowka sheep). The pig, the wild boar, the Przewalski wild horse, and the white rhinoceros were represented by the symmetrical type of arterial vascularization of the heart.
In most investigated animals representing the left type of the arterial vascularization, the subsinuosal interventricular branch is the terminating vessel of the left circumflex branch. In the roe deer heart, the left coronary artery does not reach the subsinuosal interventricular groove but terminates on the atrial surface of the left ventricle wall, just after passing the left margin of the heart. In roe deer heart, the paraconal interventricular branch elongates into the subsinuosal interventricular branch. This pattern of the left coronary artery is uncommon for other representatives of the left type of arterial vascularization.

ANALYSIS OF THE FOETAL SKULL USING THE FINITE ELEMENTS METHOD

Frątczak R[1], Panek M[1], Słowiński J[1], Kędzia A[2], Kołosowski W[2]

[1]*Institute of Materials Science and Applied Mechanics, Wrocław University of Technology, Wrocław, Poland*
[2]*Department of Normal Anatomy, Medical University, Wrocław, Poland*

The finite element method is the applied method which serves to the opinion of the stresses and strains condition of studied objects. It allows prognosis of the most probable places of material damage. It is widely used in bioengineering, in projecting processes of implants and in endoprosthesis. The aim of the work is the construction of the patternel of the skull and material strength calculations by the proper load sets. The method of investigation was to fill up the skull from the outside and inside with methylmetakryl . Sections were made stepped by 1 mm of filled skull using conventional machining. Overall there were 70 sections. Separate slices were scanned (by computer scanner), GIMP was applied after initial colour balance correction to split the proper materials. Next, the slices were applied to special processing by Roman Frątczak software that makes it possible to import any spatial model geometry to the ANSYS software, which was used to study the finite element method simulation. The imported cloud of points were automatically connected by lines using RF software, but the areas and volumes had to be built manually with regard to the best description of anatomical geometries. The spatial skull model was build using tetragonal 10 nodal elements (named Solid92, with three degrees of freedom in each node). The material model was elastic and isotropic (the properties did not depend on the examining direction) with propriety Young's modulus of 1000 MPa and Poisson's ratio equal to 0.42. The size of the element edge was 1.2 mm (the nominal value that was accordingly matched due to geometry). After all modelling processes, a static compressing force of 50 N was applied to the left temple. The opposite side, the right temple, was constrained by applying a displacement equal to 0 mm in three directions on the proper nodes — so the skull could be squeezed horizontally. The analysis results prove the stress concentration was in the whole skull, but mainly in the frontal part of the facial bone. However, from an engineering point of view, the above stress concentrations do not cause damage in the osseous structures. Individual concentrations could be noticed along the hole that probably, with a certain load case, may be the reason for cracking this structure. Considering the relatively thin bone shell in the temple, large deformation of the brain ventricle can occur. Also, large skull strains could not determine the stage of brain deformation, but the results can be used to make some evaluation of brain deformation.

IMMUNOHISTOCHEMISTRY OF PITUITARY MICROADENOMAS OCCURRING IN THE POLISH POPULATION

Furgal-Borzych A[1], Lis GJ[1], Litwin JA[1], Rzepecka-Wozniak E[2], Trela F[2], Cichocki T[1]

[1]*Department of Histology, Jagiellonian University Medical College, Cracow, Poland*
[2]*Department of Forensic Medicine, Jagiellonian University Medical College, Cracow, Poland*

According to the literature, pituitary adenomas, clinical and sub-clinical, are relatively frequent (9–27%), but their incidence in the Polish population is unknown. In the course of a retrospective study of pituitary microadenoma incidence, we evaluated the frequency of particular immunophenotypes in a pilot sample.
The pituitary glands of 100 subjects (mean age 51 years, SD = 19.9 years, range 17–95 years; 57 males, 43 females) were obtained upon autopsy at the Department of Forensic Medicine, Jagiellonian University Medical College. Each formalin-fixed, paraffin-embedded pituitary gland was cut into 8 μm thick serial sections and mounted on slides. Every 20th slide was routinely stained with haematoxylin and eosin for histopathological examination. For verification of adenomas, indirect immunofluorescence for collagen III was employed. Sections from cases with adenomas were subjected to immunophenotyping with the use of antibodies against pituitary hormones (FSH, LH, TSH, ACTH, PRL, HGH). Sections were examined under an Olympus BX50 light/fluorescence microscope.
Pituitary adenomas were found in 29 cases — all of them were microadenomas (diameter $<$ 1 cm). Multiple microadenomas (2 or 3) were observed in five cases. There was no association of adenoma occurrence with

sex, although the relationship with age was very close to statistical significance ($p = 0.06$). Among the microadenomas detected, nonsecreting (immunonegative) tumours constituted 27.6%. In the group of immunopositive adenomas, 79.3% were polyhormonal. The highest percentage of adenomas (55.2%) produced GH, followed by PRL (31.0%), ACTH (17.2%), FSH (13.8%), TSH (10.3%) and LH (3.4%).
These results, albeit preliminary, show a high incidence of pituitary microadenomas in the population and the prevalence of polyhormonal tumours.

AN ANATOMICAL STUDY OF THE ANASTOMOSIS BETWEEN THE RECURRENT LARYNGEAL NERVE AND THE SYMPATHETIC TRUNK

Gałązka A, Koleśnik A

Department of Anatomy, III Clinic of Otolaryngology, Medical University of Warsaw, Warsaw, Poland

The Recurrent Laryngeal Nerve and Sympathetic Trunk are important features of the neck anatomy. The presence of the nerval anastomosis between the two structures could be interesting from an anatomical and surgical point of view.
To determine the presence and branching patterns of the anastomosis between the recurrent laryngeal nerve and the sympathetic trunk.
Microdissection of 15 formalin preserved foetuses (30 sides).
In one case, the nerve was inappropriate for dissection. Anastomosis appeared in 23 cases. In 15 cases, it was a single branch connection. On 8 sides, a multibranch connection appeared. In only 4 cases, one of the branches of the anastomosis joined the recurrent nerve in the section superior to the inferior thyroid artery. In 19 cases, the connection was situated inferior to the inferior thyroid artery.
The anastomosis between the recurrent laryngeal nerve and sympathetic trunk is a frequent feature of the foetal anatomy. The clinical significance of this anatomical feature is yet to be evaluated.

VARIATIONS IN SIZE AND SYMMETRY OF FORAMINA AND DIAMETERS OF THE BASE OF MEDIAEVAL AND CONTEMPORARY HUMAN SKULLS

Gawlikowska A[1], Szczurowski J[2], Czerwiński F[1], Dzięciołowska E[1]

[1]*Department of Normal and Clinical Anatomy, Pomeranian Medical University of Szczecin, Szczecin, Poland*
[2]*Department of Anthropology, University of Wrocław, Wrocław, Poland*

The cranial base projection shows numerous vascular-nervous foramens that are the subject of regular interest of neurologists and neurosurgeons for whom the knowledge of this region's anatomy is extremely important for analyzing the clinical picture and planning operative technique.
The aim of this work was to estimate the variations in size and in symmetry of some foramina and diameters of skull-bases from two selected Polish historic populations and to analyze the changes that have taken place in their structure over the centuries.
The studied material consisted of two skull populations — modern, containing 82 skulls and mediaeval, containing 85 skulls. The age of the examined subjects at the moment of death was estimated using the stage of skull suture closure and was described as *adultus* or *maturus*. All skulls were well preserved and had no pathological lesions. X-rays were made in base projection. The images were scanned and calibrated by the means of MicroStation 95 Academic Edition software. Helmet's transformation was effected in order to attain a suitable geometry. The vectorization of axes and areas was performed on reference material. Tools were used for measuring the vector elements. Distances between the chosen bilateral points of both sides of the skull and distances between the analyzed points in relation to the mid-line and to the second corresponding point placed on the mid-line were measured. All data were analyzed statistically. The presence of asymmetry in the skulls of both samples was observed. A greater value of asymmetry was observed in the mediaeval group. In both examined populations, measurements of the area of the spinous foramen and one-side part of foramen magnum were significantly more frequently larger on the left-hand side. The diameter between the foraminolaterale point and midline was larger on the left side too, which means a more lateral position of the point on that side. The rest of the diameters were significantly more frequently larger on the right-hand side. The same statistically significant results were obtained when analysing the mean values of base region measurements. The methods used in this study may be served in the analysis of paleopathological materials and may also be used in modern medical diagnostics.

DIGITAL-IMAGE ANALYSIS OF THE SHAPE AND SIZE OF THE ORBIT

Gielecki J, Żurada A, Osman N

Department of Anatomy, Medical University of Silesia, Katowice, Poland

The radial method was used to study profile characteristics formed by the margins of the orbits. This method enables examination of the deviations of the local value shape for each radiation. It allows the determination of radial minimal and maximal values, mean standard and roundness deviations. It was made not only by the analysis of characteristic variations of the orbit, which relate to an individual's natural range, but also by artificial models of the orbits (ellipsoid, rectangular, circular). The term 'radial method' determines the estimation of the deviations in shape. The term 'shape deviation' is used for measurements that deviate from the standardized profile shape estimates. The standardized profile is the average squares circle (ASC), minimum circumscribed circle (MCC), maximum inscribed circle (MIC) or two concentric circles with minimal radial difference, which includes the examined profile called minimum zone circles (MZC). This theoretical study demonstrates that the definition elements of the MIC and MZC do not always lead to an unequivocal conclusion within the range of the roundness deviations previously studied. ASC was used as the element of measurement. The ASC does not fluctuate greatly when one observes a single profile position and thus it can be part of the base for the estimation of other parameters of the study profile. The radial method was utilized for the comparison of the right and left orbit asymmetry, and it enabled the harmonic analysis of profiles characteristic of the margin of the orbit.
We can obtain information about the surface, circumference, maximal width and height based on an individual's profile. The maximal width is computed relative to the maxillofrontal point, the height of the orbit and the value of the functional characteristic.
Digital image analysis was carried out by photographing 100 ancient skulls in the anthropological plane of Frankfurt to study the geometrical measurements of the asymmetry of the orbit. Radial method measurements use rectangular projection of the orbit. The outline of the orbit is marked by the Beziera's polynomials relating to the general form.
This method is very useful from an anthropological point of view and for use in forensic medicine for the comparison of the right and left orbits of various population demographics.

THE CHEMICAL CODING OF ZNT3-IR NEURONS IN THE ABDOMINAL PART OF THE OESOPHAGUS

Gocek M, Wojtkiewicz J, Gonkowski S, Bossowska A, Skobowiat C, Burliński P, Majewski M

Division of Clinical Physiology, Department of Functional Morphology, University of Warmia and Mazury, Olsztyn, Poland

ZnT3, a member of the SLC30 family of solute carriers, has recently been reported to be present in the central and peripheral nervous system of rodents and pigs. It is well known that the oesophagus is controlled by complex neuronal circuits involving both extrinsic and intramural neurons. The intrinsic nerve fibres, which represent the majority of neuronal elements in the oesophago-gastro-intestinal tract, have their neurons in intramural (enteric) ganglia. In the present report, we describe the occurrence and distribution of ZnT3-immunoreactive structures in the abdominal part of the oesophagus in the domestic pig, thus broadening our knowledge of a new component of the intramural system — ZnT3-IR nerve cell bodies. The studied part of the porcine oesophagus was analyzed for the distribution and co-localization pattern of zinc transporter 3 (ZnT3)-immunoreactivity using double-immunolabelling technique. Numerous ZnT3-IR cell bodies were seen in the myenteric and submucosal ganglia (approximately 80% of all myenteric and submucosal neurons in the studied part of the oesophagus exhibited ZnT3 immunoreactivity. Of them, approximately 80–90% of neurons simultaneously stored vasoactive intestinal peptide (VIP) and/or nitric oxide synthase (NOS). A few ZnT3-IR nerve fibres were found in the longitudinal muscle layer, yet they were moderate in number within the circular muscles. We suggest that neuronal ZnT3 may serve to modulate motor activity and secretion in the lower oesophageal region. However, the role of this transporter molecule, as well as of Zn^{2+} ions in the neural control of the lower oesophagus function, remains to be elucidated in detail.

IMMUNOHISTOCHEMICAL CHARACTERISTICS OF ENTERIC PLEXUS NEURONS IN PATIENTS WITH SIGMOID AND RECTAL CANCER

Godlewski J

Department of Animal Anatomy, Faculty of Veterinary Medicine, University of Warmia and Mazury, Olsztyn

The purpose of this work was the investigation of potential changes in the chemical coding of enteric (intramural) neurons in patients with sigmoid and rectal cancer.

Tissue samples were obtained from 15 patients operated due to colorectal cancer.

The cryostat sections were processed for double-labelling immunofluorescence to study the distribution of the intramural nerve structures (visualized with antibodies against protein gene-product 9.5) and their chemical coding using antibodies against vesicular acetylcholine transporter (VAChT), β-dopamine hydroxylase (DßH), vasoactive intestinal polypeptide (VIP), pituitary adenylate cyclase-activating peptide (PACAP), neuropeptide Y (NPY), calcitonin gene-related peptide (CGRP), somatostatin (SOM), substance P (SP) and galanin (GAL) in the inner and outer submucosal plexus, as well as in the myenteric plexus.

Unchanged and pathologically changed areas of the colon were examined to compare the chemical coding of the neurons distributed in these regions of the intestine.

The results have shown the absence of neuronal elements in cancer tissues. In the border areas of intestinal wall, a progressive decline of the number of cell bodies, especially those NPY(+) and CGRP(+), and nerve fibres immunoreactive for all examined substances was noted. The exception occurred in case of neurons GAL(+) in the myenteric plexuses pathologically changed slides, whose number was higher in comparison with the control. Immunohistochemistry revealed statistically significant changes in the expression of neurons containing NPY, CGRP and GAL.

The destruction of the enteric nervous system in the course of colorectal cancer may have caused disorder of the colon and may be responsible for some of the symptoms about which the patients complain.

CORRELATION OF mRNA EXPRESSION BETWEEN SELECTED ISOFORMS OF METALLOTHIONEIN AND PATHOLOGICAL PROGNOSTIC FACTORS IN DUCTAL MAMMARY CARCINOMA

Gomułkiewicz A[1], Dzięgiel P[1], Podhorska-Okołów M[1], Szulc R[4], Smoląg Z[4], Ugorski M[3], Zabel M[1,2]

[1]*Department of Histology and Embryology, University School of Medicine, Wrocław, Poland*
[2]*Department of Histology and Embryology, Medical University of Poznań, Poznań, Poland*
[3]*Chair of Biochemistry, Pharmacology and Toxicology, University of Natural Sciences, Wrocław, Poland*
[4]*Lower Silesian Centre of Oncology, Wrocław, Poland*

Metallothioneins (MTs) represent a group of intracellular proteins of low molecular weight (6–7 kDa) which bind metals. They include 17 isoforms differing in amino acid composition. Their principal function involves the maintenance of homeostasis for the metals which are indispensable for the body (Zn, Cu) and the binding of toxic metal ions (Pb, Cd, Hg). In recent years, the prognostic significance of the proteins in neoplastic diseases was demonstrated, including mammary carcinoma. On the other hand, no convincing data are available on the significance of mRNA expression of individual MT isoforms in mammary cancers.

The present study aimed at examining the relationship between mRNA expression for selected isoforms of MT and the degree of malignancy (G) and proliferative potential (Ki-67 antigen) in mammary carcinomas.

Material for the studies involved 55 cases of ductal mammary carcinoma of G1, G2 or G3 grade of malignancy. Following isolation of total RNA expression of mRNA for MT isoforms, including MT-1E, MT-1F, MT1-X, MT-2A and MT-3 using real-time PCR (7900HT Fast Real-Time PCR System, Applied Biosystems). In paraffin sections isolated from selected cases, immunocytochemical reactions were performed using monoclonal antibodies directed to MT, ER, PgR, Ki-67, HER-2 (Dako). Staining intensity was determined using a scale taking into account the number of positive cells and IRS scale according to Remmele, considering the number of positive cells and the intensity of colour reaction.

Among the examined MT isoforms, the highest expression of mRNA in ductal cancers of the mammary gland was noted for MT-2A and MT-3. Levels of mRNA for MT-2A and MT-3 positively correlated with the degree of malignancy (G) and proliferative potential (Ki-67) in the selected cases of cancers.

Expression of MT-2A and MT-3 mRNAs may provide a useful prognostic marker in mammary carcinomas.

DOXAZOSIN-INDUCED CHANGES IN THE NUMBER OF ZNT3-LIKE IMMUNOREACTIVE (ZNT3-LI) COLONIC NEURONS IN PIGS

Gonkowski S, Bossowska A, Wojtkiewicz J, Skobowiat C, Majewski M

Division of Clinical Physiology, Department of Functional Morphology, University of Olsztyn, Poland

ZnT3, a member of the SLC30 family of solute carriers, has recently been reported to be present in the central and peripheral nervous system of rodents and pigs. As this may implicate an important role of Zn^{2+} ions in the processes of synaptic transmission, the present study was aimed at disclosing if the expression of this transporter molecule in porcine colonic neurons may be changed by doxazosin — an agent that selectively blocks the alpha 1 adrenergic receptor, allowing a better understanding of the mechanisms involved in enteric neuron plasticity.

Pieces of distal colon were collected from three control female pigs (C group) and from three animals that were receiving doxazosin in a dose 0.1 mg/kg for 30 days *per os*. (D group) after transcardial perfusion with 4% buffered, freshly prepared paraformaldehyde. Ten-µm-thick cryostat sections were then prepared and subjected to routine double-labelling immunofluorescence using mouse monoclonal anti-PGP 9.5 and rabbit polyclonal anti-ZnT3 antisera.

In the control group, ZnT3-LI neurons constituted 25.6% of all perikarya observed in the myenteric plexus (MP), 15% in the outer submucous plexus (OSP) and 34.8% in the inner submucous plexus (ISP). In contrast, a distinct increase in the number of ZnT3-LI neurons was observed in the OSP plexus of D group (31.4%), in MP a slight increase was observed (29.3%) and in ISP the number of ZnT3-LI cells was unchanged (33.8%).

The present results demonstrate that prolonged alpha 1 adrenergic antagonist treatment produced changes within ZnT3-LI colonic neurons in pigs and further suggest that ZnT3 may participate in mechanisms of neural control of colonic activities under physiological and pathological conditions. However, the exact role of this transporter molecule, as well as of Zn^{2+} ions in the neural control of distal bowel function remains to be elucidated in detail.

THE DEVELOPMENT OF THE ATLAS AND AXIS IN STAGED HUMAN EMBRYOS

Grzymisławska M, Woźniak W

Department of Anatomy, Poznań University of Medical Sciences, Poznań, Poland

The boundary between the head and neck is at the level between occipital somite 4 and sclerotome 5. Occipital somites 1–4 fuse and form the basioccipital bone and the sclerotomes 5–7 form the central rod from which develop the upper three cervical vertebrae. The central rod was divided by O'Rahilly and Miller into segments X, Y, and Z. The atlas develops from the inferior half of the occipital somite 4 and the upper half of the sclerotome 5. Discrepancies exist as to the development of the upper cervical vertebrae, in particular to the formation of dens of the axis.

The present study was done on human embryos from the collection of the Department of Anatomy of the University of Medical Sciences in Poznań. Embryos were classified according to developmental stages and aged between 32 and 56 days (stages 13–23). All embryos were serially sectioned in 3 planes and stained according to various methods.

In embryos at stage 13 and 14, the somites are subdivided into sclerotomes and dermatomyotomes and the dense and loose zones may be distinguished. During stages 15–17, the upper three occipital sclerotomes fuse and the dense and loose zones in the central rod are still visible. The dens of the axis develops from zones X and Y, and zone Z forms the centrum (future vertebral body) of the axis. Zone X is considered by some authors as the centrum of the atlas and is named the proatlas.

MORPHOLOGICAL EVALUATION OF ORAL MUCOSA COVERING TWO-STAGE INTRAOSSEOUS IMPLANTS IN A HEALING PERIOD

Hemerling M[1], Koczorowski R[1], Brelińska R[2]

[1]*Department of Geriatric Dentistry, Medical University of Poznań, Poznań, Poland*

[2]*Department of Histology and Embryology, Medical University of Poznań, Poznań, Poland*

In modern prosthetic rehabilitation, various types of titanium intraosseous implants are used with increasing frequency. It is possible to restore single missing teeth with dental implants, but they can also be employed as abutments of fixed and removable partial or full dentures. Titanium is known to be a highly biocompatible metal. The lack of metal ion release from the implant surface to the surrounding tissue improves the healing process. However, clinical observations sometimes reveal the presence of periimplant inflammatory processes. The aim of the study was the morphological evaluation of oral mucosa above two-stage intraosseous implants in eight patients. Gingival mucosa biopsies were obtained during surgical uncovering of the intraosseous implant part, at least 16 weeks after implantation procedure. The control material involved gingival mucosa samples isolated before the procedure above the planned osseous bed. The material was fixed in Bouin's solution and embedded in paraffin. Sections were stained by means of haematoxylin and eosin and van Gieson methods. The immunocytochemical ABC technique was used to estimate expressions of Ki-67, cytokeratin 10 and S-100 protein. In all patients, a normal process of implant healing was demonstrated. As compared to the control material, the gingival mucosa after implantation manifested increased numbers of S-100 positive Langerhans cells in the epithelium and lamina propria; moreover, an increase of proliferation in basal and suprabasal epithelial layers was shown. The two layers formed branched invaginations into the lamina propria. Insignificant alterations were manifested in the direct vicinity of the implants: the epithelium contained focal lesions of keratinocyte differentiation (vacuolization, nuclear lesions and the presence of cell nuclei in the most superficial epithelial cells), infiltrates of Ig-negative lymphoid cells and Langerhans cells. In lamina propria, small or even extensive infiltrates of lymphoid and Langerhans cells were seen in the neighbourhood of blood vessels. The cellular composition of the infiltrates in both mucosal layers pointed to induction of the local cell-mediated immune reaction in the process of osteointegration.

THE INFLUENCE OF SOME ENVIRONMENTAL FACTORS ON THE MORPHOFUNCTIONAL DEVELOPMENT OF BOYS

Ignasiak Z, Domaradzki J, Sławińska T

Department of Anthropokinetics, University School of Physical Education, Wrocław, Poland

One of the most important problems for contemporary society is environmental pollution, which is the reason for children's biological development distempers. The most endangered are those areas situated near industrial factories. They are exposed to many dangerous factors devastating soil, water and air and damaging human health. However, some social-economic factors like parental education level can decrease the harmful influence of pollution on the functional traits of organisms.

This work is an attempt at the estimation of the influence of the degree of pollution in living areas and parental education levels on the basic somatic and functional traits of young rural boys.

The data of 239 boys aged 11–15 examined in 1998 were used in this work. Information about Pb and Cd in fall-out published in "Reports about environmental condition" was used to divide children into two groups: living in less and more polluted areas. Both groups were divided into groups with higher and lower levels of parental education. Some basic somatic and functional traits (motor and psychomotor) were measured. We used variance analysis to estimate differentiation between all of the groups of boys.

The results suggest that social-economical factors are more strongly related to the somatic traits and motor abilities than the degree of pollution. The latter is related to the level of psychomotor traits, but higher education can limit the unprofitable influence of the degree of pollution on the functional development of children.

ANALYSIS OF GENE EXPRESSION IN RAT EPIPHYSEAL--ARTICULAR CHONDROCYTES IN MONOLAYER CULTURE

Iwan A, Hyc A, Moskalewski S

Department of Histology and Embryology, Medical University of Warsaw, Warsaw, Poland

Evaluation of expression of genes coding chondrocyte produced extracellular matrix proteins depending on the population doublings.
Chondrocytes isolated from epiphyseal-articular cartilage complex from 4-day old rats were cultured in monolayer for 28 days (9 population doublings). Expressions of mRNA for collagen type I, II, aggrecan, versican and cathepsin B were evaluated by RT-PCR (reverse transcriptase). Changes in expression during culture were measured using the GRAB-T2.0 system.
The expression of the genes was highly time-dependent and changed over the culture time. Collagen type I expression, low in freshly-isolated chondrocytes and at the beginning of the culture, increased after the second population doubling (day 7) and achieved a high level after 4 population doublings (day 12). This high level remained stable until the end of the experiment. Collagen type II expression, very high in freshly-isolated chondrocytes and at the beginning of the culture, decreased slowly to 3 population doublings (day 10). After this time, the decrease of collagen type II mRNA level was considerable. Aggrecan expression was downregulated from 3 population doublings (day 10) to 9 population doublings (day 24). Versican expression, low at the beginning of the culture, increased from the second population doubling (day 7) to the fourth population doubling (day 12). Nevertheless, cathepsin B mRNA levels remained high during the entire culture period. These changes in expression of genes coding extracellular matrix proteins showed that chondrocytes dedifferentiated during monolayer culture. They lost the ability to produce specific cartilage matrix proteins (collagen type II, aggrecan), and simultaneously, showed augmented production of collagen type I and versican. Therefore, chondrocytes became similar to fibroblasts in the monolayer culture. In the future, we are going to try to redifferentiate cells cultivated in monolayer culture into chondrocytes using Matrigel.

THE EXPRESSION OF MELATONIN RECEPTORS MT1 AND MT2 IN NORMAL HUMAN TISSUES

Iżykowska I[1], Dzięgiel P[1], Piotrowska A[1], Podhorska-Okołów M[1], Zabel M[1, 2]

[1]*Department of Histology and Embryology, Wrocław Medical University, Wrocław, Poland*
[2]*Department of Histology and Embryology, Poznań University of Medical Sciences, Poznań, Poland*

Melatonin, the pineal hormone, is secreted from the pineal gland. The specific actions of melatonin are mediated by two subtypes of G-protein-coupled receptors: MT1 and MT2. Hitherto, the data about distribution of MT1 and MT2 receptors in human organs has still been controversial and incomplete.
The aim of the study was to provide immunohistochemical evidence for the localization of MT1 and MT2 melatonin receptors in selected human tissues.
The study was performed on normal tissues of the small intestine, gallbladder and thyroid embedded in paraffin blocks received from the archives of the Department of Histology and Embryology, Wrocław Medical University., Immunohistochemical reactions were performed in paraffin sections of studied tissues by using rabbit polyclonal antibodies directed to MT1 and MT2 receptors. Positive control reaction was performed on the kidney.
Our results showed the presence of melatonin MT1- and MT2-receptors in all examined tissues, albeit with different intensities. The expression of MT1 receptor in all studied tissues was always stronger than the expression of MT2 receptor. MT1 and MT2 immunoreactivity was present in the cell membrane as well as in the cytoplasm of positive cells. The obtained results could suggest the essential role of melatonin receptors in the cell. Additional studies are needed to elucidate the function of MT1 and MT2 receptors in different organs.

COMPARATIVE MORPHOLOGY OF THE TONGUES OF SELECTED SPECIES OF ARTIODACTYLA

Jackowiak H

Department of Animal Anatomy, Agricultural University of Poznań, Poznań, Poland

Studies on the morphology of the tongues of mammals have indicated that the chief factor causing the diversity of lingual papillae are the type of food and ecological conditions. In the Artiodactyls, the tongue, together with the teeth and palate, play an important function during mastication and grinding plant food. So far, microscopic studies of the morphology of the tongue have been conducted on the goat, cattle, buffalo, lesser mouse deer and camel. The aim of the present work was to describe and compare the morphology of the tongue and microstructure of the lingual papillae in the species belonging to the order Artiodactyla.
The study was performed on the tongues of representatives of the families *Suidae, Hippopotamidae, Cervidae, Bovidae*, and *Girraffidae* donated by the Zoological Garden in Poznań. Samples of the apex, body, intermolar prominences and root of the tongue were fixed in neutral formalin and conventionally processed for light and scanning electron microscopic observations.
The characteristic morphological features of the tongue in the studied animals are flat apex and elongated body of the tongue with distinct lingual prominence. We observed anatomical differences in the shape of the apex of the tongue, which show species-specific presence of median sulcus. The elongated body of the tongue is the constant flat part of the tongue covered, similarly to the apex, with short filiform and fungiform papillae. Species-specific features include the shape and size of intermolar prominence. Regarding the diversity of the distribution of the mechanical highly keratinized filiform papillae, the obtained results showed conical papillae and/or lentiform papillae on the surface of the intermolar prominence and the connection of their microstructure with the type of plant food. The distribution and shape of the gustatory vallate papillae on the posterolateral parts of intermolar prominence seem to be specific for particular families of the Artiodactyla, but the number of the vallate papillae is a species-specific feature.

ARCHITECTURE OF THE VASCULATURE IN THE HUMAN GALLBLADDER AS REVEALED BY SCANNING ELECTRON MICROSCOPY

Jackowiak H[1], Godynicki S[1], Ciesielczyk B[2], Lametschwandtner A[3]

[1]*Department of Animal Anatomy, Agricultural University of Poznań, Poznań, Poland*
[2]*Department of Surgery, Raszeja Hospital, Poznań, Poland*
[3]*Department of Organismic Biology, University of Salzburg, Salzburg, Austria*

While the microvascularisation of the wall of the gallbladder of laboratory animals is well studied, work on the vascular system of the human gallbladder were concentrates on its arterial supply, branching modes and variability of the course of the cystic artery, and on blood outflow patterns to the portal system, which are of great importance in clinics. Here we for first time report on the detailed microvascular anatomy of the wall of the human gallbladder using scanning electron microscopy of vascular corrosion casts.

Ten infammed gallbladders with stones were removed either by traditional or laparoscopic surgery were studied. Briefly, the cystic artery was cannulated and the vascular bed of the gallbladder was rinsed free blood with 25 ml heparinized saline (1,000 IU/ml saline). Then the polymerizing resin Mercox® was injected using manual pressure. After hardening of the injected resin gallbladders were macerated in 15% NaOH, rinsed and deep frozen in distilled water, and freeze-dried. Casts were examined with a SEM ZEISS 435 VP.

SEM observations showed two vascular networks within the wall of the human gallbladders, one in the mucosa and one in the subserosa. Branches of the cystic artery divide on the free surface of the gallbladder 1. into arterioles which supply the subserous and muscular layers of the gallbladder and 2. into arterioles which feed the dense subepithelial capillary network of the mucosal folds. Capillaries form also a dense network around the mucosal glands.

The venous blood from the folds of the mucosa drains into the vertically collecting venules into a horizontally extending plexus venosus, located on the basis of mucosal folds. At the subserosal level a well-developed venous plexus is present from which blood is collected via 4–7 veins towards the hepatic parenchyma.

In specimens with acute *cholecystitis* capillaries locally revealed vascular sprouts indicating that angiogenesis takes place in the pathologically changed mucosa.

SCANNING ELECTRON MICROSCOPIC STUDY OF THE LINGUAL PAPILLAE OF THE EGYPTIAN SPINY MOUSE (*ACOMYS CAHIRINUS, DESMAREST*)

Jackowiak H[1], Godynicki S[1], Szczurkowski A[2], Kuder T[2]

[1]*Department of Animal Anatomy, Agricultural University of Poznań, Poznań, Poland*

[2]*Department of Comparative Anatomy, Institute of Biology, Świętokrzyski University, Kielce, Poland*

The aim of this scanning electron microscopic study was to describe the morphology and microstructure of the lingual papillae on the surface of the tongue in the Egyptian spiny mouse.

For the study, 4 tongues fixed in 5% formalin were used. The tissues were dehydrated in a series of ethanol and acetone, critical point dried and sputtered with gold. The samples were observed with a SEM Zeiss 435 VP at accelerating voltage 15–20 kV

The characteristic morphological features in spiny mouse area are median sulcus on the broad apex of the tongue, narrow body of the tongue and lingual prominence. The SEM study allowed the description of four types of lingual papillae on the dorsal surface of the mucosa. Lingual papillae are also distributed on the antero-ventral surface of the borders of the tongue. The mechanical papillae are represented only by filiform papillae. Dependant on the area of the tongue, three morphological subtypes of filiform papillae were observed. The filiform papillae on the apex and body of the tongue have one keratinized process with an oval or sharpened tip, whereas the filiform papillae on the posterior part of the lingual prominence have a bifid keratinized process.

The gustatory papillae are represented by three types of papillae. Most numerous are flat, oval fungiform papillae. On the root of the tongue, in the midline of the tongue, only one rounded vallate papillae with distinct border was observed. The foliate papillae are situated posterolateral in front of the palatolaryngeal folds and consist of three or four leaflets.

The surface of the posterior part of the root of the tongue, behind the vallate papilla, is flat.

The results showed a similarity to the structure of the tongue in rodent species belonging to Muridae.

PATTERN OF DISTRIBUTION OF THE LINGUAL PAPILLAE IN FRUGIVOROUS MAMMALS; LM AND SEM STUDY

Jackowiak H, Trzcielińska J, Godynicki S

Department of Animal Anatomy, Agricultural University of Poznań, Poznań, Poland

Important factors affecting the structure of the lingual mucosa are the type of ingestion of food, the method of its grinding in the oral cavity and the method of its passage to further segments of the alimentary tract. In the present study, the aim was to describe the morphology of the tongue in two frugivorous species of mammals i.e. small marsupial feathertail glider (*Acrobates pygmaeus*) and in the Egyptian fruit bat (*Rousettus aegyptiacus*) and examine the distribution and microstructure of lingual papillae on the dorsal surface of the tongue in view of the adaptation to its diet.

The study was conducted on 7 tongues of adult feathertail gliders and on 6 tongues of adult Egyptian fruit bats donated by the Zoological Garden in Poznań (Poland). The tongues were fixed in 10 % formalin and routinely processed for LM and SEM observations.

The results of the study on the feathertail glider show that the unique arrangement of lingual mechanical papillae is strongly adapted to the effective holding of parts of fruits and the collection of pollen and nectar. The arrangement, shape and size of filiform papillae and the direction of their keratinized processes change depending on the part of the tongue, so that the surface of the apex and the body of the tongue resembles a kind of special brush. SEM observations in both species showed that in the anterior part of the tongue filiform papillae and their processes are reflected posteriorly, as in other mammals. Further, at ¾ distance from the apex of the tongue, these elongated papillae form two groups of filiform papillae on the left and right side of the tongue located opposite one another. On the root of the tongue, medially located filiform papillae are tilted posteriorly, which helps to collect the pieces of food and pass them in the median line of the tongue to the pharynx.

The appearance of such an arrangement of mechanical papillae in taxonomically different groups of animals indicates their close adaptation and efficiency in the uptake of semi-liquid food.

LOCALIZATION OF ROS-GC1 TRANSDUCTION MACHINERY IN SPERMATOZOA

Jankowska A, Burczyńska B, Warchoł JB

Department of Cell Biology, University of Medical Sciences, Poznań, Poland

In sperm from vertebrates as well as invertebrates, several cellular processes including capacitation and acrosomal reactivity are regulated by cyclic nucleotides and calcium ions. Both calcium and cyclic nucleotides play a crucial role during various stages of fertilization. Recently we showed the presence of Ca^{2+}-modulated membrane guanylate cyclase transduction machinery in bovine testes. The machinery is both inhibited and stimulated by free Ca^{2+} levels. The Ca^{2+} sensor component of the inhibitory mode of the machinery is GCAP1 and for the stimulatory mode is S100B. Guided by our previous study demonstrating that ROS-GC1 transduction machinery is present, especially in spermatogenic cells, we questioned if a guanylate cyclase signal transudation system, regulated by intracellular Ca^{2+}, is also present in spermatozoa.

Immunohistochemistry methods were used to show ROS-GC1 transduction machinery. The enzyme was localized in the cell membrane of the apical and equatorial segments of the acrosomal cap, postacrosomal region as well as in the middle piece of the bovine spermatozoa tail. Both Ca^{2+} sensor proteins (S100B and GCAP1) were detected in the apical part and principal segment of the acrosomal cap. Additionally,

GCAP1 was present both in the middle-, principle- and end-piece of the spermatozoa tail.
This study documents, for the first time, the functional identity of a Ca^{2+} modulated membrane guanylate cyclase transduction machinery in bovine spermatozoa. The transduction component is the guanylate cyclase ROS-GC1. The enzyme coexists with its two Ca^{2+} dependent modulators, GCAP1 and S100B. These proteins, by binding to the specific domains of the cyclase, can inhibit or stimulate ROS-GC1 activity. In this manner, Ca^{2+} pulses precisely regulate the levels of cyclic GMP generated in the spermatozoa.

THE ESTIMATION OF THE SAPHENO-POPLITEAL JUNCTION IN THE INTRAOPERATIVE VIEW AND DURING DOPPLER ULTRASOUND EXAMINATIONS IN PATIENTS WITH CHRONIC VEIN DISEASE

Janowski K, Topol M
Department of Angiology, Chair of Anatomy MU of Łódź, Łódź, Poland

The aim of the study was the estimation of the morphology of the saphe-no-popliteal junction (SPJ) during Doppler ultrasound examinations and varicose vein surgery.
The estimation of SPJ was based on the preoperative Colour Doppler ultrasound examinations and on the intraoperative view during varicose vein surgery procedure with subligation of SPJ. The patients were selected during preoperative ultrasound examinations. Patients with insufficient valve in the SPJ in which varicose veins occurred, were taken to the study. Our material consisted of 42 patients, both gender, aged between 22 and 83. Patients were qualified to the operation according to the physical examination and Doppler ultrasound examination.
During Doppler ultrasound examination, we took the diameter of the SPJ, the position of the SPJ above the knee joint and the presence of the femoro-crural vein (the so-called Giacomini vein).
The above mentioned parameters were estimated during the operations. We compared the parameters from the Doppler ultrasound examinations and intraoperative views and estimated the correspondence between them. We described two types of SPJ depending on the presence of the Giacomini vein. Type I (type "T") — with the Giacomini vein and type II — without it.
The position of the SPJ varied between 2 and 8 cm above the knee joint; in most cases, 4 cm superior to the knee joint.
The intraoperative views and ultrasound views were the same in about 75% of cases.
Type II without the Giacomini vein occurrence was the most frequent. The SPJ occurred on the level of 4 cm superior to the knee joint in most cases. Doppler ultrasound examination was very helpful in 75% of cases in the estimation of the SPJ.

THE FREQUENCY OF CAVUM SEPTI PELLUCIDI ON CT SCAN IMAGES

Jaworek JK[1, 2], Chrzan R[2], Mróz I[1], Zawiliński J[1], Zawilińska-Sienkiewicz J[1], Nowak W[1], Urbanik A[2]

[1]*Department of Anatomy, Collegium Medicum, Jagiellonian University, Cracow, Poland*
[2]*Department of Radiology, Collegium Medicum, Jagiellonian University, Cracow, Poland*

The cavum septi pellucidi (CSP) is a fluid-filled cavity located between the membranes of the septum pellucidum. Persistent CSP is a congenital anomaly of the midline structures of the adult human brain. The CSP is triangular and demarcated anteriorly by the genu of corpus callosum, posteriorly by the corpus and columns of the fornix, superiorly by the body of the corpus callosum and inferiorly by the rostrum of the corpus callosum.
The reported incidence of CSP in the normal adult population varies from 0.10% to 85%. The wide variance in reported prevalence may be due to several factors, including the method of detection (postmortem/pneumoencephalography/computed tomography/magnetic resonance imaging), definition of the CSP (based on its size) and inhomogeneity of the populations studied. The aim of this study was to assess the prevalence of CSP in the adult Polish subpopulation using computed tomography.
All brain CT exams performed at the Radiology Department CM UJ during 2000–2006 were reviewed for the presence of a persistent CSP. CT examinations were performed using a spiral CT scanner (Siemens Somatom Sensation 10). Secondary coronal and sagittal MPRs (multiplanar reconstructions) were then generated from the original axial slices.
Out of the 25,277 brains that were examined, a cavum septi pellucidi was present only in 353 brains, an incidence of 1.40%.

THE FREQUENCY OF CAVUM VERGAE ON CT SCAN IMAGES

Jaworek JK[1, 2], Chrzan R[2], Mróz I[1], Zawiliński J[1], Zawilińska-Sienkiewicz J[1], Nowak W[1], Urbanik A[2]

[1]*Department of Anatomy, Collegium Medicum, Jagiellonian University, Cracow, Poland*
[2]*Department of Radiology, Collegium Medicum, Jagiellonian University, Cracow, Poland*

Persistent cavum vergae (CV, cavum psalterii) is a brain midline cystic abnormality. The CV is bound superiorly by the body of the corpus callosum, inferiorly by the hippocampal commissure, laterally by the crus of the fornix, and posteriorly by the splenium of the corpus callosum. It can be a posterior extension of the cavum septi pellucidi (CSP) and it can be found with the CSP.
The reported incidence of CV in the normal adult population varies from 1.9% to 39%. The aim of this study was to assess the prevalence of CV in the adult Polish subpopulation using the method of computed tomography.
All brain CT exams performed at the Radiology Department CM UJ during 2000–2006 were reviewed for the presence of persistent CV. CT examinations were performed using a spiral CT scanner (Siemens Somatom Sensation 10). Secondary coronal and sagittal MPRs (multiplanar reconstructions) were then generated from original axial slices.
Out of the 25,277 brains that were examined, a cavum Vergae was present only in 197 brains, an incidence of 0.78%.

THE ARTERIA LUSORIA IN ADULT PATIENTS WITH A LEFT-SIDED AORTIC ARCH IN MULTI-SLICE COMPUTED TOMOGRAPHY: A REPORT OF THREE CASES

Jaworek JK[1, 2], Chrzan R[2], Szafirska M[2], Nowak W[1], Urbanik A[2]

[1]*Department of Anatomy, Collegium Medicum, Jagiellonian University, Cracow, Poland*
[2]*Department of Radiology, Collegium Medicum, Jagiellonian University, Cracow, Poland*

The aberrant right subclavian artery (ARSA), also known as the arteria lusoria, is the most common anomaly of the aortic arch, with a reported prevalence ranging from 0.4% to 2%. In this anomaly, the right subclavian artery

does not arise from the brachiocephalic truncus but instead develops as a fourth branch of the aortic arch that is distal to the left subclavian artery. In most cases, ARSA runs posterior to the oesophagus (80%), but it may run between the trachea and oesophagus (18%) or in front of trachea (4%).
Most adult patients are asymptomatic; however, this anomaly may give rise to the conditions known as dysphagia lusoria or dyspnoea lusoria.
We report three cases of right subclavian artery, which were diagnosed by multi-slice computed tomography (CT). In one of the three cases, CT angiography (angio-CT) was performed. No patient had any symptoms attributable to arteria lusoria — in all cases, ARSA was an incidental X-ray finding.

THE SEPTUM OF SPHENOID SINUSES — BONY OR MEMBRANOUS?

Jaworek JK[1,2], Chrzan R[2], Sztuk S[2], Jaworek RT[3], Nowak W[1], Urbanik A[2]

[1]*Department of Anatomy, Collegium Medicum, Jagiellonian University, Cracow, Poland*
[2]*Department of Radiology, Collegium Medicum, Jagiellonian University, Cracow, Poland*
[3]*Department of Microbiology, Faculty of Biochemistry, Biophysics and Biotechnology, Jagiellonian University, Cracow, Poland*

The aim of this study was to assess the presence of complete or incomplete bony main septum of sphenoid sinuses in the adult Polish subpopulation.
A retrospective study of 207 patients (101 male, 106 female) referred from the Otorhinolaryngology Department to the Radiology Department CMUJ for CT examination of the paranasal sinuses was performed. Since the aim of this study was to evaluate anatomical variations of SS septation, only patients with no SS diseases were included. All the subjects were Polish, with a mean age of 44 years, ranging from 18 to 84 years.
CT examinations were performed using a spiral multirow CT scanner (Siemens Somatom Sensation 10) with the following parameters: the extent fully covering all paranasal sinuses, detector configuration 10 × 0.75 mm, feed 4.1 mm, reconstruction thickness 1 mm, reconstruction increment 0.7 mm and kernel H60s for bone structures, or reconstruction thickness 4 mm, reconstruction increment 4 mm and kernel H31s for soft tissue structures. Secondary coronal and sagittal MPRs (multiplanar reconstructions) were then generated from original axial slices.
No intravenous contrast media was required. Siemens CARE Dose 4D option was used to reduce maximally the X-ray dose.
In every case, we measured the total height of the main septum parts with attenuation below the following threshold values: –200 HU, –100 HU, 0 HU, 100 HU and 200 HU. A complete main septum had no parts with attenuation values below 200 HU. An incomplete main septum had parts with lower attenuation values, reaching even –200 HU.
The main septum was completely bony in 57% patients (55% males and 59% females). In 43% of patients, the MS was partially membranous.

THE TOTAL NUMBER OF SEPTA WITHIN SPHENOID SINUSES

Jaworek JK[1,2], Chrzan R[2], Sztuk S[2], Jaworek RT[3], Nowak W[1], Urbanik A[2]

[1]*Department of Anatomy, Collegium Medicum, Jagiellonian University, Cracow, Poland*
[2]*Department of Radiology, Collegium Medicum, Jagiellonian University, Cracow, Poland*
[3]*Department of Microbiology, Faculty of Biochemistry, Biophysics and Biotechnology, Jagiellonian University, Cracow, Poland*

The aim of this study was to assess the septation of the sphenoid sinuses in the adult Polish subpopulation.
A retrospective study of 207 patients (101 male, 106 female) referred from the Otorhinolaryngology Department to the Radiology Department CMUJ for CT examination of the paranasal sinuses was performed. Since the aim of this study was to evaluate anatomical variations of SS septation, only patients with no SS diseases were included. All the subjects were Polish, with a mean age of 44 years, ranging from 18 to 84 years.
CT examinations were performed using a spiral multirow CT scanner (Siemens Somatom Sensation 10) with the following parameters: the extent fully covering all paranasal sinuses, detector configuration 10 × 0.75 mm, feed 4.1 mm, reconstruction thickness 1 mm, reconstruction increment 0.7 mm and kernel H60s for bone structures, or reconstruction thickness 4mm, reconstruction increment 4 mm and kernel H31s for soft tissue structures. Secondary coronal and sagittal MPRs (multiplanar reconstructions) were then generated from original axial slices. No intravenous contrast media was required. Siemens CARE Dose 4D option was used to reduce maximally the X-ray dose.
The assessment of the CT scans revealed the presence of at least one septum in all cases (100%). In 42% of patients, there was only one septum (MS), which divided SS in two sinuses. In 58% of patients, we found more then one septum (AS) in the posterior part of the SS. Usually there was only one AS (33%), but the presence of two AS's was frequent (21%). It was a very unusual to find three AS's (4%). We found no SS with more than three accessory septa.

ANASTOMOSES BETWEEN THE TESTICULAR ARTERY AND PAMPINIFORM PLEXUS IN THE HUMAN SPERMATIC CORD

Jędrzejewski KS, Okraszewska E

Department of Anatomy, Medical University of Łódź, Łódź, Poland

The reason for the interest in the presence of arterio-venous anastomoses in human spermatic cords was the previously experimentally proved flow of blood passing over the intratesticular vessels. The amount of the blood flowing through the testicles is one of the most important factors in spermatogenesis as well as in endocrine function. Most of the available studies were based on animal material. Another encouraging factor for the following study is the increasing infertility in men.
A total of 50 human testicles were studied. The testicle, epididymis and spermatic cord were removed in one piece. The testicular artery was canulated, and the testis together with the spermatic cord were filled with a casting medium (Mercox). After polymerisation of the resin, the tissue was digested and corrosion casts prepared for scanning electron microscope examination.
Each of the examined specimens contained the testicular artery tightly surrounded by pampiniform plexus. The winding course of the testicular artery, as well as circular imprints of smooth muscles, were noticed. We did not find any direct arterio-venous anastomoses between the testicular artery and the pampiniform plexus veins. In every specimen, we observed a thick net of capillary vessels placed in the tunica media and tunica adventitia of the testicular artery — a kind of "vasa vasorum". SEM pictures clearly show that this vessel net is connected with the testicular artery, as well as with the pampiniform plexus. This leads to the conclusion that there are numerous, indirect connections between the testicular artery and pampiniform plexus. It seems clear that for the spermatogenesis as well as for endocrine function of the testicles, proper blood supply is one of the main factors. The "vasa vasorum" are actually arterio-venous anastomoses mediating in direct flow between the testicular artery and pampiniform plexus. The circular smooth muscles might act as the functional contractors of the testicular artery regulating the flow through the testicle. To recapitulate — the amount of blood reaching the testicle depends on many factors and the angioarchitecture of the spermatic cord (especially arterio-venous anastomoses) is only one of them.

NEUROCHEMICAL CHARACTERIZATION OF PARACERVICAL GANGLION (PCG) NEURONS SUPPLYING THE PORCINE URINARY BLADDER — A PRELIMINARY STUDY

Józefowicz O, Bossowska A, Jurkowska M, Wojtkiewicz J, Majewski M

Division of Clinical Physiology, Department of Functional Morphology, Faculty of Veterinary Medicine, University of Warmia and Mazury, Olsztyn, Poland

The PCG is thought to be one of the most important parasympathetic coordination centres of the peripheral nervous system that controls the function of the abdominal and pelvic viscera, including the urinary bladder. While the distribution pattern and chemical coding of PCG neurons projecting to the urinary bladder of animals from various species is relatively well documented, data on the distribution and chemical characterization of parasympathetic neurons located in the PCG and supplying the porcine urinary bladder are still, in spite of the conducted research, very fragmentary. Therefore, this study was aimed at disclosing the origin and neurochemical phenotypes of PCG neurons projecting to the urinary bladder in pigs. The urinary bladder wall was injected with retrograde tracer Fast Blue (FB) in three juvenile female pigs. After three weeks, the PCG were collected from all animals and processed for single and double-immunofluorescence labelling on 10-μm-thick cryostat sections using combinations of primary antisera raised in different species and directed towards choline acetyltransferase (ChAT), tyrosine hydroxylase (TH), neuropeptide Y (NPY), vasoactive intestinal polypeptide (VIP), pituitary adenylate activating polypeptide (PACAP), somatostatin (SOM), leucine enkephalin (LEU) and nitric oxide synthase (NOS). The vast majority of FB+ neurons contained ChAT and/or NPY (about 80% and 75%, respectively). A smaller number of FB-labelled cells contained NOS, TH, SOM and VIP (about 50%, 30%, 20% and 15%, respectively). PACAP and LEU were absent from FB+ PCG neurons, but the majority of these cells were supplied by numerous PACAP-immunoreactive (IR) and LEU-IR terminals. Some of them were also surrounded with nerve fibres containing VIP and SOM, but only single cells were supplying with ChAT-, TH- and NPY-IR nerve terminals. Thus, the present study demonstrated that the pelvic projection to the urinary bladder is complex and consists of both sympathetic (minor) and parasympathetic (major) components.

EXPRESSION OF ACTIVE ZONE PROTEINS IN RAT CEREBELLUM DURING DEVELOPMENT

Juranek J[1], Całka J[1], Mukherjee K[2], Ahnert-Hilger G[3], Li J[4]

[1]*Department of Functional Morphology, Faculty of Veterinary Medicine, University of Warmia and Mazury, Olsztyn, Poland*
[2]*Southwestern Medical Centre, University of Texas, Dallas, USA*
[3]*Charité-Universitätsmedizin, Humboldt University, Berlin, Germany*
[4]*Wallenberg Neuroscience Centre, Lund University, Sweden*

The study was designed to reveal differences in expression patterns and subcellular localization of synaptic active zone (AZ) proteins -Piccolo, Bassoon, Munc13, Rim1α, Liprinα3 and ELKS2 in rat cerebellum during development. The experimental procedure, performed in accordance with the Local Ethical Committee guidelines for animal care, included: immunofluorescent labelling of rat cerebellum dissected on embryonic days 15, 19 and postnatal days (PD) 1, 5, 10, 15 and 20 with antibodies against AZ proteins and synaptic and Purkinje cell markers, Synaptophysin and Calbindin, respectively, followed by confocal microscope imaging and quantitative analysis of the data and SDS-PAGE electrophoresis and immunoblotting of homogenates and subcellular fractions of PD20 rat cerebellum. The obtained immunofluorescence results revealed a differential distribution of active zone proteins in the developing cerebellum at given time points. The most abundant protein was Liprin, followed by Munc13 and subsequently by Piccolo, Bassoon, Rim and ELKS. The most significant difference between AZ proteins in number of labelled puncta was observed on PD15 and the least significant difference was observed on PD5. On PD5 and PD10, significant correlations in expression pattern were noted for Bassoon and RIM and for ELKS and RIM. Immunoblotting studies revealed that all the studied proteins are present in cerebellar homogenates and subcellular organellar fractions, but, except for Liprin, they are not present in cytosol. The given results show that AZ protein expression and subcellular localization in rat cerebellum during development are spatially and temporally diverse and depend on the protein and developmental stage of the studied tissue.

MORPHOLOGICAL ANALYSIS OF MANDIBULAR GLANDS IN THE PRENATAL PERIOD OF THE PIG

Juszczyk M[1], Pospieszny N[1], Pospieszna J[2]

[1]*Department of Anatomy and Histology, Faculty of Veterinary Medicine, Wrocław University of Environmental and Life Sciences, Wrocław, Poland*
[2]*Institute of Basic Electrotechnic and Technology, Wrocław University of Technology, Wrocław, Poland*

The morphology and the development of the mandibular salivary gland in the prenatal period of the pig has not yet been explained completely [Latshaw WK (1987) Veterinary development of anatomy. A clinically oriented approach. BC Decker Inc., Philadelphia-Toronto: 90–93. Marrable AW (1971) The embryonic pig. A chronological account. Pitman Medica: 17–98. Pospieszny N (1993) Morfologia i rozwój części pozaczaszkowej nerwu błędnego świni okresie płodowym. Rozprawa habilitacyjna. Wydawnictwo Akademii Rolniczej, Wrocław: 5–64, 122]. The purpose of the study was a morphological and histological analysis of the mandibular gland in the prenatal period of the pig.

One hundred and nineteen foetuses aged from 36 to 120 days were involved in this study. The foetuses were divided into six age groups. The morphological characteristics, vascularisation and innervation of the mandibular gland were investigated by morphological, radiological and histological methods. The differences between the examined parameters were analysed using the Anova test , Kruskal-Wallis median test and the coefficient of rang Spearman's correlation. A p value < 0.05 was considered significant.

The morphology and development of the mandibular gland is significantly correlated with the development of neighbouring organs. The most intensive growth of the mandibular gland was observed in the $10^{th} - 11^{th}$ week of prenatal life, i. e. in the isometric phase of growth. In the course of pregnancy, the connective tissue of the gland diminishes, while the secretory structure and excretory ducts of the gland proliferate. Histological analysis revealed that on the 36^{th} day of life the secretory structures and the excretory ducts are already visible, on the 63^{rd} day, the secretory follicles are grouped into salivary lobules surrounded by a network of capillaries. On the 112^{th} day of life, the mandibular gland is completely developed. In relation to the angle of the mandible, the gland moves centripetally and cranially. The position of the foetus in the uterus and its sex has no influence on the morphology and development of the mandibular gland.

CELLULAR EXPRESSION OF β-CATENIN AND PROLIFERATIVE ACTIVITY IN CHRONIC, LONG LASTING HEPATITIS C VIRUS (HCV) INFECTION

Kasprzak A[1], Adamek A[2], Biczysko W[3], Przybyszewska W[1], Olejniczak K[1], Juszczyk J[2], Zabel M[1,4]

[1]*Department of Histology and Embryology, Medical University of Poznań, Poznań, Poland*
[2]*Department of Infectious Diseases, Medical University of Poznan, Poznań, Poland*

[3]*Department of Clinical Pathomorphology, Medical University of Poznań, Poznań, Poland*
[4]*Department of Histology and Embryology, Medical University of Wrocław, Wrocław, Poland*

Catenins represent cytoplasmatic proteins exhibiting a strong affinity to cadherins. β-catenin is thought to transactivate mostly unknown target genes, which may stimulate cell proliferation or inhibit apoptosis. Aberrations of β-catenin are frequent in the course of hepatocellular carcinoma and may promote its development in the course of chronic hepatitis, including chronic hepatitis C. In the course of liver regeneration following partial hepatectomy, the protein undergoes translocation to the cell nucleus. It remains unclear to what extent the cellular expression of β-catenin *in vivo* represents an index of the progression of the disease and of proliferative activity in the liver in chronic hepatitis C. The aim of the studies included the detection of β-catenin in liver biopsies from adults (n = 21) with chronic, long-lasting hepatitis C as related to hepatocyte proliferative activity.

The immunocytochemical ABC (avidin biotin-peroxidase complex) technique was applied, alone or associated with the ImmunoMax technique. Results of the immunocytochemical tests were compared to histological alterations in liver biopsies (*grading*, *staging*, steatosis), proliferation index and with selected clinical data concerning the patients.

In all chronically HCV-infected patients, cytoplasmic and membrane localization of β-catenin dominated over nuclear localization. No direct relationship could be demonstrated between expressions of β-catenin and of Ki-67 antigen. Moreover, no correlation could be demonstrated between cellular expression of β-catenin and *grading/staging,* steatosis, alanine aminotransferase (ALT), serum concentration of HCV RNA and alpha-fetoprotein (AFP). Our results suggest that the total tissue expression of β-catenin in the liver does not correlate with proliferative activity of HCV-infected hepatocytes.

CELLULAR EXPRESSION OF HEPATITIS C VIRUS (HCV) PROTEINS (C, NS3, NS5A) DOES NOT CORRELATE WITH KI-67 ANTIGEN EXPRESSION

Kasprzak A[1], Adamek A[2], Biczysko W[3], Seidel J[1], Przybyszewska W[1], Olejniczak K[1], Juszczyk J[2], Zabel M[1]

[1]*Department of Histology and Embryology, Medical University of Poznań, Poznań, Poland*
[2]*Department of Infectious Diseases, Medical University of Poznań, Poznań, Poland*
[3]*Department of Clinical Pathomorphology, Medical University of Poznań, Poznań, Poland*

The detection and subcellular localization of three HCV proteins (core, NS3 and NS5A) in liver biopsies from adults with chronic long-lasting hepatitis C as related to hepatocyte proliferative activity and selected histological and clinical data.

The immunocytochemical ABC (avidin-biotin peroxidase complex) associated with the ImmunoMax technique was applied in liver biopsies from adult patients with chronic hepatitis C. Commercially available monoclonal antibodies were used. Semiquantitative scoring of the tissue protein expression were compared to grading and staging of liver biopsies, proliferation index (Ki-67 antigen expression) and with selected clinical data.

A significantly higher expression of NS3 protein was noted, as compared to expressions of NS5A and C proteins. In all the patients, cytoplasmic localization of all proteins dominated over nuclear localization ($p < 0.05$). Immunoelectron microscopy showed that all three proteins were located along the membranes of the endoplasmic reticulum (ER) and in its cisternae, in mitochondria, perinuclear region and occasionally in the cell nucleus. No direct relationship could be demonstrated between expressions of HCV proteins and of Ki-67 antigen. Moreover, no correlations could be demonstrated between cellular expressions of any HCV protein on one hand and inflammatory activity (grading) or staging, alanine transaminase (ALT), serum level of HCV RNA or alpha-fetoprotein (AFP) on the other. However, positive correlations were disclosed between the proliferative activity of hepatocytes and the patient's age, grading and staging. Advanced hepatic fibrosis also correlated with serum levels of AFP. The studies indicate that in HCV infection grading and staging, proliferative activity of hepatocytes and serum AFP level represent more valuable indices of the disease progress than those provided by cellular expression of three potentially oncogenic HCV proteins *in vivo*.

CHARACTERISATION OF INTRAVENTRICULAR HAEMORRHAGES IN THE FOETAL PERIOD

Kędzia A[1], Glonek M[2], Derkowski W[3]

[1]*Department of Normal Anatomy, Medical University of Wrocław, Wrocław, Poland*
[2]*Neurological Department, State Neuropsychiatric Hospital, Opole, Poland*
[3]*Neurological Outpatient Clinic and Neurophysiological Laboratory, Kluczbork, Poland*

The aim of our study was to describe intraventricular and periventricular haemorrhages during the 1st and 2nd trimesters of foetal life using computer image analysis systems and to compare the findings with results obtained by ultrasound imaging or MRI. Our material consisted of 75 foetuses from spontaneous abortions, 5.4–26 cm crown-rump length (10–27 hbd). In 10 cases, intra- and periventricular haemorrhages were found. The methods included: anthropological methods (crown-rump measurements, head and thorax dimensions), preparative methods (craniotomy and brain sections), Pickworth method and computer image analysis (video camera and computer acquisition and image analysis systems: ELF v 4.62, GIMP 2.0 and Scion for Windows 98). In our material, we mainly observed typical development of the supratentorial ventricular system. Lateral ventricles appeared during the hemisphere rotation process: first frontal and temporal horns and later, from the 11th hbd, occipital horns. From the 16th hbd, Magendi and Luschki foramina appeared. There is a ventricular triangle between the temporal and occipital horn of the lateral ventricle, and its width is almost constant during the foetal period - not more than 10 mm. The width of the 3rd ventricle did not exceed 3.5 mm. These measurements correlate well with foetal ultrasound findings. The characterisation of intra- and periventricular haemorrhages in our material has been illustrated with digital images of foetal brains; computer image analysis allowed measurements to be taken with accuracy to a single pixel. We used classification of intra- and periventricular haemorrhages to 4 stages: 1st — to germinal matrix (or subependymal region), 2nd — with extension to lateral ventricles without ventriculomegaly, 3rd — with extension to lateral ventricles with ventriculomegaly and 4th — intraparenchymal haemorrhage. In 55 foetuses, horizontal sections of the brain were undertaken. In 47 cases, the ventricular system was exposed; in 2 cases large defects of CNS (meningoencephalocele and anencephalia) appeared and in 6 cases severe damage did not allow the evaluation of the ventricular system. In 17 foetuses, there were no macroscopic abnormalities in the brain hemispheres. In 30 foetuses, abnormalities of brain hemispheres appeared: 13 cases of leukomalacia, 10 intra- and periventricular haemorrhages, 5 cases of ventriculomegaly, 1 case of colpocephaly and 1 case of blood vessel malformation. Our studies showed that the evaluation of brain ventricles shape and symmetry during prenatal period has practical significance. We noticed that the frontal horns often had a triangular shape with the base of the triangle directed outward to the front in intraventricular haemorrhages. The frontal horns were less enlarged and the significant asymmetry was observed more frequently in intraventricular haemorrhages than in other cases of ventriculomegaly. The shape of the

ventricular system, especially the frontal horns, is important in the diagnostics of foetal CNS. Computer image analysis systems allow foetal brains to be described in physiological and pathological conditions with a high degree of accuracy — this is very useful when comparing anatomical findings with ultrasound findings and fast MRI.

RECIPROCALITY OF OUTFLOW OF VEIN BLOOD FROM THE BRAIN DURING THE FOETAL AND ADULT PERIODS

Kędzia A[1], Kędzia E[2], Kędzia W[3]

[1]*Department of Normal Anatomy, Medical University of Wrocław, Wrocław, Poland*
[2]*Department and Clinic of Anaesthesiology and Intensive Therapy, Medical Academy of Wrocław, Wrocław, Poland*
[3]*Department of Internal and Occupational Diseases, Medical University of Wrocław, Wrocław, Poland*

The paper is aimed at the evaluation of the reciprocality of the outflow of vein blood i.e. monitoring inter relations and balancing overlap of separate vein systems. This phenomenon has been observed in sinuses durae matrix as well as the overlapping of two vein regions - surface and deep ones. Reciprocality comprises mainly large vessel truncus but not microangioarchitecture. Examinations were carried out for 200 foetuses and 100 adults. This material allowed exact investigation of changes related to age. The following techniques were applied: anthropological methods, filling of vessels with contrasts, the Pickworth method and computer image analysis in incompatible systems: Imtron 2000, Scion for Windows 98 and the Krefft method. Overbalance, development and regression of overbalance were observed during the foetal period. The foetal period included two characteristic sinuses: tentorium and occipitales. The quantitative analysis of vein blood outflow from the brain during foetal and adult periods has been carried out according to the Anna Krefft method. The level of vein blood outflow has been indicated by the synthetic variable "Z". Three various types of vessel systems were distinguished in adults: foetal, intermediate and adult. The foetal type maintained the most elements from the foetal period of life; it had a low outflow level indicated by the synthetic variable "Z" (due to the Krefft method) with the presence of lattice forms. The adult type had well-developed vessels, especially anastomoses veins, and a high outflow level corresponding to values of "Z". Spearman found the higher correlation factor range for foetuses: 0.83 compared to adults 0.45, which suggests that hemisphere cerebri are more correlated during the foetal period than in the case of adults. Persons of adult age were characterized quantities named weights due to the absence of important correlation of features. For the left hemisphere, the central surface vein plays a more important role — value of weight (from –0.2025 to 8) left, (from –0.1206 to 8) right, anastomoses upper vein — (from –0.2045 to 6) left, right (from –0.1042 to 6). In the basis cerebri, the vena cerebri profunda medii has the most important influence on outflow of vein blood with higher values of the left side (from –0.5357 to 1), right (from 0.3726 to 1), whereas vena pontis and vena cerebri posterior were more important for the right side.

APOLLONIAN CIRCLES IN FOSSA CRANII POSTERIOR AND FLOW OF LIQUOR CEREBROSPINALIS

Kędzia A[1], Rybaczuk M[2], Andrzejak R[3], Kędzia W[3]

[1]*Department of Normal Anatomy, Medical University of Wrocław, Wrocław, Poland*
[2]*Division of Continual Media Mechanics, Institute of Materials Science and Applied Mechanics, Wrocław University of Technology, Wrocław, Poland*
[3]*Department of Internal and Occupational Diseases, Medical University of Wrocław, Wrocław, Poland*

The paper aimed at modelling the observed structures in terms of Apollonian-like circles. Such an approach is missing in current literature. These special structures of arachnoids were observed in fossa cranii posterior and they have a circular form. The examined material comprised 100 sagittal and horizontal cross sections of heads of foetuses from 4 to 7 months of foetal life. The preparations were cut down with the help of a special device with a self-sharpening blade and an electric motor. This allows ideal flat cuts. Photos of foetuses were acquired with the help of a digital camera and measured according to the special options in the Scion for Windows 98 system. Cross-sections have the form of tangent circles with various radii. The above constructions fill the area situated beyond the fossa cranial posterior. It lies below the cerebellum. The corresponding mathematical model allowing the determination and estimation of the mechanical properties has been elaborated. Systems of the Apollonian circle type are characterised with the power dependence describing the number of circles with radii greater than the given radius R. Then the number of circles with radii between R and R+dR will be given as a derivative of the basic characteristic. The model of flow employed the three-dimensional analogue of the Apollonian circles. The cascade model of flow has been proposed. The balance equation must be fulfilled when liquid flows from the domain with radius r into area with radius r' ($r > r'$), which constitutes correspondence between velocity of flow. Simultaneously, the Bernoulli equation entails shifts of pressure due to flow velocity. We assume laminar flow with constant density. In this case, energy dissipation from viscosity will be proportional to the area of the wall in each cross-section of the Apollonian circle-like structure. When discussing layer-cross-sections with equal thickness, it is easy to find that the damping corresponds to the same basic power dependence with the same power exponent (differentiating lowers the exponent by one and multiplication by length of the perimeter increases the exponent by 1). This is true in the case of the approximate model with point contacts between circles. However, if the contact length remains proportional to the radius of the circles (holes between and in circles) then the only modification reduces itself to the pre-factor but without changes of power exponent. Another modification of damping may follow from deformations of the described structure. In the last case, the changes of contact areas (in the three-dimensional case) may be not proportional to the radii. The model proposed in this paper neglects all such effects.

FRACTAL ANALYSIS OF REN VESSELS

Kędzia A[1], Rybaczuk M[2], Andrzejak R[3], Kędzia W[3]

[1]*Department of Normal Anatomy, Medical University of Wrocław, Wrocław, Poland*
[2]*Division of Dynamics, Institute of Materials Science and Applied Mechanics, Wrocław University of Technology, Wrocław, Poland*
[3]*Department of Internal and Occupational Diseases, Medical University of Wrocław, Wrocław, Poland*

Analysis of literature suggests that fractals have not been applied for the proper evaluation of microangioarchitecture until now. In our own research, this method was employed in fractal evaluation of the microangioarchitecture of the brain, stomach and ossification centres. The ren vessels are not examined with the help of the above method. The examinations comprise 10 rens without visible changes for adults within the age range 20–30 years. The Pickworth method, computer image analysis in two incompatible systems, Imtron and Scion for Windows 98 as well as fractal analysis, were applied. Ready preparations under the Pickworth method were treated with nonlinear transformations: filtering, binarization, visualisation (enlarging, colouring, shifts of brightness and contrast) to improve image quality. The threshold and density slice functions allowed

objects to be split according to shadow scale. A plotter enabled spatial visualisation of grey levels. The shadow correction restores relief of examined surfaces and this indicates convex fragments of objects. Each fragment of image requires special treatment and choice of transformations due to differentiated structure. The fractal analysis followed special preparation of images. The convert and fd3 programs under Linux were applied to carry out fractal analysis. The level of complexity was evaluated according to the fractal dimensions. Capacity, information and correlation dimensions were determined. It has been noticed that the capacity dimension appears to be best suited for the evaluation of complexity level. Next, the grey level was chosen for each image. The vessel system in rens has a tendency to separate itself at a straight angle. Vessels of the glomerulus are very specific; the surface is extremely folded having the form of a sine function with many connected lakes. The fractal dimension is very high (1.99), which refers to fast energy exchange with close packing and high complexity level. The fractal dimension of close to 2 indicates that the object occupies the entire surface.

NEURONES CONTAINING CALCIUM BINDING PROTEINS IN THE OPOSSUM (*MONODELPHIS DOMESTICA*) MIDBRAIN

Klejbor I[1], Ludkiewicz B[1], Spodnik J[1], Turlejski K[2], Moryś J[1]

[1]*Department of Anatomy and Neurobiology, Medical University of Gdańsk, Gdańsk, Poland*
[2]*Department of Molecular and Cellular Neurobiology, Nencki Institute of Experimental Biology, Warsaw, Poland*

Among its many functions, the mesencephalic neuronal system is involved with stress-related disorders and defensive behaviour. The midbrain nuclei differ in connections and content neurotransmitter and calcium binding proteins (CaBPs) such as calbindin (CB), calretinin (CR) and parvalbumin (PV). CaBPs are involved in buffering intracellular calcium, thus they may provide neuroprotective influences. Recent studies also showed that CaBPs neurons might be responsible for stress response. Based on analyses of spontaneous behaviour, it is possible to observe differences between rats and opossums. Opossums showed a higher rate of locomotor activity and explored new object faster. The distinction of these behavioural strategies might be a reflection of difference in morphology and function of selected brain systems in CaBPs expression. In the present study, we used immunohistochemistry to examine the distribution and morphology of neurons containing CaBPs, including CB, CR and PV in the midbrain nuclei (VTA and SN) in the adult gray short-tailed opossum. The material consisted of nine adult animals. After perfusion, the brain sections were stained using the antibodies against CB, CR and PV. The immunohistochemically stained slides were examined by fluorescent microscope BX-51 (Olympus, Japan). Our results showed that in all studied regions, expressions of CaBPs were present. However, we observed differences in expressions of separate CaBPs. CR-ir cells were most numerous. VTA contained round, oval or triangular densely packed CR-ir cells with visible dendrites. CR-ir fibres were long and sometimes showed varicosities.

In the SN area, CR-ir cells were observed mainly in SNc whereas in SNr showed neuropil rich in immunoreactive fibres and points. PV-ir cells occupied all studied nuclei but in the VTA area, PV-ir neurons rarely occurred while neuropil was rich. In the SN area, we observed many PV-ir cells with long processes. In the VTA region, as well as in SN, a few CB-ir cells and fibres were observed. CB-ir cells were oval or triangular and they possessed long fibres. Anterior region VTA and SN showed more CB-ir elements than the posterior one. We may conclude that generally, the distribution of CaBPs in VTA and SN in the opossum and the rat is similar except for CB-ir cell patterns.

DISTRIBUTION OF CART-IR NEURONS AND FIBRES IN THE DENTATE GYRUS AND HIPPOCAMPUS PROPER IN THE GUINEA PIG (*CAVIA PORCELLUS*)

Kolenkiewicz M, Robak A

Department of Comparative Anatomy, University of Warmia and Mazury, Olsztyn, Poland

CART (cocaine- and amphetamine-regulated transcript) is one of the neuropeptides and it is present in different parts of the brain (hypothalamus, limbic system and cortex).

This neuropeptide was first studied during amphetamine and cocaine administration and its influence on the psychomotor stimulants. Later studies showed that CART plays a key role in stress response and the regulation of food intake.

The hippocampus is one of structures in which CART is present. The Ammon's horn is known to regulate learning and memory processes and stress response. CART is probably able to protect and promote the survival of hippocampal neurons.

The aim of this study was to gain details about the distribution of CART-immunoreactive (CART-IR) neurons and fibres in the dentate gyrus and the Ammon's horn in guinea pigs aged 10 and 14 days of postnatal life (P10 and P14). The animals were euthanized by use of pentobarbital sodium. The brains were immersed in 4% paraformaldehyde for 15 minutes and stored in 19% and 30% sucrose solution until they sank. CART-IR neurons and fibres were immunocytochemically identified with rabbit polyclonal antibody against CART peptide on 10 μm thick frozen sections. Secondary antibody was conjugated with CY^3.

Studies showed a few large, oval-shaped CART-IR perikarya in the granular layer of the gyrus dentatus. Some single immunoreactive varicose fibres that had gone through the granular layer were also observed. The most intensively stained part of dentate gyrus was a band of puncta in the inner molecular layer. The hilus of the dentate gyrus contained numerous mossy cells with multipolar stomata and thin mossy fibres which passed throughout the CA3 sector of the hippocampus and ended with a typical end bulb. In the hippocampus proper, only few varicose fibres were observed in the stratum radiatum.

HUMAN STERNUM MORPHOMETRY IN THE PRENATAL PERIOD

Korczak I[1], Kędzia A[1], Dudek K[2]

[1]*Department of Normal Anatomy, Medical University of Wrocław, Wrocław, Poland*
[2]*Institute of Machine Design and Operation, Wrocław University of Technology, Wrocław, Poland*

Analysis of developing human sterna was performed on a total of 46 human foetuses of both sexes and with crown-rump length (CRL) ranging from 98 mm to 225 mm. The methods were: preparation, anthropological, computer measurement using Scion for Windows software, Gimp 2.2.14 software for photo retouching composition and statistics: Shapiro-Wilks test, t-Student test. The sterna were prepared and photographed in the frontal projection. Pictures were sent to the computer and measured using Scion for Windows software. Pixels were converted into millimetres using a millimetric scale located on each foetus. The accuracy of measurements was $\pm$ 0.01 mm. The obtained results were subjected to statistical analysis using: t-Student test, Shapiro-Wilks test. Shapiro-Wilks test and t-Student test were applied to the verification hypothesis regarding the absence of important differences between male and female foetuses to estimate difference in growth rate in the $4^{th} - 5^{th}$ foetal months and $6^{th} - 7^{th}$ foetal months. The relevance between the measurements and the embryo age was performed. Mathematical models describing the measurement accretion in the age function were made; it was

a logarithmical model. To estimate the sternum geometry, 24 measurements were taken. The length-width index of the manubrium, mesosternum and particular segments were constant. Length accretion of the entire sternum was supreme in the 4th foetal month and elevated 8 mm; however, in the 7th foetal month, it was minimal and elevated 4.2 mm. Accretion of the manubrium in the 4th, 5th, 6th, 7th foetal months elevated adequately: 1 mm, 0.7 mm, 0.6 mm and 0.5 mm. Accretion of the mesosternum in the 4th, 5th, 6th, 7th foetal months elevated adequately: 4.5 mm, 3.5 mm, 2.8 mm and 2.4 mm. The most intense growth of the manubrium and mesosternum was in the 4th foetal month. The growth rate of the manubrium was lower than the entire sternum in the following period. Conclusion: the sternum increases in a cephalocaudal direction; growth rate is regular except for the manubrium which grows intensely in the 4th foetal month. Sexual dimorphism was not found. Primary sternal ossification centres appear in the manubrium. Processus xiphoideus characterized a great variation in the shape and geometry. It takes a cone shaped, cylindrical, irregular figure.

RENAL FAILURE DUE TO EXPERIMENTAL ACUTE PANCREATITIS IN RATS

Kostek H, Wieczorkiewicz-Płaza A, Płaza P, Staśkiewicz G, Anasiewicz A

Department of Anatomy, Medical University of Lublin, Lublin, Poland

Renal disorder (apart from pulmonary, hepatic and cardiovascular) during acute pancreatitis has a significant influence on prognosis. The aim of this study was to observe histopathological changes in renal tissue during the first 48 hours of experiment, and evaluate their correlation with histopathological changes in pancreatic tissue and with levels of selected lysosomal enzyme activity.

Seventy male Wistar rats with a mean body weight of 300 g were included in the study. They were divided into 3 groups: I — healthy rats (normal group), II — rats with 0.9% NaCl solution injected into the hepatopancreatic duct (control group), III — rats with acute pancreatitis induced by the injection of 5% sodium taurocholate (according to Aho and Heinkel's method) (experimental group). Groups II and III were randomly divided into 5 subgroups. At 2, 6, 12, 24 and 48 hours after the induction of acute pancreatitis, the rats were anesthetized and their kidneys and pancreases used for histopathological investigations. The study was fully approved by the University Ethics Commission.

Histopathological changes were noticed in both organs. In the kidneys, cortical and medullar passive hyperaemia, parenchymatous and hydropic degeneration of epithelium of the convoluted tubules and inflammatory parenchymal infiltration were observed. In pancreatic tissue, haemorrhagic necrosis and in interstitial tissue, multifocal pyogenic inflammation, Balser necrosis and cellular parenchymal inflammatory infiltration (composed with granulocytes, lymphocytes and macrophages) were observed.

Histopathological changes in the kidneys and pancreas were more intensified in the group receiving injections of 5% sodium taurocholate than in group receiving injections of 0.9% NaCl solution into the hepatopancreatic duct and were correlated with time period. There was no correlation between activity of selected lysosomal enzymes and intensification of histopathological changes in renal tissue.

CHARACTERISTICS OF AGE-RELATED CHANGES WITHIN MEDULLA OF THE FEMALE RAT THYMUS

Kowalska K, Brelińska R

Department of Histology and Embryology, Medical University of Poznań, Poznań, Poland

In all species, the principal traits of age-related involution include a decrease in thymic weight, associated with reduced lympho-epithelial compartment, which involves the active region of thymopoiesis, with parallel increase in connective tissue compartment. The alterations commence abruptly in the period when the animal reaches sexual maturity. During early involution, the architecture of the epithelial network remains intact and changes in thymus develop mainly due to loss of thymocytes. With progressing age, the age-related alterations in thymic epithelial cells (TEC) organization were described to develop in the cortex. Changes in the medulla and their kinetics have been less recognized. Therefore, the aim of this work was to provide a morphometric description of the changes within the thymic medulla in female rats during the first two years and to relate them to processes of medullary TEC differentiation. Medullary TEC have been studied by a panel of antibodies directed to cytokeratine polypeptides (Ck) and by expression of Ki67. Using various combinations of single and double immunostaining 5 TEC subtypes were identified in the medulla of three-month-old rats, each characterized by different Ck expression and Ki67. Their relative frequencies of occurrence are about 19% of TEC1 and TEC2, 11% of TEC3 and 70.5% of TEC4 with high mitotic activity. Subtype 4 comprised 1% of undifferentiated TEC. Subtype 5 of TEC comprised cells forming Hassall's corpuscles.

In the 24 months period of a rat's life, its thymus weight and entire volume showed peak values in the second and the third months. In morphometric analysis, the most dynamic changes in the entire period of life involved the cortex, while the medulla showed itself to be a rather "stable" region. However, changes in organization of the epithelial network in the medulla preceded those observed in the cortex. Beginning in the 5th month of life, perivascular spaces in the medulla gradually became widened. It could be suggested that signals acting locally within perivascular spaces may influence the architecture of the medulla through a direct effect on TEC. In the present study, this has been confirmed by the evident reduction of medullary TEC, which may be linked to inhibited processes of renewal and differentiation of the 4th subtype of TEC.

MECHANISMS OF APOPTOTIC ACTIVATION IN THE COURSE OF EXPERIMENTAL CEREBRAL ISCHAEMIA IN RATS

Kowiański P, Lietzau G, Karwacki Z, Dziewiątkowski J, Moryś J

Department of Anatomy and Neurobiology, Medical University of Gdańsk, Gdańsk, Poland

Cerebral ischaemic stroke is the third most common cause of death after heart infarct and neoplasm. Morbidity varies from 100–330/100,000 per year. This relatively high value and the lack of effective therapeutic procedures result in the persistent focus of scientific interest on the problems of cerebral ischaemia.

The final result of pathophysiological processes occurring in the region of ischaemia is neuronal death of both necrotic and apoptotic character. Hence, the aim of this work was an assessment of two forms of apoptosis induction (caspase-dependent and caspase-independent) in the course of experimental transient focal cerebral ischaemia in rats.

The experimental model was applied to 25 Wistar rats of both sexes (weight 250 g and 360 g). The middle cerebral artery was occluded for 1 h. The reperfusion varied from 1 h to 3 days. To determine the presence of caspase-dependent apoptotic death, immunocytochemical staining for caspase-8 and caspase-3 was performed. The caspase-independent pathway was studied on the basis of the presence of apoptosis inducing factor (AIF). The results were assessed qualitatively using the confocal microscopy system.

Our results indicate that both forms of apoptotic neuronal death (caspase-dependent and caspase-independent) are observed in the ischaemic region. The concentration of neurons undergoing apoptotic activation varies according to their localization within the ischaemic region and length of reperfusion period. Additionally, characteristic changes of AIF distribution within neuronal cell bodies concerned with the length of reperfusion period are reported.

Our results indicate a significant role of caspases and AIF in apoptosis-induction during transient focal cerebral ischaemia. This observation may have implications in the development of specific protective procedures concerned with the selective inhibition of neuronal death during cerebral infarct.

OPIOID-LIKE IMMUNOREACTIVITY IN THE MAMILLARY BODY OF PIGS

Kozdryk M[3], Robak A[1], Bogus-Nowakowska K[1], Równiak M[1], Wylot B[2], Majewski M[3]

[1]Department of Comparative Anatomy, University of Warmia and Mazury, Olsztyn, Poland
[2]Department of Animal Physiology (Faculty of Biology), University of Warmia and Mazury, Olsztyn, Poland
[3]Division of Clinical Physiology, Department of Functional Morphology (Faculty of Veterinary Medicine), University of Warmia and Mazury, Olsztyn, Poland

Our preliminary studies have suggested that some opioid precursor (proenkephalin and prodynorphin) genes are expressed in the mamillary region of mature female pigs. The purpose of the present study is to elucidate the presence of opioid-like immunoreactivity in the mamillary body (Mbs) of immature pigs, aged 10–14 weeks postnatally. The pig brains were perfused and postfixed (4% paraformaldehyde in phosphate buffer, pH 7.4), then washed in PBS and cryoprotected in a 30% solution of sucrose, before cutting into slices (10 or 20 μm thick). The slicess were immunostained with a standard fluorescence technique using the primary antibodies against dynorphin A (DYN A), α-neoendorphin (α-neoEND), and the species specific secondary antibodies conjugated with fluorochromes FITC or CY3. The medial (MM) and lateral (ML) mamillary nuclei as well as the supramamillary (SM) and posterior part of the tuberomamillary nuclei (TMp) were investigated. Generally, the perimamillary area (SM, TMp) showed a stronger immunoreactivity than the mamillary nuclei. Throughout the entire mamillary body, the opioid-ir fibres were observed. These fibres were segregated into three different morphological types: 1) fine, slender, faintly-ir fibres consisting of dots, they coursed alone (MM) or formed a network (SM, TMp) that sometimes looked like a basket structure (TMp); 2) strongly fluorescent varicose fibres (short or relatively long) containing thick irregular varicosities and thin intervaricose segments. In general, the distribution of DYNA-ir and α-neoEND-ir fibres was similar, but some differences were observed. These opioid-like immunoreactivities were higher in the anterior sector of MM than in the posterior one. The α-END-ir and DYN A-ir single rounded or triangular perikarya were found in SM and MM.

EXPERIMENTAL PHOTOTOXICITY AND PHOTOSENSIVITY — HISTOPATHOLOGICAL CHARACTERISTICS OF INFLAMMATORY SKIN REACTION

Krajnow A, Domeradzka K, Palmowska M, Stetkiewicz J

Department of Pathomorphology, Nofer Institute of Occupational Medicine, Łódź, Poland

Phototoxicity and photosensivity are inflammatory skin reactions caused by exposure to a chemical and subsequent exposure to sunlight or ultraviolet radiation. In the course of testing several non-steroid anti-inflammatory drugs for phototoxicity and photosensivity, we noticed a need to validate our procedures by experimental *in vivo* methods.
Ethanol solutions containing 25, 50 and 100 ppm of 8-methoxypsoralen (8-MOP) were used as a reference substance for phototoxicity control; 1% 6-methylcumarine (6-MC) ointment was applied for the photosensitivity test. The experiments were performed on guinea pigs. The animals were exposed to 280–315 nm UV light at 0.047 UVA/UVB ratio, 10 J/cm^2 UVA and 0.1 J/cm^2 UVB dose. The phototoxicity test was performed according to modified OECD TG-404 method — dermal application of 8-MOP was followed by a single exposure to UV light. The photosensitivity test was performed according to a modified Bahler test (OECD TG-406) — after dermal application of 6-MC, the animals were exposed each second day to UV light (induction). Two weeks after the last exposure, a control test was carried out. Twenty-four and forty-eight hours after the single exposure (phototoxicity test) or control test (photosensitivity test) skin specimens from UV-exposed and non-exposed animals were subjected to histopathological examination.
Microscopic examination performed after the phototoxicity test revealed spongiosis of the epidermis and perivascular infiltration containing polymorphonuclear cells in the upper dermis. The degree of change was dependent on 6-MC concentration.
Acanthosis, spongiosis and diffuse mixed infiltration in the dermis were most prominent after the control photosensitization test, while pyknosis and vesicles in the epidermis were related to phototoxicity.

MORPHOLOGY OF THE INCUDO-MALLEAL AND INCUDO-STAPEDIAL JOINT IN HUMANS

Krasucki KP[1], Skarżyńska B[2], Skarżyński PH[3]

[1]Head and Neck Clinical Anatomy Laboratory, Warsaw Institute of Physiology and Pathology of Hearing, Warsaw, Poland
[2]Department of Normal Anatomy Centre of Biostructure, University of Medical Sciences of Warsaw, Warsaw, Poland
[3]Inter-Center Students Research Study Group, Warsaw Institute of Physiology and Pathology of Hearing, Warsaw, Poland

It is commonly thought that joints are the connections between auditory ossicles. The authors of this paper verified 10 human ossicle-tympanic specimens and by applying histological methodology they assessed the character of the structure of the auditory ossicle connections. The specimens were covered by Histocryl-acrylic resin and then coloured by HE. The research revealed significant variations of some of the structures. The surface of the incudo-malleal joint is elliptic; they separate from each other in various degrees, which often do not make a proper cavity. The research revealed the presence of a thin meniscus of fibrous structure going straight from the joint capsule. The structure of this connection bears more resemblance to a synchondrosis than a regular joint. The joint capsule of the incudo-stapedial joint is hardly visible. A total lack of joint cavity was observed between the surfaces connecting the ossicles (head of the stapes and surfaces of the lenticular process). The lenticular process of the incus has on its surface cartilage a convexity that forms the head of the joint.

BLOOD SUPPLY OF THE PRIMARY OSSIFICATION CENTRES OF THE BODY OF LUMBAR VERTEBRAE IN HUMAN FOETUSES

Krzanowski K, Czerwiński F, Sławiński G, Michalska-Krzanowska G, Sulisz T

Department of Anatomy, Pomeranian Medical University of Szczecin, Szczecin, Poland.

The blood supply of the spine in foetuses differs from that observed in adults. Some vessels observed in foetal development disappear with the end of the ossification process. The aim of the study was to describe the blood supply of the primary ossification nuclei the in bodies of the lumbar vertebra in human foetuses.

Fourteen foetuses of both sexes, aged between 12 and 15 weeks of gestational age were examined. X-rays of the lumbar vertebral column in antero-posterior and lateral projection were taken to identify the presence and size of the primary ossification nuclei. Next, the contrast medium (micropaque) was injected through the common carotid artery and X-rays in both projections were again taken. Then, particular vertebra were separated. Cross-sections of each lumbar vertebra were made and their structural X-rays were taken. Based on radiological images, the course of the main arteries and their branches supplying the centres of ossification were analysed.
The lumbar vertebrae begin to ossify in the 10th week of foetal life, and usually of two ossification nuclei located in the body and in the arch. The most advanced ossification is observed in first lumbar vertebra and the least in the fifth. The primary centre of mineralization is observed in the rostral part of the body and develops in the dorsal direction. This region is supplied mostly by the spinal branches of the lumbar and highest lumbar arteries. In 47%, the ossification nuclei were supplied by the large single symmetrical branches of the segmental artery, which went to the ossification centre from the anterior or antero-lateral surface of the body by the artery only on left side in 14.4% of cases and 11.6% only n the right side. In 27% of cases, the primary nuclei were supplied by numerous thin branches.

HISTOCHEMICAL LOCALIZATION OF AUTONOMIC GANGLIA FUNCTIONALLY CONNECTED WITH TYMPANIC CHORDA IN MONGOLIAN GERBILS (*MERIONES UNGUICULATUS*)

Kuchinka J, Nowak E, Szczurkowski A, Kuder T

Department of Comparative Anatomy, Institute of Biology, Świętokrzyski University, Kielce, Poland

The aims of our investigation were the morphological and histochemical observations of autonomic structures in the lingual and sublingual regions in Mongolian gerbils (*Meriones unguiculatus*).
The investigation was performed on five adult Mongolian gerbils of both sexes. Two individual heads of animals were prepared using stereomicroscopy and studied in situ using the thiocholine method of Koelle-Friedenwald modified by Gienc for use in macromorphological specimens. For histochemical investigations, tissues from three individuals were cut with the cryostat in 10 μm sections and stained using the AChE method.
Macromorphological investigations showed about ten spindle-shaped ganglia connected with the cholinergic fibres in the hilus of salivary gland. Moreover, delicate cholinergic fibres with some aggregations of neurocytes were observed along the salivary ducts and along the lingual nerve.
The frozen sections showed a large nummber of cholinergic fibres surrounding the secretory units. Numerous small (about a few nerve cells) ganglia were observed in interstitial connective tissue. Moreover, cholinergic fibres surrounded the salivary ducts and blood vessels.

VARIABILITY OF BLOOD SUPPLY TO THE EYEBALL IN CHINCHILLAS (*CHINCHILLA LANIGER*, MOLINA)

Kuchinka J, Nowak E, Szczurkowski A, Kuder T

Department of Comparative Anatomy, Institute of Biology, Świętokrzyski University, Kielce, Poland

The aim of our studies was the anatomical analysis of blood supply to the eyeball in chinchillas (*Chinchilla laniger*, Molina).
Investigations were performed on ten chinchillas of both sexes after slaughter in a professional farm. The animals were injected using stained acryl latex through the left heart ventricle. The heads of animals were fixed in 10% formalin and after calcification in 5% HNO_3, the injected arteries were prepared.
In most cases, the maxillary artery or stapedial artery in rodents is a source of blood supply to the eyeball. In chinchillas, three individual variants of the course of eyeball arteries were observed. In the first variant, the eyeball is supplied by a "double" ophthalmic artery, which branches from the maxillary artery. In the second variant, the ophthalmic artery branches from the last part of the basilar artery. In the third variant, blood supply to the eyeball is form both the maxillary artery and the last part of the basilar artery.

THE INFLUENCE OF CAFFEINE ON THE DEVELOPMENT OF THE CORNEA AND LENS IN CHICKS

Kujawa-Hadryś M, Bartel H

Department of Histology and Tissue Ultrastructure, Medical University of Łódź, Łódź, Poland

Caffeine is one of the most often consumed psychoactive chemicals. It has been known for several years that high doses of caffeine negatively affect the fertility of women and laboratory animals and during the prenatal period, can also damage the normal development of many organs.
So far, a few studies have suggested any destructive effects of caffeine on structures of eye development, especially on the cornea and a lens. The aim of this study is to show the relationship between different doses of caffeine administered to chicken embryos and the ultrastructural changes in the developing cornea and lens.
The experimental materials were chicken embryos from eggs incubated in an electric cabinet at 37–38°C, and 50–60% relative humidity. In the experiment, 60 chicken embryos were used. Statistically, chicken embryos develop from only 60% of the eggs. The eggs were divided into 3 groups at random. The first group was a control group. Beginning from the 24th hour of the incubation (7–8 stages of development according to Hamburger-Hamilton) every 12 hours (ending to the 72nd hour of the incubation) Ringer's solution has was administered to the 4 eggs of this group. In the second group, a teratogenic dose of caffeine was used — 3.5 mg/egg. The scheme of administration of caffeine was analogical to the scheme used in the first group. The eggs from the third group were affected by caffeine in doses equal to half of the teratogenic dose — 1.75 mg/egg. The solutions were administered with a syringe to all the chicken embryos through an observation window in the eggshell, directly into the amniotic sac. After closing the window in the eggshell with glass plates and paraffin, the eggs were put back to the electric cabinet. On the 10th day (36 stages of the development according to Hamburger-Hamilton) and on the 19th day of incubation (45 stages of the development according to Hamburger-Hamilton), the corneas and the lenses were taken to conduct morphological analysis under an electron microscope.
The initial results of the study showed a negative influence of caffeine on the development of the cornea and the lens. Further results of the study can contribute to a better understanding of the pathomechanism of innate opacification of the cornea and the lens.

THE DEVELOPMENT OF FOLIATE PAPILLAE OF THE TONGUE IN RABBITS (*ORYCTOLAGUS CUNICULUS F. DOMESTICA*) IN VIEW OF MORPHOMETRIC STUDIES

Kulawik M, Godynicki S

Department of Animal Anatomy, Agricultural University of Poznań, Poznań, Poland

The aim of this study was to describe the dynamics of the development of foliate papillae on the tongues of rabbits based on the statistical analysis of the height of foliate papillae and their primordia and the thickness of the epithelium tat covers them in individual periods of pre- and postnatal life. Studies were conducted on 59 tongues collected from rabbits (*Oryctolagus*

cuniculus f. domestica) of both sexes, being at days 15, 18, 20, 22 and 26 of prenatal life (p.c.) and from rabbits at days 1, 15 and 30 and in the 6th month of postnatal life (p.p.).
Specimens for observation under a light microscope were fixed in 10% neutralized formalin or Bouin's solution, dehydrated in a series of alcohols with increasing concentrations, embedded in paraplast and sliced into sections. Masson-Goldner staining or HE were applied in this study.
Morphometric studies were conducted on the basis of images of histological specimens, observed under a light microscope, mounted with a camera with a computer image analysis program MultiScan V. 6.08. The height of the foliate papillae, their primordia and the thickness of the epithelium covering them in individual periods of pre- and postnatal life were analyzed morphometrically. Using the F-test, statistical differences were determined for mean values of the measured trait in successive periods of pre- and postnatal life.
Primordia of foliate papillae were observed starting from day 22 of foetal development in the rabbit in the posterior part of the tongue, on its dorsolateral side.
Morphometric analyses showed that the height of foliate papillae and their primordia, as well as the thickness of the epithelium covering developing foliate papillae increased in the successive investigated periods of pre- and postnatal life in the rabbit. The highest growth rate of foliate papillae was recorded between day 30 and the 6th month p.p., while the lowest was between days 26 p.c. and day 1 p.p. The highest dynamics of changes in the thickness of the epithelium were recorded between days 15 and 30 p.p., while the lowest was between day 26 p.c. and day 1 p.p.

THE DEVELOPMENT OF MUCOSA ON LATERAL SURFACES OF THE LINGUAL BODY IN THE PRE- AND POSTNATAL LIFE OF RABBITS

Kulawik M, Godynicki S

Department of Animal Anatomy, Agricultural University of Poznań, Poznań, Poland

The aim of this study was to describe the structure of the lateral surfaces of the body of the tongue in rabbits in the period from day 15 of prenatal life (p.c.) to the 6th month of postnatal life (p.p.).
Studies were conducted on 77 tongues collected from rabbits (*Oryctolagus cuniculus f. domestica*) being at days 15, 18, 20, 22 and 26 of prenatal life and from rabbits at days 1, 15 and 30 and in the 6th month of postnatal life. Samples for observation under a light microscope were fixed in 10% neutralized formalin, dehydrated in alcohols, embedded in paraplast and sliced into sections in three planes, i.e. in the median, transverse and horizontal planes. Masson-Goldner staining, HE, orcein, resorcin-fuchsin and PAS were applied in this study.
Morphometric studies were conducted based on images of histological specimens observed under a light microscope mounted with a camera with the computer image analysis program MultiScan V. 6.08. The thickness of the epithelium covering the lateral surfaces of the body of the tongue in individual periods of the pre- and postnatal life of rabbits was analyzed morphometrically.
For the observation of the connective tissue core of the lateral surfaces of the body of the tongue, samples were first fixed in Karnovsky fixing solution and then placed in a 10% NaOH solution at room temperature. After the epithelium was removed, samples were dehydrated, critical point dried and sputtered with gold.
As a result of the conducted studies, it was shown that the epithelium covering the lateral surfaces of the body of the tongue in the period from day 15 p.c. to the 6th month p.p. changed from a 1–2-layer epithelium into a non-keratinized stratified squamous epithelium. The thickness of the epithelium increases in successive analyzed periods of life in rabbits. Starting from day 22 p.c., structurally differentiating lamina propria mucosae was observed, in which elastic fibres were identified, arranged primarily perpendicularly to the longitudinal axis of the tongue. The connective tissue core was formed by numerous, irregular in shape connective tissue papillae. From day 15 to 20 p.c., glycogen grains were found in the cytoplasm of epithelial cells.

THE DEVELOPMENT OF VALLATE PAPILLAE ON THE TONGUES OF RABBITS (*ORYCTOLAGUS CUNICULUS F. DOMESTICA*)

Kulawik M, Godynicki S

Department of Animal Anatomy, Agricultural University of Poznań, Poznań, Poland

The aim of the study was to investigate the development of the mucosa on the tongues of rabbits in the area where vallate papillae are formed, starting from day 15 of prenatal life (p.c.) to the 6th month of postnatal life (p.p.).
Studies were conducted on 93 tongues, collected from rabbits being at days 15, 18, 20, 22 and 26 of prenatal life and from rabbits at days 1, 15 and 30 and in the 6th month of postnatal life.
Tongues for observations under a light microscope were fixed in 10% neutralized formalin or Bouin's solution. Tissue samples with vallate papillae were dehydrated in a series of alcohols (with concentration increasing from 50 to 96%), embedded in paraplast and sliced in three planes, i.e. in the sagittal, transverse and dorsal planes, into sections with thickness from 3 to 5 μm. Masson-Goldner and HE staining were applied in the study.
The first form of primordia of vallate papillae were a thickening of the epithelium, observed in the period from day 15 to day 20 p.c. From day 22 p.c., lamina propria of the lingual mucosa formed the connective tissue core for the developing vallate papillae. The connective tissue core of primordia was surrounded by a circular primary epithelial streak, which from day 26 p.c. elongated more in certain places, giving rise to posterior serous lingual glands. From day 26 p.c., the epithelium covering primordia of vallate papillae grew into connective tissue forming secondary epithelial streaks. Furrows of vallate papillae started to form from day 22 p.c. Taste buds were observed from day 1 p.p. in the place where the primary epithelial streak cleaved forming the furrow of papilla. After the formation of vallate papillae, taste buds were identified both in the epithelium of papillae and in the epithelium of the outer wall from the side of the furrow. Occasionally, single taste buds were found dorsally in the epithelium covering the vallate papillae, where they accompanied the openings of excretory ducts of posterior serous lingual glands. The epithelium covering the developing vallate papillae changed in the investigated periods from a three-layer epithelium into non-keratinized stratified squamous epithelium.

THE MUCOUS MEMBRANE OF THE TONGUE WITH SPECIAL EMPHASIS ON FUNGIFORM PAPILLAE IN THE PERIOD FROM DAY 1 TO MONTH 6 OF POSTNATAL LIFE IN RABBITS

Kulawik M, Godynicki S

Department of Animal Anatomy, Agricultural University of Poznań, Poznań, Poland

The aim of this study was to investigate the development of the mucosa on the tongue in the rabbit in the area where fungiform papillae are formed in the period from day 1 to the 6th month of postnatal life.
Studies were conducted on 29 tongues of the domestic rabbit (*Oryctolagus cuniculus f. domestica*), which were collected at days 1, 15 and 30, and in the 6th month of postnatal life (p.p.).
Samples for observation under a light microscope were fixed in 10% neutralized formalin or Bouin's solution, dehydrated in alcohols, embedded

in paraplast and sliced in three planes, i.e. median, transverse and horizontal, into a series of slices with a thickness of 3 to 5 μm. Masson-Goldner staining, HE, orcein or resorcin-fuchsin were applied in this study.
Specimens for observations under a scanning electron microscope were fixed in a Karnovsky fixing solution, dehydrated, critical point-dried and sputtered with gold.
As a result of observations under a light microscope and a scanning electron microscope, changes were examined in the mucosa on the dorsum of the apex and on the dorsum of the body of the tongue, where fungiform papillae are located.
The epithelium covering fungiform papillae at day 1 of postnatal life was a non-keratinized stratified squamous epithelium, whereas starting from day 15 of postnatal life it was found that the epithelium was a keratinized stratified squamous epithelium. Also starting from day 15 of postnatal life, in the area of the connective tissue core of some fungiform papillae, solitary lymphatic nodules were observed.
At day 1 of postnatal life, elastic fibres are well marked and are arranged primarily in the transverse direction in relation to the longitudinal axis of the tongue. Their concentration increases medially and caudally on the dorsum of the apex and on the dorsum of the body of the tongue in front of the torus of the tongue. In the area of the torus of the tongue, the concentration of elastic fibres decreases in the caudal direction. Such a distribution of elastic fibres was also observed in successive investigated periods in the life of the rabbit.

CLINICALLY IMPORTANT STRUCTURES OF A DOG'S NOSE VESTIBULE

Kupczyńska M, Makowiecka M, Skibniewski M

Department of Morphological Sciences, Faculty of Veterinary Medicine, SGGW, Warsaw, Poland

The application of new diagnostic imaging methods (CT, endoscopy) requires detailed morphological knowledge. However, the anatomical descriptions available in literature cannot be used as the sole basis for the interpretation of the images produced by those examinations. The description mentioned above usually concerns isolated organs; they do not consider their syntopy nor take into account the aspects fundamental to the correct examination. These problems are resolved by clinical anatomy. Nasal cavity diseases are very common in dogs and rhinoscopy has become an important method of examination in their diagnosis. This investigation examined those structures of the vestibule of the nose, which, in literature, are briefly mentioned (or not at all) and which are essential for the proper application of rhinoscopy.
A standard anatomical preparation of the vestibule of the nose was carried out on the corpses of 74 dogs of both sexes, various breeds and morphotypes. The vestibule of the nose is the area of irregular shape, which leads to a nostril limited by the medial and lateral wing of the nose. The first one is stronger and reinforced with the dorsal lateral nasal cartilage. The other one rests on the lateral accessory nasal cartilage. The medial wings are divided by the philtrum. On the lateral wall of the nose, both wings are divided by the wing groove. The skin of the medial wing curls up into the light of the vestibule and transforms into the alar fold, which rests on the strong medial accessory nasal cartilage. The nasal cartilages mentioned above are made of hyaline cartilage, which is responsible for the low flexibility of this area. The alar fold creates an elevated area in the nostril and presses against the nostril septum. In mesati- and dolichocephalic dogs, this structure fills a great part of the light of the vestibule. In brachycephalic dogs, however, it practically fills this space. On the superior wall of the vestibule lie two, occasionally three, parallel folds. A few other folds close at the limen of the nose. On the lateral wall of the vestibule there are two other folds: the straight and the oblique, which disappear at the bottom of the alar fold. The dorsal and ventral folds of mucosal membrane, which sit on the septum of the nostril, also disappear in this area. On the bottom of the vestibule lies the basal fold, which is the weakest one. The folds mentioned above are developed in different manners in each individual. This fact is the most important in the morphology of brachycephalic dogs. The researched structures can make rhinoscopy significantly difficult or even impossible.

THE PLANTAR CALCANEONAVICULAR LIGAMENT. ITS ANATOMICAL STUDY AND ROLE IN STABILIZING THE LONGITUDINAL FOOT ARCH

Kwapisz A[1,2], Król A[1], Domżalski M[2], Jędrzejewski K[1]

[1]*Department of Anatomy, Medical University of Łódź, Łódź, Poland*
[2]*Second Department of Orthopaedics, Medical University of Łódź, Łódź, Poland*

The plantar calcaneonavicular ligament complex, also known as the spring ligament fibrocartilage complex SLFC, is a part of the acetabulum pedis. Accompanied by surrounding tendons, ligaments and bony structures, the SLFC plays an important role in stabilizing the longitudinal foot arch. Dysfunction of the aforementioned elements were reported to be the cause of adult flat foot. In our study, we emphasized the precise structure of the SLFC and the understanding of its role.
Our materials consisted of 19 lower limbs, being the property of the Department of Anatomy. The examined limbs were ablated in the inferior talar joint following careful removal of the head of the talus. Next, the surrounding fatty tissue was excised to insure a proper view of the SLFC. In 12 cases (63.16%), we identified three ligaments of this complex: superomedial, inferior and a structure known as the "third ligament" (TL). In the remaining 7 (36.84%) cases, we could not identify any structure that could be considered as the third ligament (TL).
We observed that the spring ligament fibrocartilage complex is composed of three structures although in some cases we could not find a distinct third ligament. However, our study requires further confirmation on larger material.
Acquired adult flat foot is commonly a result of a torn tendon of the tibialis posterior muscle. It has been reported several times that isolated damage of the SLFC also may result in adult flat foot. Understanding of the anatomy of this structure might help surgeons in the reconstruction of this fibrocartilage ligament complex.

FORMATION OF THE HUMAN CERVICAL LORDOSIS

Lewandowski J, Szulc P, Marecki B

Department of Functional Anatomy, Academy of Physical Education of Poznań, Poznań, Poland

The spondylometric features may serve as the indicators of human organism reactions to various biological factors — particularly musculoskeletal system pathology — and may be effectively used in diagnostics and prophylaxis.
The aims of the study were to measure the cervical lordosis angle in both sexes and across various age categories to determine dimorphic differences and to investigate the relationship between the cervical lordosis and selected somatic features.
Spondylometric measurements of the cervical lordosis were carried out using tensiometric electrogoniometer based on the original method developed by the authors. The subjects totalled 24,517 individuals (12,161 females and 12,356 males) aged 3–25 years. The results were submitted for statistical analysis.
The highest developmental gradient of the cervical lordosis, both in males and females, can be observed at 17–18 years of age. The rate at which cervical lordosis deepens in males and females is highest between years 12–16. In the early years of the period of ontogenesis analysed, in adolescence and the

post-adolescent stage, the cervical lordosis is more pronounced in males. The cervical lordosis angle moderately correlates with somatic features in females between 3 and 7 years of age, and in males at 4 years of age.
A percentile grid and graphic depiction of normal values of the cervical lordosis have been included in the work.

INNERVATION OF THE PIG PINEAL GLAND BY NERVE FIBRES CONTAINING CATECHOLAMINE-SYNTHESIZING ENZYMES, NEUROPEPTIDE Y (NPY) AND C-TERMINAL FLANKING PEPTIDE OF NPY (CPON) DURING FOETAL LIFE

Lewczuk B, Bulc M, Prusik M, Przybylska-Gornowicz B

Division of Histology and Embryology, Department of Functional Morphology, Faculty of Veterinary Medicine, University of Warmia and Mazury, Olsztyn, Poland

Sympathetic nerve fibres originating in the cranial cervical ganglia play the most important role in the regulation of pineal gland function in mammals. It is generally assumed the mammalian pineal shows very low secretory activity, if any, during foetal life. In rodents, the sympathetic innervation and the mechanisms of adrenergic regulation of melatonin secretion develop intensively during the first weeks of postnatal life. In our previous studies, it was shown that the sympathetic innervation of the pig pineal gland undergoes large modifications from birth to sexual maturation. The aim of the present study was to check the presence of nerve fibres containing catecholamine-synthesizing enzymes, NPY and CPON, in the pig pineal during foetal life.
Pineals were collected from 70-day-old and 90-day-old pig foetuses. The glands were fixed with 4% paraformaldehyde in 0.1 M phosphate buffer (pH 7.4) for 60 minutes, rinsed with the same buffer, cryoprotected and cut into 12-µm-thick sections using a cryostat. The sections were processed for double-immunofluorescence staining using primary antibodies against tyrosine hydroxylase (TH), dopamine β-hydroxylase (DβH), NPY and CPON.
Numerous TH-positive nerve fibres were found in the pineal glands of both 70- and 90-day-old foetuses. The fibres formed bundles in the pineal capsule and penetrated from these structures into the connective tissue septa, where they were located close to the blood vessels. Positive nerve fibres were also found in the glandular parenchyma, where they were evenly distributed. TH-positive fibres were usually also DβH-, NPY- and CPON-immunoreactive. Sporadically, TH-positive/DβH-negative, DβH-positive/NPY-negative and DβH-positive/CPON-negative nerve fibres were observed. The proximal part of the pineal gland contained some NPY-/CPON-positive/DβH-negative nerve fibres. They were thicker and possessed larger varicosities than DβH-positive fibres. All studied nerve fibres were more numerous in the pineal glands of 90-day-old than in 70-day-old foetuses.
The obtained results show that the pig pineal, during the last trimester of foetal life, posses quite well developed innervation by TH-, DβH-, NPY- and CPON-immunoreactive nerve fibres. It is reasonable to suspect that the majority of these fibres (with the exception of NPY-/CPON-positive/DβH-negative fibres) originate in the cranial cervical ganglia and represent the sympathetic innervation. The functional significance of these fibres remains to be established.

THE STRUCTURES AND TOPOGRAPHY OF THE AMYGDALA OF THE CHINCHILLA

Lonc G, Szalak R, Krakowska I, Boratyński Z

Department of Animal Anatomy, Faculty of Veterinary Medicine, Agricultural University of Lublin, Lublin, Poland

The aim of this study was to describe the structures and topography of the nuclei of the amygdaloid complex in chinchillas.
The material for the study consisted of five chinchilla brains. The brains were fixed in formalin, dehydrated in ethyl alcohol and embedded in paraffin blocks. Next, the blocks were cut in a transversal plane into 12-µm-thick slices. The slices were coloured according to Klüver and Barrer's method and examined under a light microscope.
One can distinguish three parts of the amygdala: the corticomedial amygdaloid complex (CMC), basolateral complex (BLC) and other amygdaloid areas (OA). The BLC is divided into three nuclei: the lateral amygdaloid nucleus (LA), basolateral amygdaloid nucleus (BL) and basomedial amygdaloid nucleus (BM). The BLC is situated in the posterior part of the chinchilla amygdala. The lateral amygdala is situated above the BL and is laterally bordered by the external capsule. The basolateral amygdaloid nucleus in the chinchilla is situated between the LA and BM. The basomedial amygdaloid nucleus is located ventromedially to the BM and dorsally to the cortical nucleus (CO). The corticomedial amygdaloid complex consists of the following: cortical nucleus (CO), medial nucleus (M), central nucleus (CE), amygdalohippocampal area (AHA), nucleus of the lateral olfactory tract (NLOT) and bed nucleus of the olfactory tract (BOAT). The nucleus of the lateral olfactory tract in chinchilla begins at the rostral part of the amygdala. It is bordered medially and dorsally by the anterior amygdaloid area (AAA) and laterally by anterior part of the cortical nucleus. The chinchilla bed nucleus of the olfactory tract is situated behind the NLOT. Dorsally, it borders the M, and laterally the CO. The central nucleus makes the dorsomedial part of the medial and caudal amygdala. The amygdalohippocampal area in the chinchilla is located in the caudal part of the amygdala between the subicular complex and CO. The cortical nucleus is long band of neurons, which make up the ventral part of the amygdala. The other amygdaloid areas consist of the anterior amygdaloid area (AAA) and nucleus intercalated (I). The intercalated nucleus is composed of neurons between amygdala nuclei. AAA make the anterior pole of the chinchilla amygdala.

FOOT FUNCTIONAL ANATOMY IN PATIENTS WITH PEDES CAVI

Lorkowski J[1,2], Teul I[3], Trybus M[1], Hładki W[1], Brongel L[1]

[1]*Department of Emergency Medicine and Multitrauma Injury, II Chair of Surgery, Jagiellonian University Medical College, Cracow, Poland*
[2]*Division of Anatomy and Biomechanics of the Movement System, "Zdrowie" Rehabilitation Centre, Cracow, Poland*
[3]*Chair of Anatomy, Pomeranian Medical University, Szczecin, Poland*

The aim of this study was to analyse functional foot anatomy in subjects with pedes cavi.
The examination group consisted of 21 patients (both sexes, aged 20–70) with this type of foot deformity. The control group consisted of 40 healthy individuals.
We used physical examination, radiological study and underfoot pressure measurements using static and postural pedobarographic tests. The plantar pressure was determined at foot regions distinguished on the basis of the classification by Cavanagh.
Pedes cavi was diagnosed using clinical, radiological and pedobarographic examination in 12 subjects. Correct diagnosis was made in 9 patients with the use of only pedobarography despite minimal or non clinical signs. The differences in clinical and pedobarographic examination resulted from a prominent adipose layer present within the foot. Those patients did not present pedes cavi in clinical examination, but pedobarographic methods confirmed the presence of these feet anatomy deformities. Pedobarographic examination revealed in these 9 patients a bilateral lack of underfoot pressure under the mid-foot regions (MM, LM).
Pedobarography as a quantitative method of estimation of underfoot pressure distribution is indicated in patients with not fully diagnosed

feet malformations as well as in patients with pedes cavi. The pedobarographic examination is a proper visual diagnostic method of pedes cavi, especially in those with atypical anatomy e.g. presence of adipose layer within the foot.

UNDERFOOT PRESSURE DISTRIBUTION IN PATIENTS WITH MEDIAL MENISCUS INJURY

Lorkowski J[1,2], Trybus M[1], Hładki W[1], Brongel L[1], Teul I[3]

[1]Department of Emergency Medicine and Multitrauma Injury, II Chair of Surgery, Jagiellonian University Medical College, Cracow, Poland
[2]Division of Anatomy and Biomechanics of the Movement System, "Zdrowie" Rehabilitation Centre, Cracow, Poland
[3]Chair of Anatomy, Pomeranian Medical University, Szczecin, Poland

Estimation of the underfoot pressure distribution in patients with changes of medial knee compartment anatomy due to medial meniscus injury.
Twenty patients (6 women, 14 men), aged 17 to 58 with unilateral injury of the medial meniscus. Twenty-five healthy volunteers made up the control group.
Case history, physical examination, radiological study of the knee joints, postural pedobarographic examination and arthroscopy were used. For the analysis of underfoot pressure distribution, the plantar side of the foot was divided into regions according to Blomgren's classification.
Injury of the medial meniscus was observed in arthroscopy in every patient. The following results of postural pedobarography were obtained: in most cases — 16 patients with medial meniscus injury (on affected side) — decreased (by up to 25%) of maximal pressure under H region, increased (up to 20%) maximal underfoot pressure in mid-foot especially in the MT2, MT3 regions, decreased foot contact area with the base (up to 7%). In the remaining four patients, the underfoot pressure changes were not so significant.
In patients with medial meniscus injury of the knee, abnormalities of plantar pressure distribution exist. The most common changes are found in the foot pressure under the heel and mid-foot.

STRESS AND NEURONS CONTAINING CALCIUM BINDING PROTEINS AND NITRIC OXIDE SYNTHASE IN THE RAT AMYGDALA DURING DEVELOPMENT AND AGING

Ludkiewicz B, Klejbor I, Domaradzka-Pytel B, Wójcik S, Dziewiątkowski J, Moryś J

Department of Anatomy and Neurobiology, Medical University of Gdańsk, Gdańsk, Poland

The stress system coordinates the adaptive responses of the organism to stressors of any kind. Amygdala, throughout its connections, activates the hypothalamo-pituitary-adrenal axis by emotional stressors such as unfriendly and unfamiliar environments.
Nitric oxide synthase (NOS) and calcium binding proteins (CaBPs): calretinin (CR), calbindin (CB) and parvalbumin (PV), are widely distributed in amygdala. Neuronal NOS is the brain-specific isozyme that makes nitric oxide, which can probably mediate stress responses in the amygdala. CaBPs may function mainly as a calcium buffer.
The aim of the present study was to ascertain whether NOS-, CR-, CB- and PV-containing neurons of the amygdala are activated in the open field test (OF), a model of emotional, aversive stress stimulation.
The material consisted of rat brains of various postnatal ages (from P0 to P720). OF was applied for 10 minutes, 90 minutes before the death of the animals. The brain sections were double stained using the antibodies against the c-Fos protein (marker of neuronal activation) and against NOS, CB, CR, PV.
Both the number and the distribution of c-Fos- immunoreactive (-ir) cells in the response to the OF were differentiated among individual animals, but the highest density of c-Fos-ir neurons was observed in the ventral part of medial nucleus (MeV; from P4), anterior cortical nucleus (from P7) and bed nucleus of the accessory olfactory tract (BAOT; from P14). The double immunolabelling study revealed that:
— Nuclei of the amygdaloid body show relatively low density of CB-, PV/c-Fos cells and low degree of co-localization and did not differ with regard to both these parameters.
— MeV and BAOT show a high degree of co-localization and density of adequately: NOS/c-Fos and NOS-, CR/c-Fos neurons; these populations are probably a decisive factor regarding the high activation of these nuclei after stress stimulation.

THE MORPHOLOGY AND TOPOGRAPHY OF NUCLEUS AMYGDALOIDEUM CENTRALIS IN PIGS

Łuszczewska-Sierakowska I[1], Eustachiewicz R[1], Radzikowska E[2], Sulejczuk D[3], Krakowska I[1], Matysek M[1]

[1]Department of Animal Anatomy, Agricultural University of Lublin, Lublin, Poland
[2]Human Anatomy Department, Medical Research Institute, Polish Academy of Sciences, Warsaw, Poland
[3]Department of Experimental Pharmacology, Medical Research Institute, Polish Academy of Sciences, Warsaw, Poland

The aim of this research was the morphology and topography of nucleus amygdaloideum centralis in pigs.
The brains of six one-year-old domestic pigs of both sexes were used as the material for the examination. The brains were removed and processed conventionally by microscope (the brains preserved in paraformaldehyde, dehydrated in alcohol and overexposed in turpentine were paraffin embedded; paraffin blocks were cut frontally into 15 μm-thick pieces; the preparations were coloured according to Klüver and Barrer's method and according to Nissel). Corpus amygdaloideum has been an object of numerous neuroanatomical, neurophysiological and histochemical examinations in many species of experimental animals, domestic animals as well as man. Corpus amygdaloideum is like other structures of the limbic system.
The nucleus amygdaloideum centralis is located in one-half of the nucleus amygdaloideum anterior on the level of the lateral nucleus amygdaloideum base. The anterior part of the described nucleus has, on transverse cross-sections, an irregular shape, while at the same time its borders fuse with other neighbouring structures of the nucleus amygdaloideum.
The posterior part of the nucleus amygdaloideum centralis makes a more eliminated cell group which has, on transverse cross-sections, a longitudinally positioned oval shape. The nucleus amygdaloideum centralis, on its medial side, borders with internal capsule fibres and the lateral edge of the optic tract, laterally with the nucleus amygdaloideum lateralis and in the the posterior part with the nucleus amygdaloideum baso-lateralis. The abdominally described nucleus borders with the nucleus amygdaloideum medialis and dorsally with crust cells.
The nucleus amygdaloideum centralis is made up of two distinctly different cell groups. The medial part of the nucleus amygdaloideum centralis anterior end is made up of nervous cells of medium size, relatively well-straining, with fusiform, triangular or oval shape. The lateral part of the described nucleus anterior end and its posterior end are made up of nervous cells of medium size, a bit smaller than the cells described above, as well as relatively weakly-straining and relatively loosely distributed.

ANATOMY OF CALOT'S TRIANGLE IN LAPAROSCOPIC CHOLECYSTECTOMY

Maciejewski R[1,2,3], Torres K[1,4], Chrościcki A[4], Torres A[1,5], Staśkiewicz G[1], Styliński K[5], Łętowska-Andrzejwicz K[1]

[1]*Human Anatomy Department, Medical University of Lublin, Lublin, Poland*
[2]*Second General Surgery Department, Medical University of Lublin, Lublin, Poland*
[3]*Department of Rescue Medicine, UITM of Rzeszów, Rzeszów, Poland*
[4]*Department of General Surgery, District Specialist Hospital, Lublin, Poland*
[5]*Anaesthesiology and Intensive Care Department, District Specialist Hospital, Lublin, Poland*

Proper recognition of particular structures that form the triangle of Calot is essential for the proper and safe performance of laparoscopic cholecystectomy. The triangle of Calot formed superiorly by the hepatic edge, medially by common bile duct and inferiorly by cystic duct usually contains the cystic artery. Proper recognition, ligation and cutting of the cystic duct and cystic artery with branches (dorsal and ventral) remain an integral condition for the removal of the gallbladder. Calot's triangle as an orientation structure which determines the most common location of the cystic artery. The aim of this study was to evaluate the most common position of the cystic artery with its main branches (if visible) and structures forming Calot's triangle during laparoscopic cholecystectomy. The relations of these structures were evaluated in 50 patients that underwent laparoscopic cholecystectomy at the Department of General Surgery of the District Specialist Hospital of Lublin. The anatomical relations of the cystic duct and artery were classified into different types. Correlations between these parameters, basic patient data (age, gender, BMI) and operation parameters were evaluated. The obtained results were statistically analyzed. Evaluation of anatomical conditions in Calot's triangle can be an important predictive factor during laparoscopic cholecystectomy. We observed that some anatomical variations in this region significantly complicate the operation and increase the risk of complications like bile leaking or bleeding caused by improper ligation of the cystic artery and duct.

DISTRIBUTION OF PARVALBUMIN, CALRETININ AND CALBINDIN IN THE CLAUSTRUM AND THE ENDOPIRIFORM NUCLEUS OF THE OPOSSUM

Majak K, Domaradzka-Pytel B, Moryś J

Department of Anatomy and Neurobiology, Medical University of Gdańsk, Gdańsk, Poland

To understand the organization of inhibitory circuitries in the rat claustrum and endopiriform nucleus, the distribution of parvalbumin (PV), calretinin (CR), and calbindin (CB) immunoreactivity (-ir) were investigated within the nuclei.
Brains from six adult opossum (both sexes) were stained for PV, CR and CB and analyzed using fluorescent or confocal microscopy.
Moderate-to-dense CB-ir was observed within the ventral claustrum. The staining was the highest in the posterior half of the nucleus. PV-ir and CR-ir were light in density and distributed evenly throughout the whole extent of the nucleus. In the endopiriform nucleus, light-to-moderate CR-ir was observed within the neurons and neuropil, whereas staining for PV and CB was light. In addition, several CR-ir fibres going towards the adjacent piriform cortex were noted.
Our observations provide baseline information for studies that aim to compare the distribution of calcium binding proteins in different species, particularly rat, monkey and human.

SUBPOPULATIONS OF THYMIC DENDRITIC CELLS IN DEVELOPING THYMUS: PROLIFERATION, DIFFERENTIATION

Malińska A, Brelińska R

Department of Histology and Embryology, Medical University of Poznań, Poznań, Poland

In the study, the manifestation of the dendritic cell (Dc) subpopulation was analysed in rat foetal thymuses between 12 and 21 E and Dc differentiation and proliferative activity were appraised in the thymic microenvironment. In paraffin sections, Dc were identified by expression of S-100 protein and in ME by the presence of Birbeck's granules. Proliferative activity of Dc was evaluated by double labelling with S-100 protein and Ki-67. ME observation of foetal thymuses allowed two Dc subpopulations to be distinguished, differing in ultrastructure and appearing at various stages of foetal life. The first subpopulation migrated to the thymus with the first wave of colonisation (between 13 and 16 E) and appeared in the lymphoepithelial compartment beginning at 15 E. This subpopulation manifested morphological exponents of migration toward the thymic medulla at its stage of formation, in which, in contact with epithelial cells of the region, it differentiated to forms of strongly branched cytoplasm. The first subpopulation of Dc demonstrated proliferative activity in two regions: in 15 E in the capsular connective tissue in direct or close contact with the subpopulation of superficial TEC and in the other region, involving thymic medulla in which Ki67-positive Dc remained in direct contact with superficial TEC, forming perivascular tunnels.
The second subpopulation of Dc appeared in the thymic region starting at 17E, and it remained in the cortex until the end of foetal life. The size of the second Dc subpopulation gradually increased in increasingly deep cortical layers. The cells were vastly equipped in organella and manifested traits of interaction with thymocytes and epithelial cells of the thymic cortex.
The two distinguished subpopulations of Dc probably differed in origin: the first subpopulation migrated to the primordium from the foetal liver and may correspond to myeloid Dc, described in several species; the second subpopulation may correspond to lymphoid Dc, as indicated by their preliminary appearance in the thymic subcapsular zone and differentiation to the lymphoid Dc form, described as IDc.

EFFECTS OF CASTRATION AND OESTROGENS ON THE THYMUS OF FEMALE RATS IN DIFFERENT PERIODS OF LIFE

Malińska A, Kowalska K, Podemska Z, Brelińska R

Department of Histology and Embryology, Medical University of Poznań, Poznań, Poland

Thymic atrophy becomes most evident from the onset of puberty, predominantly due to elevated sex steroid levels. Accordingly, surgical or chemical castration of aged animals causes "regeneration" of the thymus, which is reversed by administration of synthetic sex steroids. Re-examination of this phenomenon revealed, however, that, while castration resulted in increased thymus size, its effects were transient.
Therefore, we have decided to monitor morphological changes that occur in the thymus of six-month-old female rats after ovariectomy in 1, 2 and 4.5 months of life, and then in a subsequent group of castrated rats after a single 1 mg dose of oestradiol 7, 14 and 21 days before decapitation. In each experimental group, the thymuses were evaluated based on morphometric analyses in correlation with epithelial cell organization in different thymic compartments as detected by cytokeratine immunoreactivity and expression of Ki67. In the entire group after castration, thymic weight increased in comparison to 6-month-old control rats. Thymus weight and entire volume showed the highest values in rats castrated in the first month of life. In the same group, the most pronounced decrease

in thymic weight was noted after oestradiol. In animals castrated after 2 and 4.5 months of life, thymic weight in the 6th month corresponded to values demonstrated in control animals in the second and the third months. In all groups after castration, the most pronounced reduction in thymus weight was demonstrated after a single dose of oestradiol injected 14 days before decapitation. The thymuses demonstrated morphological modifications in response to castration and the following oestradiol, the dynamics of which varied between thymic compartments, subpopulations of thymic epithelial cells. The effect of oestradiol was manifested by a decline in number of thymocytes and, in parallel, by high mitotic activity of superficial thymic epithelial cells. The subpopulation of epithelial superficial cells was the first to respond to involution induced by oestradiol, in subseptal/subcapsular layers and, in perivascular tunnel in the medulla, always in direct contact with the connective tissue compartment. The studies showed that the effects of castration on the thymus depended on the age at which the animals were castrated.

THE COURSE VARIABILITY OF THE OPHTHALMIC ARTERY IN SOME SPECIES OF RODENT

Marynowska P[1], Kuchinka J[2]

[1]*Student in Institute of Biology, Świętokrzyski University, Kielce, Poland*
[2]*Department of Comparative Anatomy, Institute of Biology, Świętokrzyski University, Kielce, Poland*

The aim of the investigation was the comparative anatomical analysis of the topography of the ophthalmic artery in some species of rodent.
Investigations were performed on three species of rodent: South American bush rat (*Octodon degus*), Mongolian gerbil (*Meriones unguiculatus*) and Egyptian spiny mouse (*Acomys cahirinus*, Desmarest). The animals were injected using stained acryl latex through the left heart ventricle. The heads of the animals were fixed in 10% formalin, and after calcification in 5% HNO_3, the injected arteries were prepared.
Comparative anatomy analysis showed a different course of the ophthalmic artery in the investigated species. In the South American bush rat, the ophthalmic artery branched from the maxillary artery, in the Egyptian spiny mouse, it is a branch of stapedial artery and in the Mongolian gerbil a high variability of the ophthalmic artery course was observed.

PELVICALYCEAL COLLECTING SYSTEM OF SWINE — OWN ANATOMICAL CLASSIFICATION

Matusewicz M, Szymański J, Puczkowska-Surowiak U, Konarska S, Oszukowski P

Department of Clinical Morphology in the Chair of Anatomy, Medical University of Łódź, Łódź, Poland

The pelvicalyceal collecting system is a clinical concept including urinary tracts from minor calices, through major calices, to the renal pelvis. In humans, there are many classifications of urinary tract types, mainly based on the shape of the renal pelvis. We decided to simplify the classification of renal collecting system to the one with the first-order or primary and the second-order or secondary major calices. Taking into account our consideration, we investigated the shape and main dimensions of the renal collecting system in swine.
The study was carried out on 36 kidneys of adult swine (*Sus scrofa domestica*) of both sexes. We generated the corrosion specimens applying durable, chemohardenable, yellow-stained mass named Plastogen G.
Considering the results, the renal collecting system in swine is an irregular body in shape, visibly elongated in the upper-down dimension. Its length ranges from 47 mm to 92 mm, breadth from 15 mm to 36 mm, and thickness from 7 mm to 21 mm. In the studied material, the renal system originates from minor calices. Their number varies from 4 to 16, forming flattened cones in shape, with diameters of 3 mm to 22 mm and heights of 1 mm to 10 mm. Major calices, taking the form of cylindrical bodies, emerge from minor calices. Always two major calices (primary, secondary or both), mainly the secondary ones, go into the renal pelvis. The primary calices inserted in the renal pelvis were observed in lengths of 7 mm to 34 mm and in diameters of 4 mm to 11 mm; indeed, those which came into the secondary ones were 3–14 mm long and 3–15 mm in diameter. The length of the secondary calices varied from 5 mm to 30 mm, and their diameter from 4 mm to 14 mm. The minor calices in the number of 1 to 5 united to each primary calyx (inserted in the renal pelvis), whereas numbers 2 to 4 united to those inserted in the secondary calices. We paid attention to the configuration where both: 1 to 4 primary calices, but also 0 to 6 minor calices arrange secondary calices. In 17 cases, minor calices (numbers 1 to 5) come directly into the renal pelvis. The renal pelvis is the last part of the urinary tract, which takes the form of a distorted triangle, with the range of 6 mm to 28 mm in breadth and 6 mm to 25 mm in height.

THE REPAIR OF BONE DEFECTS WITH BIOGLASS IMPLANTS. A HISTOCHEMICAL STUDY

Menaszek E[1], Niedzielski K[2,3], Demczuk B[1], Cholewa-Kowalska K[4], Łączka M[4]

[1]*Department of Cytobiology and Histochemistry, Jagiellonian University, Cracow, Poland*
[2]*Clinics of Orthopaedics and Traumatology of the Polish Mother Memorial Institute, Łódź, Poland*
[3]*Unit of Childrens' Orthopaedics and Traumatology, Medical University of Łódź, Łódź, Poland*
[4]*Department of Technology of Glass and Amorphous Coatings, AGH University of Science and Technology, Cracow, Poland*

The objective of this study was to investigate the effect of a new generation of bioglass on bone regeneration. Many ceramics have been used widely as bone implant materials. Among them, bioactive glasses, which were discovered in 1969, have drawn attention because of their favourable biological properties. Since then, numerous glasses and glass ceramics have been extensively studied. Recent findings show very promising results in bone regeneration due to controlled release of the ionic dissolution products of bioactive glasses.
The study was performed on 40 male rabbits. Defects of size 20 mm × 5 mm × 5 mm experimentally made in radius of both limbs were filled with bioglass S2 (CaO-SiO_2–P_2O_5 system) obtained by sol-gel method or SiO_2. Inert silica (SiO_2) glass was used as a control. Both materials were used in the form of granules ranging from 0.5 to 0.8 mm in diameter. After 3, 7, 21, 42 and 90 days from the surgery, the animals were killed and fragments of bones containing implants were excised, frozen in liquid nitrogen and sectioned at 10 μm. The cryosections were processed for examination by light microscopy. The activity of enzymes involved in the bone turnover: Alkaline Phosphatase (ALP), Acid Phosphatase (ACP) and Tartrate Resistant Acid Phosphatase (TRAP), was determined histochemically. The presence of calcium deposits was analysed by Alizarin Red S (ARS) staining. The number of stained cells and the percentage of enzyme-positive surfaces to totally rebuilt tissue surface were measured using MultiScan 11.06 software (CSS Ltd, Poland).
In all samples with implanted bioglass, there was a significant increase in the percentage of ALP, TRAP and ARS labelled tissue surface when compared to samples with SiO_2 ($p \leq 0.05$). Consequently, new bone forming around the bioglass implants was observed in almost all cases.
These results demonstrate the suitability of bioactive glasses as scaffolds for bone tissue engineering as they not only provide an osteoconductive and osteoproductive substrate, but also stimulate the activity of bone cells.

FORMATION OF SPHEROIDS COMPOSED OF HENLE LAYER CELLS AND FAT DROPLETS IN CULTURES OF RAT HAIR FOLLICLES

Niderla-Bielińska J, Jankowska-Steifer E, Moskalewski S

Katedra i Zakład Histologii i Embriologii, Akademia Medyczna of Warsaw, Warsaw, Poland

The aim of the study was to elucidate the structure of dark-looking spheroids, which appeared in the cultures of hair follicles, isolated from rat dermis. These spheroids were particularly numerous when keratinocyte growth medium with a reduced amount of supplements was used.

Light microscopic observations disclosed that these spheroids consisted of fat droplets covered by cells reacting with the antitrichohyalin AE15 monoclonal antibody. These fat droplets originated from subcutaneous adipocytes, damaged during isolation, and remained in cultures. The morphological appearance of cells covering fat droplets studied at the EM level corresponded with that of the cells in the Henle layer of the intact hair follicles in the dermis. EM observations further suggested that in cultures the Henle layer detached from the Huxley layer and that the fat droplets penetrated under the Henle layer resulting in the formation of a spheroid.

Since from 2 cm^2 of rat skin more than 400 spheroids were regularly obtained, it seems conceivable that they could be exploited for isolation of Henle layer cells.

PATHOLOGY OF A THYROID CARTILAGE

Nowaczyk MT[1], Karczmarek I[1], Radziemski A[2], Osmola K[1]

[1]*Department of Maxillo-Facial Surgery, Medical University of Poznań, Poznań, Poland*

[2]*Department of Anatomy, Poznań University of Medical Sciences, Poznań, Poland*

The study aimed at presenting lesions of unknown origin in the thyroid cartilage of a patient operated due to squamocellular carcinoma of the oral cavity floor.

The material originated from a 57-year-old patient operated in the Department of Maxillo-Facial Surgery due to squamocellular carcinoma of the oral cavity floor with metastases to regional cervical lymph nodes T3 Nb M0. During postoperative monthly USG control of cervical lymphoid system, a lesion was detected, suggestive of a metastasis to a paralaryngeal lymph node on the operated side. The image of the lesion suggested a solid tumour of non-uniform echogenic character with central destruction with contact to thyroid cartilage suggesting its infiltration.

In the course of the operation, the suspected lymph node could not be localized and intraoperative USG disclosed pathological tissue linked to thyroid cartilage. On the frontal aspect of the cartilage, on the left hand side close to its upper edge, an oval, elastic-solid tumour was disclosed of 15 × 8 mm in size.

The pathological lesion was covered by a normal perichondrium, which in its central part was evidently soft. Incision of the perichondrium demonstrated whitish, amorphic masses, which could easily be separated from their bed. Margins of the defects were serrated and passed into unaltered cartilage. On the side of larynx interior, the perichondrium was very thin and underwent tearing. In order to prevent development of subcutaneous emphysema, a lower tracheotomy was conducted which was maintained until the cervical wound healed. Histopathological examination of the obtained material disclosed no neoplastic or inflammatory processes.

SUBMUCOSUS PLEXUS OF THE INTESTINES OF CHINCHILLAS (*CHINCHILLA LANIGER*, MOLINA)

Nowak E

Department of Comparative Anatomy, Institute of Biology, Świętokrzyski University, Kielce, Poland

The aim of the investigation was the morphological observation of autonomic structures in mucosa of the intestine in chinchillas (*Chinchilla laniger*, Molina).

Investigations were performed on five chinchillas of either sex, after slaughter in a professional farm. The individual parts of the intestine: duodenum, small intestine and large intestine were rinsed in isotonic salt solution. Three different techniques were used. Tissues were studied in situ with the thiocholine method of Koelle-Friedenwald modified by Gienc for use in macromorphological specimens. For histochemical investigations, tissues from three individuals were cut with a cryostat in 10 μm sections and stained using AChE, SPG and routine histological methods.

Macromorphological observations showed that the submucosus plexus in chinchilla forms a regular net on the whole surface of the intestine. Moreover, small aggregations of neurocytes (3–5 cells) form autonomic ganglia. Histochemical specimens allowed observation of cholinergic and adrenergic fibres. The connection between the submucosus and myenteric plexus was not found.

EXPRESSION OF SELECTED NEOPLASTIC MARKERS (HER2, COX2, MT, Ki-67) IN MAMMARY ADENOCARCINOMAS IN BITCHES

Nowak M[1], Madej JA[1], Dzięgiel P[2]

[1]*Department of Pathological Anatomy, Pathophysiology, Microbiology and Forensic Veterinary Medicine, Faculty of Veterinary Medicine, Wrocław University of Environmental and Life Sciences, Wrocław, Poland*

[2]*Department of Histology and Embryology, Medical University of Wrocław, Wrocław, Poland*

The study was aimed at the immunocytochemical demonstration of HER2 (Human Epidermal Growth Factor Receptor), COX2 (Cyclooxygenase), MT (Metallothionein) and Ki-67 antigen and at examining the relationship between the markers in mammary primary adenocarcinomas in bitches. Material for the studies was sampled in the course of surgery in 60 bitches of various breeds, aging from 6 to 16 years, diagnosed with tumours of the mammary gland. The tumours were verified histopathologically and then immunohistochemical reactions were performed to detect the studied markers.

Expression of HER-2, COX2, MT and Ki-67 was detected using, respectively, mouse monoclonal antibodies, clone PN2A; DakoCytomation, Denmark, (1:50); goat polyclonal antibodies, clone M-19; Santa Cruz Biotechnology, Inc., USA, (1:100); mouse monoclonal antiMT antibodies, clone E9, DakoCytomation, Denmark, (1:100) and anti-Ki-67 antibodies, clone MIB-1, DakoCytomation, Denmark, (1:100). Microphotographs of the preparations were subjected to computer-assisted image analysis in a stand consisting of an Axiophot light microscope (Carl Zeiss). The assembly had the potential to record image patterns and to perform its digital analysis. The analysis took advantage of MultiScaneBase V 14.02 software, working in the Windows environment.

The studies of mammary adenocarcinoma sections demonstrated the presence of HER2 (69% cases), COX2 (57% cases), MT (95% cases) and of Ki-67 antigen (78% cases). Application of statistical techniques (Spearman's correlation) demonstrated a significant positive correlation between intensity of HER2 and Ki-67 expressions, a moderate correlation between intensities of COX2 and Ki-67 expressions and between MT and Ki-67 expressions and a weak correlation between expression intensities of HER2 and COX2.

Expression and correlation between individual markers in tumours of the mammary glands of bitches and of women were similar. This may suggest that the animal model (dog) may be used in studies on neoplastic transformation in human mammary gland.

SIGNIFICANCE OF CAVEOLIN-1 EXPRESSION IN PARIETAL EPITHELIAL CELLS OF THE BOWMAN'S CAPSULE

Nowicki M[1], Ostalska-Nowicka D[2], Miskowiak B[1], Zachwieja J[3], Partyka M[1], Witt M[4]

[1]*Histology and Embryology, Poznań University of Medical Sciences, Poznań, Poland*
[2]*Paediatric Nephrology, Poznań University of Medical Sciences, Poznań, Poland*
[3]*Paediatric Nephrology, Poznan University of Medical Sciences, Poznań, Poland*
[4]*Anatomy, Technical University, Dresden, Germany*

To analyze the expression of caveolin-1 in normal human kidneys and during diseases leading to nephrotic syndrome in children and compare its pattern to results observed in both human and animal control samples. The study group was composed of 104 children diagnosed with minimal change disease (MCD), focal segmental glomerulosclerosis (FSGS), lupus glomerulonephritis (LGN) and Schoenlein-Henoch glomerulopathy (SH). The research protocol employed direct immunohistochemical assay with the use of mono- and polyclonal antibodies against caveolins. Additionally, the kidney samples of Wistar rats, wild type mice and caveolin-1 deficient mice were analyzed in the study.
In the control human samples, caveolin-1 was most abundant in the muscle layer of blood vessels and PECs. Expression of caveolin-1 in PECs was significantly lower in children diagnosed with FSGS and LGN than in MCD, SH and controls. Moreover, FSGS and LGM patients who performed proteinuria lower than 50 mg/kg/day were accompanied by lipiduria. In the control animal tissues, except for knock-out mice, caveolin-1 was present in distal convoluted tubules, PECs, endothelial cells and muscles.
Caveolae are extremely conservative elements of the cell membranes of parietal epithelial cells in the Bowman's capsule. They could be excluded from the cell membrane only in response to the dramatic cell reconstruction as observed in focal segmental glomerulosclerosis and lupus erythematosus glomerulopathy. Parietal epithelial cells of the Bowman's capsule in human kidneys participate probably in cholesterol homeostasis by regulation of its primary urine uptake from the filtration space of glomerulus.

ANATOMY OF THE SEPTOMARGINAL TRABECULA IN THE ADULT HUMAN HEART

Nowiński J, Kosiński A, Grzybiak M, Piwko G, Kuta W, Makarewicz W

Department of Clinical Anatomy, Medical University of Gdańsk, Gdańsk, Poland

The septomarginal trabecular is an element found in every human heart, in the hearts of all primates and in interior mammals. It is distinguished as a muscular band deriving from the interventricular septum. This structure connects the interventricular septum with the anterior wall of the right ventricle. It has a connection with anterior papillary muscle, also called the large one. However, there are an abundant number of studies focusing on septomarginal trabecula, but the opinions are not homogenous. Considering the incoherence of views in the range of its structure and phylogenesis, as well as numerous publications suggesting its significant influence on haemodynamics and electrical phenomena in the heart, the trabecula underwent a detailed analysis. The study was performed on the material of 100 hearts of adult humans of both sexes, aged 19 to 79 years. The hearts were preserved in formalin-ethanol solution. The trabecula was present in all studied hearts. The size and the run of the trabecula differentiated vastly. The width of the trabecula was measured in the region of its branching-off of the supraventricular crista. The parameter revealed some significant differences between the specimens ranging from 2 to 10 mm. In many cases, the trabecula became thinner the further it had run from the interventricular septum to the anterior wall of the right ventricle. However, the width along the trabecula was constant in the majority of cases. Another element of the analysis was the evaluation of the level it derived from the interventricular septum. In most cases of studied hearts, it had its beginning at 1/3rd (38 cases — 38%) and 2/5th (27 cases — 27%) of the upper part of the septum. The results of the study confirmed that septomarginal trabecula is a constant element of the human heart, connecting the interventricular septum with the anterior wall of the right ventricle, and its morphological structure is significantly diverse. In all studied hearts it was a visibly and fully-developed, solid muscular band, in most cases branching off the upper part of the interventricular septum.

VASCULAR SEGMENTS OF THE HUMAN PANCREAS IN CORROSION CASTS AND CT SCANS

Palczak A[1], Król A[1], Rotkiewicz A[2], Wolski A[2]

[1]*Department of Normal and Clinical Anatomy, Medical University of Łódź, Łódź, Poland*
[2]*Department of Radiology, Medical University of Łódź, Łódź, Poland*

Numerous embryological, anatomical and clinical observations show that the pancreas has a complex segmental structure. The existence of these segments plays an important role in limited surgical resection. The purpose of our paper was to evaluate the accuracy of helical CT three-dimensional (3-D) reconstruction in the visualization of pancreatic segments and small arteries compared to corrosion casts.
In our study, we used 15 helical angio-CT scan 3-D reconstructions with intravenous contrast injection from patients of the Department of Radiology and 5 Plastogen G corrosion casts of the arteries of pancreases obtained from cadavers. The resolution of the images from helical angio-CT obtained by scans of 0.625 mm was 0.3 mm. We used the Maximum Intensity Projection (MIP) technique for visualizing vessels of small diameter.
The CT scan 3-D reconstruction allowed us to observe segmental arteries and their branches up to 1 mm of diameter. We identified similar segments including the minor segments in the 3-D reconstruction as in the corrosion casts. Our study confirmed that the pancreas is always formed by two major vascular parts, the head and tail, separated by a less vascularised area. These parts are usually divided further into four minor segments: the anterior head, posterior head, body and tail.
CT helical scan three-dimensional reconstruction (3-D) is a useful method of visualizing pancreatic vessels and could be used in surgical practice as an alternative for classical methods such as angiography. CT helical scan (3-D) allows pancreatic vessels to be shown in order to better recognize pancreatic segments as compared to corrosion casts.

CONSTRUCTION AND ANALYSIS OF THE FEM MODEL OF FOETAL SHOULDER BLADE BONE

Panek M[1], Frątczak R[1], Słowiński J[1], Kędzia A[2], Stankowski J[2]

[1]*Institute of Materials Science and Applied Mechanics, Wrocław University of Technology, Wrocław, Poland*
[2]*Department of Normal Anatomy, Medical University of Wrocław, Wrocław, Poland*

In recent times, the finite element method is one of the more widely applied investigative methods in many fields of science. It is widely used in industry, architecture, motorization and aviation, and in recent years in

medicine, orthopaedics, dentistry and anatomy. The finite element method enables three-dimensional visualisation of the stress and strain state and tell us about the deformation of an examined body. Increasingly, it is becoming the general course of behaviour, and, besides investigations of real objects, is used to create virtual models and conduct research with its usage. So far, the authors have not met such a case of numerical analysis of the foetal shoulder blade in the available literature. The goal of the presented work was the preparation of a three-dimensional virtual model of the foetal shoulder blade and the finite element method analysis of places of accumulated stress caused by applied loads. The studied bone, after preparation, was immersed in epoxy resin (Epidian 5). It was made 20's intersections in sagittal plane, then each layer was scanned and edited in a graphics program (Gimp), by modification of brightness, contrast and colour settings. To contrast the examined structures (bone and resin), the samples were additionally coloured to obtain clear separation of the studied elements. The pictures obtained in such a way were transformed onto a set of points and lines (with the author's software of Frątczak, designed for folding three-dimensional geometry from flat images), which was read into Ansys software (designed for FEM analysis). Afterwards, by linking the appropriate points and lines, a set of layers was obtained which described the shoulder blade solid. In next step, this solid was divided into a mesh of finite elements (model discretization). During the division of the model into a mesh, tetra element types were used, causing each element to have 10 nodes and three degrees of freedom in every node (Solid 92). The material model which was used to conduct the simulation was characterized by Young's elasticity modulus (E = 1000 MPa) and Poisson coefficient equal to 0.42. As a result of the conducted investigation, a discrete model (FEM) of the foetal shoulder-blade bone was obtained, which allowed the realization of a wide range of simulations for different cases of loading, both static and dynamic. The results of the simulation make possible an estimation of the appearance the places which are subjected on damages and loss of material cohesion (cracks, fractures and oversized deformations). Simple static loads in the frontal and sagittal planes do not create a risk of shoulder-blade fracture. The biggest stress concentration occurs in the shoulder appendix region. Investigations of the finite element method give the places that are exposed on potential injuries as possibilities of designation.

THE FEM METHOD OF ANALYSIS OF THE FOETAL CLAVICLE BONE

Panek M[1], Frątczak R[1], Słowiński J[1], Kędzia A[2], Szymański M[2]

[1]*Institute of Materials Science and Applied Mechanics, Wrocław University of Technology, Wrocław, Poland*
[2]*Department of Normal Anatomy, Medical University of Wrocław, Wrocław, Poland*

Until now, the finite element method (FEM) has been used in the technical sciences (building industry, durability of materials, mechanics of fluids). It has a wide field of use, except for bioengineering, especially in biomechanics, orthopaedics and dentistry. It allows the evaluation of the stress and strain state of examined objects and what it for this goes potential points of damages, without the necessity of constructing device prototypes and building, sometimes expensive, research statements. Until now, FEM was not applied in the analysis of foetal clavicles. The goal of the presented work was the potential places of break of continuity in osseous tissue of foetal clavicle analysis, for a set load, by application of the finite element method. The preparation of the foetal clavicle was executed in the initial stage of investigation and then the specimen was flooded in epoxy resin (Epidian 5). The next stage was to obtain the cross-sections necessary to create the virtual three-dimensional model. For this reason, there was a 1 mm layer removed from the specimen. Thanks to the computer scanning of the obtained surface and editing in a graphics program (Gimp), a digital image was obtained which represented a cross-section of the investigated clavicle. Frątczak's program allowed the conversion of these pictures and the construction a three-dimensional model of clavicle. A cloud of points was received which was linked by lines, such as: Bezier's curves, straight lines and contiguous. The planes were stretched on the received lines: simple — described by three lines, and complex — described by Bezier's curves.

The constructed 3-D model was elaborated with the finite element method using Ansys 8.0 software. The dividing on the finite element mesh was conducted using a tetra element. The following material properties were assumed during the investigation: Young's modulus 1000 MPa and Poisson coefficient equal to 0.42. In the simulation, the surfaces of the paracentrical end were fixed in all three axes, while the lateral end surface was loaded by force which lay perpendicular to the long bone axis and had a 100 N value. Analysis of the stress state in such a loaded structure showed a stress concentration which occured in the middle of the diaphysis. This concentration could lead, in certain cases, to the damage of bone tissue. The results of clinical investigations confirm these conclusions.

ROLE OF NF-κB IN CELL APOPTOSIS AND PROLIFERATION IN RAT RENAL TUBULES AFTER ACUTE EXERCISE

Piotrowska A[1], Podhorska-Okołów M[1], Iżykowska I[1], Dzięgiel P[1], Zabel M[1,2]

[1]*Department of Histology and Embryology, Medical University of Wrocław, Wrocław, Poland*
[2]*Department of Histology and Embryology, Poznań University of Medical Sciences, Poznań, Poland*

It is widely accepted that acute physical exercise can induce pathological changes in untrained organisms. Our previous studies have demonstrated that exercise-induced apoptosis was confined to the renal distal tubular cells. Under normal conditions, the process of regeneration via neighbouring cell proliferation occurs in response to tubular cell injury. NF-κB is a transcription factor that plays a pivotal role in the expression of various target genes regulating both cell proliferation and apoptosis.

The aim of this study was to examine if NF-κB could control exercise-induced apoptosis and cell proliferation in renal proximal and distal tubules.

Twenty male Wistar rats formed groups of running (n = 10) and control animals (n = 10). The animals from the exercise group were subjected to running on a treadmill at 1.0 km/h until exhaustion. The control animals remained in their cages throughout the experiment.

Apoptosis was detected in paraffin sections by the TUNEL technique. Expressions of Ki-67 and NF-κB were examined on paraffin sections by immunohistochemistry, using mouse monoclonal antibodies and rabbit polyclonal antibodies, respectively.

Apoptosis was detected only in the cells of distal tubules. Expression of nuclear proliferation marker Ki-67 was more prominent in distal renal tubular cells. Expression of NF-κB was different in both renal tubules; in proximal tubular cells, it was confined to the nucleus, while in distal tubular cells to the cytoplasm.

The obtained results could suggest that apoptosis of distal tubular cells is followed by cell proliferation that could allow the regeneration of damaged cells. The nuclear translocation of NF-κB could be involved with the protection of proximal tubular cells against apoptosis while the cytoplasmic location could suggest that apoptosis inhibition in distal tubular cells does not exist.

EARLY DIFFERENTIATION OF THE FIRST PHARYNGEAL ARCH IN HUMAN EMBRYOS DURING THE FIFTH WEEK

Piotrowski A, Woźniak W

Department of Anatomy, University of Medical Sciences, Poznań, Poland

The pharyngeal arches are temporary structures developing during the 4 and 5 weeks, and they contribute to the formation of the head and neck. Each arch consist of: 1) mesenchymal core from the paraxial mesenchyme and neural crest cells; 2) pharyngeal pouch which is lined by endoderm; 3) pharyngeal cleft (groove) which is covered by ectoderm; and 4) pharyngeal membrane which extends between two adjacent arches. In each arch, there is also a nerve and artery arising from the aortic sac. The first arch contributes very much to the development of the face, mouth cavity and ear. The aim of study was to trace the development of the structures derived from this arch in embryos aged 5 weeks.
Investigations were made on 10 embryos aged 5 weeks (developmental stages 13, 14, 15). Embryos were from the collection of the Department of Anatomy of the Medical University in Poznań. All embryos were embedded *in toto* in paraplast and were serially sectioned in various planes. Sections were stained with routine histological methods and were impregnated with silver.
In stage 13 (32 post-fertilization days), four pharyngeal arches were present. Pharyngeal arch 1 divides into maxillary and mandibular processes and these processes, together with frontonasal prominence, bound the primary mouth (the stomodeum). The mandibular processes of this arch begin to fuse. The first pharyngeal pouch laterally forms a wide tubotympanic recess. In embryos at stage 14 (33 post-fertilization days), the maxillary processes of the first arch are more prominent and are in contact with lateral nasal processes. The pharyngeal cleft invaginates deeply and forms the primordium of the external auditory meatus. In embryos at stage 15 (36 post-fertilization days), the mandibular processes fuse and the maxillary processes grow laterally and the external auditory meatus is well developed. The primordia of the auricular hillocks in pharyngeal arches 1 and 2 develop.

THE INFLUENCE OF PHARMACOLOGICALLY INDUCED IMMUNOSUPPRESSION ON BLOOD LEUKOCYTE ACTIVITY IN CHICKENS STIMULATED WITH ANTIGEN

Pliszczak-Król A, Janaczyk B, Graczyk S

Division of Pathophysiology, Department of Pathological Anatomy, Pathophysiology, Microbiology and Forensic Veterinary Medicine, Wrocław University of Environmental and Life Sciences, Wrocław, Poland

The aim of study was to investigate if experimental dysfunction of bursal- and thymic-dependent lymphatic structures affects blood leukocyte activity and organization and the functions of the organelles of these cells.
The investigations were carried out on 42 chickens. The birds were divided into three groups with 14 chickens in each group. The first group served as a control. The second group included birds treated with cyclophosphamide (CY) for B lymphocyte dysfunction. For the induction of thymic-dependent cell dysfunction, the birds belonging to the third group were treated with cyclosporine A (CsA). Cytostatics were administered by i.m. injections during three consecutive days in 100 mg/kg b.w. doses. In addition, 7 chickens from each group were immunized with SRBC on the fourth day of the experiment. Blood for tests were collected on the sixth day after immunization. The following parameters were evaluated: leukocyte count, leukogram, phagocytic activity of leukocytes toward yeasts, the ability of leukocytes for nitro blue tetrazolium reduction (NBT test), and the ability of mononuclear leukocytes for the creation of radial segmentation of nuclei — RS (test of cytoskeleton ability for reorganization).
Administration with CY and CsA caused a slight decrease in leukocyte numbers in chickens, which became greater after immunization with SRBC. Simultaneously, in the chickens after CY administration and immunization with SRBC, the percentages of lymphocytes and heterophils were changed — the percentage of lymphocytes was increased and the percentage of heterophils was decreased. It was also observed that the percentage of phagocytic cells was increased and the ability of leukocytes for NBT reduction was intensified. The treatment with cyclosporine A had the opposite effect. The analysis of cells with segmented nuclei showed that the treatment of birds with CsA and immunization SRBC caused an increase in the percentage of cells with RS.

THE INFLUENCE OF SPLENECTOMY OR CYCLOPHOSPHAMIDE TREATMENT ON LEUKOCYTES AND SOME HAEMOSTATIC PARAMETERS IN RATS STIMULATED WITH LPS

Pliszczak-Król A, Janaczyk B, Graczyk S

Division of Pathophysiology, Department of Pathological Anatomy, Pathophysiology, Microbiology and Forensic Veterinary Medicine, Wrocław University of Environmental and Life Sciences, Wrocław, Poland

Splenectomy (Spx) and cyclophosphamide (CY) treatment are followed by an increased risk of infection and DIC syndrome. This suggests that they may alter coagulation processes and haemopoietic function. The aim of this study was to investigate the effect of Spx or CY treatment on leukocytes and some haemostatic parameters in rats with LPS induced systemic inflammation.
Sixteen- to twenty-week-old female Wistar rats underwent Spx or received a single dose of CY (25 mg/kg b.w.). Two to three weeks after Spx or 72 hours after CY administration, blood was collected for tests. Some of the animals received LPS from *E. coli* (0.5 mg/kg b.w.) 24 hours prior to material collection. Leukocyte number and leukogram were evaluated. Prothrombin time (PT), thrombin time (TT), activated partial thromboplastin time (APTT) and fibrinogen and platelet count were evaluated.
Leukocyte number increased after Spx and decreased considerably after CY treatment. LPS administration almost doubled that number in control and Spx animals. In CY rats, it increased only slightly. The number of thrombocytes was similar in Spx and CY treated rats, but LPS administration resulted in a considerable decrease of this number, especially in the CY/LPS group. PT was slightly prolonged in Spx as well as in CY treated rats, and LPS administration did not seem to influence it. TT was shortened in Spx LPS treated rats. In addition, APTT was shortened in that group, but in the case of this parameter it corresponded to results in CY treated animals. Surprisingly, APTT in Spx and CY/LPS treated rats did not change. Levels of fibrinogen increased slightly in the CY group. However, after LPS administration, there was a dramatic increase of fibrinogen levels in both Spx and CY treated animals. These results show that Spx and CY administration, as well as systemic inflammation, have little effect on coagulation times. However, they distinctly influence fibrinogen and platelet counts, which indicates that changes in haemostasis after Spx or chemotherapy have their main source in those factors levels and/or function.

THE EFFECT OF ACUTE AND ENDURANCE EXERCISE ON METALLOTHIONEIN EXPRESSION IN RENAL TUBULES OF RATS

Podhorska-Okołów M[1], Dzięgiel P[1], Dolinska-Krajewska B[1], Cegielski M[1], Zabel M[1,2]

[1]*Department of Histology and Embryology, Medical University, Wrocław, Poland*

[2]*Department of Histology and Embryology, University of Medical Sciences, Poznań, Poland*

The induction of exercise-induced apoptosis in organs not actively involved in exercise, such as the kidneys, could be a result of oxidative stress. Metallothionein (MT) has a protective effect on the cell against oxidative stress and apoptosis. We have previously demonstrated an increased incidence of apoptosis in distal tubular cells and collecting ducts in rat kidneys after acute exercise. The present study was designed to test the hypothesis that MT may play a protective role in rat renal tubules against exercise-induced apoptosis after acute exercise and regular training. Male Wistar rats were divided into control, acute exercised and 8-wk regularly trained groups. The kidneys were removed after a rest period of 6 h and 96 h. The ultrastructure of renal tubular cells was examined by electron microscopy. Apoptosis was detected in paraffin sections by the TUNEL technique. Expression of MT was examined by immunohistochemistry. The level of lipid peroxidation TBARS (thiobarbituric acid reactive substances) was assayed in renal tissue homogenates. After acute exercise, the occurrence of apoptosis was restricted to distal tubules and collecting ducts of rat kidneys, whereas the proximal tubules remained unaffected. The 8-wk training did not result in increased apoptosis in tubular cells. MT expression was confined exclusively to proximal tubules in all groups. However, it was significantly increased in acutely exercised animals, as compared to control and trained rats. After the 8-wk training, MT expression remained unaltered compared to the control group. TBARS levels were significantly increased after acute exercise, while after regular training they remained unchanged. A significant correlation between TBARS levels and MT expression was demonstrated. The findings could suggest a protective role of MT against oxidative stress and apoptosis in proximal tubular cells.

THE EFFECTS OF AXOTOMY ON THE CHEMICAL CODING OF NEURONS OF THE PARACERVICAL GANGLION INNERVATING PIG UTERI

Podlasz P, Wąsowicz K

Division of Animal Anatomy, Department of Functional Morphology, Faculty of Veterinary Medicine, University of Warmia and Mazury, Olsztyn, Poland

The aim of the study was to investigate the reaction of neurons responsible for innervation of the uterine horn located in the paracervical ganglion (PCG) of the pig to hysterectomy-induced axotomy. The expression of tyrosine hydroxylase (TH), dopamine hydroxylase (DβH), choline acetyltransferase (ChAT), vesicular acetylcholine transporter (VAChT), neuronal nitric oxide synthase (nNOS), neuropeptide Y (NPY), vasoactive intestinal polypeptide (VIP), pituitary adenylate cyclase-activating peptide (PACAP), galanin (GAL), somatostatin (SOM) and substance P (SP) was studied in control and experimental animals. Methods used were: retrograde axonal tracing combined with double immunofluorescence to determine the neurochemical coding of neurons innervating the uterus under normal conditions and after axotomy, as well as RT-PCR and in situ hybridization to study expression at the molecular level. Immunohistochemical methods revealed that the number of neurons containing TH and DβH decreased from 100% to 63 % and from 100% to 65%, respectively. The expression of GAL rose dramatically (from 0% to 44% of neurons) and the number of neurons containing NPY rose only slightly (from 64% to 77%). No changes were observed in the number of neurons containing other substances. In situ hybridization and RT-PCR studies confirmed the immunohistochemical results except for NPY where no changes were found. Presumably, this was due to the retention of NPY in the cell somata, and not because of the rise of NPY production. Particularly interesting was the lack of changes in the expression of neuroprotective peptides — VIP and PACAP, whose expression significantly rose in rodents after axotomy. The presented data show significant differences in reaction of neurons to axotomy between species.

THE INFLUENCE OF ETHANE 1.2-DIMETHANESULPHONATE ON HeLa CELLS

Polak U, Warchoł JB

Department of Cell Biology, Karol Marcinkowski University of Medical Sciences, Poznań, Poland

Ethane 1.2-dimethanesulphonate (EDS) is a glutathione-dependent alkylating agent, which induces apoptotic death of cells, although the molecular basis of this processes is not well understood. Furthermore, the agent destroys HeLa cells. Our study was performed to examine an effect of EDS on HeLa cells and to determine whether this process is influenced by inhibition of protein synthesis using cycloheximide (CHX).
The experiments were carried on HeLa cells growing in RPMI 1640 medium, supplemented with 10% FBS (37°C; 5% CO_2). The HeLa cells were exposed to EDS alone at concentrations of 10, 20, 50 mmol/l or EDS with constant concentration of CHX (100 µmol/l). Simultaneously, the cells were treated with CHX alone and DMSO (at the highest concentration used for dissolving EDS). Morphological changes were observed after 24 and 48 h intervals, under a fluorescent microscope, using propidium iodide and Hoechst 33, 342 staining.
After incubation with EDS alone there were observed chromatin changes different from those usually noticed in apoptotic cells. After simultaneous treatment with EDS and CHX, apoptotic cells were noticed there.
The ultrastructure of HeLa cells after treatment with EDS alone showed many vesicles in the cytoplasm and chromatin condensation without nuclear fragmentation. After incubation with EDS and CHX, the cells showed typical apoptotic changes, such as lumpy chromatin condensation, fragmentation in the nuclei and changes in mitochondrial structure.
The obtained results revealed that the synthesis of antiapoptotic proteins plays a very important role in HeLa cell death induced by EDS.

ANGIOARCHITECTURE OF INTRATESTICULAR VESSELS OF HUMAN AND BOVINE MASCULINE GONADS

Polguj M, Bolanowski W, Jędrzejewski KS

Department of Normal and Clinical Anatomy, Chair of Anatomy, Medical University of Łódź, Łódź, Poland

Topography of mediastinum testis is one of the most significant structural differences between human and bovine testis. In humans, the mediastinum testis is located at the posterior margin of the gonad in its proximal part. In bovines, the mediastinum testis is located in the central part of the gonad. The consequence of this difference in mediastinum testis topography influences the vascular pattern of masculine and bull gonads.
The aim of the study was to compare the intratesticular vascular network of masculine and bovine gonads with special focus on differences resulting from mediastinum testis localisation.
Two groups of specimens were compared. Both groups consisted of 50 corrosive die casts of intratesticular and spermatic cord vessels, respectively of bovine and human gonads. In twenty gonads of each group only arterial vessels were injected, in the next 20 — only veins, while in 10 gonads both arteries and veins were injected. The die casts were examined with stereoscopic binocular and optical microscopes. Photographic documentation was collected for each of the 100 specimens.
The different intratesticular vascular patterns in humans and bulls were observed. In humans, intratesticular arteries come off the arterial network of tunica albuginea and mediastinum testis. The first ones run centripetally, while the latter run centrifugally. Analogically, intratesticular veins empty into the tunica albuginea venous plexus running centrifugally, and those emptying into the mediastinum testis plexus run centripetally. In bulls, arterial vessels run centripetally and later form a helical, screw-like layer to give off centripetal branches. Venous vessels run centripetally and empty into the venous plexus of the tunica albuginea.

MORPHOLOGICAL ANALYSIS OF SUBLINGUAL GLANDS IN THE PRENATAL PERIOD OF PIGS

Pospieszny N[1], Juszczyk M[1], Pospieszna J[2]

[1]*Department of Anatomy and Histology, Faculty of Veterinary Medicine, University of Environmental and Life Sciences, Wrocław, Poland*
[2]*Institute of Basic Electrotechnic and Technology, University of Technology, Wrocław, Poland*

The morphology and development of the sublingual salivary glands in the prenatal period of the pig has not yet been explained completely [Bielańska-Osuchowska Z (2004) Zarys organogenezy. Różnicowanie się komórek w narządach. PWN, Warszawa, 261–263, Marrable AW (1971) The embryonic pig. A chronological account. Pitman Medical, 17–98, Pospieszny N (1989) Morphological analysis of the cervicothoracic ganglion of 10-week-old pig foetuses. Anat Histol Embryol, 18: 327–333]. The research was carried out in order to assess the morphology, histology and development of the sublingual glands in the prenatal period of the pig.
The study included 119 foetuses aged 36 to 120 days, divided into six groups of age . The morphological characteristic, vascularisation and innervation were examined by morphological, statistical, radiological and histological methods.
The development of the sublingual glands is correlated with the development of surrounding organs. The most intensive growth was between the 10th and 11th week of prenatal life. The comparison of the examined parameters of the sublingual glands with the mandibular gland revealed that the level of development is similar in both organs. In the course of pregnancy, the connective tissue decreases, while the secretory parts and excretory ducts proliferate. The longitudinal dimension of the sublingual glands increases faster than the adequate dimension of the mandibular gland. The comparison of the morphological data revealed that the sublingual glands develop simultaneously on both sides of the foetus. The morphology and development of the sublingual glands were not influenced by the sex of the foetus or its position in the uterus.

MENTALIS NERVES IN PIG FOETUSES ON THE 110TH DAY OF FOETATION

Pospieszny N[1], Rozpędek W[1], Pospieszna J[2]

[1]*Department of Anatomy and Histology, Faculty of Veterinary Medicine, University of Environmental and Life Sciences, Wrocław, Poland*
[2]*Institute of Basic Electrotechnic and Technology, University of Technology, Wrocław, Poland*

The mentalis nerves (*nn.mentales*) are a branch of the mandibular alveolar nerve, which in turn belongs to the mandibular nerve. When talking about the mentalis nerves, we mean the nerves leaving the mandibula canal through the mentalis openings in the mandibula. The mentalis nerves form the following branches: mentalis branches and labial mandible branches. Those branches sensorially equip the area of the mentalis and, partly, the mandibula branches. Through their mediation, it is possible to transfer touch sensations from suitable touch receptors which are on the labium surface, on the mentalis and also on the tentacles. It is one of many elements indispensable during nutrition intake. Because of the lack of elaboration about these nerves in swine in the prenatal period and because of our curiosity, we decided to analyse thoroughly the behaviour of major mentalis branches in swine foetuses to define the number of major branches, the number of mentalis openings and their localization and to compare subjects of different side and gender.
The research was carried out on six pig foetuses, which came from one litter, on the 110th day of foetation (3 male and 3 female). The material was fixated with 5% formaldehyde solution and then it was prepared. Preparation was done under an optical microscope. During preparation, the method of neurofibrillary syringing with 2–3% acetic acid solution was used to expose neurofibrils in a better way. Detailed photographic documentation was also carried out; this was done using a Nikon digital camera. The photographs were then processed using Lucia computer software. The software enabled precise analysis of the examined material.
The mandibular alveolar nerve, in its last fragment, has a different number of branch lines in the form of mentalis nerves. The number fluctuates from 5–8. It corresponds with the number of mentalis openings in the mandibula, through which the mentalis nerves leave the mandibula canal. One cannot find distinct differences in the mentalis nerve branch course after leaving the mandibula canal in subjects of different gender. In addition, the functioning of both the mentalis branches and the labial mandible branches is similar on both sides. The total number of nerve branches amounts from 10–14 on both sides. The mentalis openings occur in different numbers from 6–9. Their localization is variable and there is some kind of asymmetry in their number and localization, but it is not considerable.

THE STOMATOGNATHIC SYSTEM — PROCESS OF VARIABILITY

Prośba-Mackiewicz M[1], Mackiewicz J[2]

[1]*Department of Dental Techniques and Dysfunctions of the Masticatory System, Medical University of Gdańsk, Gdańsk, Poland*
[2]*Department of the Maxillo-Facial Surgery, Medical University of Gdańsk, Gdańsk, Poland*

The aim of the paper is to present an idea of the stomatognathic system and to describe the variability of the processes that take place after loss of the teeth.
The stomatognathic system is a morphological and functional unit with occlusal and articular relations between the upper and lower dentition arches. It describes the functional relations of teeth or in situations when the loss of teeth has stimulated other functions.
Patients with full natural dentition, partial dentition and edentulous were investigated.
Clinical investigations with lingual — functional tests: of the deglutition, articulation of the phonemes and localization of the plica of the sublingual salivary gland, were used.
In the group with edentulous patients, two pathological functions were observed.
The results of the investigations are a base for the presentation of the scheme of the stomatognathic system after loss of the teeth — in processes of variability.

THE MORPHOLOGY OF THE PINEAL GLAND OF THE COMMON GULL (*LARUS CANUS*)

Prusik M[1], Kalicki M[2], Lewczuk B[1], Bulc M[1], Przybylska-Gornowicz B[1]

[1]*Division of Histology and Embryology, Department of Functional Morphology, Faculty of Veterinary Medicine, University of Warmia and Mazury, Olsztyn, Poland*
[2]*Municipal Zoological Garden of Seacoast, Gdańsk, Poland*

The morphology of the avian pineal gland shows a large interspecies variability. Until now, detailed studies concerning the histology and ultrastructure of the pineal organ have been carried out only in a few birds, mainly domestic species — the chicken, the turkey and the goose. Our knowledge about the structure of pineals in wild avian species is still poor. In the present study we have examined the pineal gland of the common gull.
The study was performed on the pineal glands of young common gulls (*Larus canus*) living in natural conditions, which had been untreatably injured (usually serious multiple fractures) during strong storms and qualified for euthanasia. The birds were killed by administration of a lethal dose of pentobarbital and then the pineals were immediately removed and prepared for histological as well as ultrastructural studies.
The gull pineal gland consisted of a wide, triangular, superficially

localized distal part and a narrow, elongated proximal part, attached via the choroid plexus to the diencephalon. The pineal was covered by a thin capsule closely connected to the dura mater. The connective tissue penetrating from the capsule inside the organ divided the parenchyma into small, incompletely separated lobes. The pineal represented a follicular type with elongated follicles in the distal part and small, round follicles in the proximal part of the organ. They were formed by two or more layers of cells: 1) columnar or cuboidal cells in contact with the lumen and 2) oval cells forming the outer part of the follicular wall. Sometimes, clusters of cells characteristic for the pineal of the solid type were observed in the proximal part of the gland. Based on ultrastructural studies, pinealocytes of rudimentary-receptor type and ependymal-like supporting cells were identified among the cells limiting the follicular lumen. The oval cells, laying on the outer part of the follicular wall or forming clusters without lumen, were represented by secretory pinealocytes and astrocyte-like supporting cells. Rudimentary-receptor pinealocytes differed with each other in size and shape; however, they shared a common feature which was the stratified distribution of organelles, which create zones with rough endoplasmic reticulum, the Golgi apparatus and mitochondria above the nucleus. In contrast, secretory pinealocytes formed a rather uniform population and contained irregularly dispersed organelles.

DIFFERENTIATION OF SKELETAL UNITS OF THE MANDIBLE IN THE HUMAN EMBRYOS

Przystańska A, Bruska M, Woźniak W

Department of Anatomy, Poznań University of Medical Sciences, Poznań, Poland

The mandible, being a major part of the viscerocranium, is the second bone of the skeleton to ossify, the clavicle being the first. According to Sperber (1989) the mandible consists of 6 skeletal units: coronoid, angular, condylar, basal (or neural), alveolar and mental. During development of the mandible, several important factors affect and control its growth. These factors include: 1) Meckel's cartilage which forms a morphogenic template that guides the mandibular bone, 2) epitheliomesenchymal interactions between oral epithelium and subjacent mesenchyme, 3) prenatal muscular activity, 4) the growth and changing the shape of the tongue, 5) inferior alveolar nerve, 6) teeth.

The aim of this work is to trace the development of the mandible in human embryos between 5 and 8 weeks with special consideration to differentiation of the skeletal units.

For the study, 20 embryos from the Collection of the Department of Anatomy Medical University of Poznań were used. The embryos were staged according to 23 developmental stages. Serial sections of embryos were made in frontal, sagittal and horizontal planes. Sections 10 μm thick were stained with haematoxylin and -eosin, cresyl violet, and impregnated with Bodian's protargol.

In embryos at stages 13, 14, and 15 (5 weeks), the mandibular processes of the first pharyngeal arch fuse in the median plane and the maxillary processes are prominent (stage 13). At the end of the 5th week (stage 15), the medial and lateral nasal processes differentiate and the maxillary process elongates. In the mandibular processes, condensed mesenchyme forms Meckel's cartilage in the centre of these processes.

In embryos at the 6th week (stages 16, 17 and 18), Meckel's cartilage is in the shape of an elongated rod and passes from the otic capsule to the future chin. The trunk of mandibular nerve lies superiorly and medially to the cartilage. From the trunk, arise the lingual and inferior alveolar nerves. The mandible appears externally to Meckel's cartilage.

In embryos at stage 18, ossification of the mandible begins. The initial ossification site is at the future mental foramen and is considered the primary growth centre.

During the 7th week (stages 19, 20), the mandibular body (basal unit), alveolar unit (dental lamina) and the condylar unit may be distinguished. In embryos at the 8th week (stages 21 to 23), all skeletal units of the mandible are evident. The condylar blastema is associated with the lateral pterygoid muscle, and other muscles of mastication are repositioned from Meckel's cartilage to the mandible. The growth spurt of the mandible during the 8th week is associated with the formation of the secondary palate and elongation of the tongue.

THE ANALYSIS OF HUCUL HORSE BODY PARAMETER GROWTH RATES

Purzyc H, Kobryńczuk F

Department of Morphological Sciences, Faculty of Veterinary Medicine, Warsaw Life Science University, SGGW, Warsaw, Poland

The evaluation of growth rates of 37 body dimensions in postnatal development of Hucul horses was the aim of our study.

The study was conducted in Hucul horses bred in Poland, including 112 stallions, 185 mares and 44 geldings aged between 6 days and 28 years, which had been divided into 6 groups on the grounds of age. The measurements of 37 morphometric traits were carried out in each specimen. The findings served to calculate growth rates of particular parts of the animals' bodies according to the Szmalhauzen-Brodi equation:

$$S = \frac{\log V_1 - \log V_0}{t \times 0.4343},$$

where: V_0 — mean parameter value of the adjacent younger age group; V_1 — mean parameter value of the adjacent older age group; t — the difference between mean age values of adjacent groups; 0.4343 — coefficient.

Hucul horse body dimension growth rates, as we go from the youngest (I) to the oldest (VI) groups demonstrate sharp drops, reaching values close to zero or even negative in the last stage of the animals' lives. For 12 out of 37 investigated parameters among stallions and mares the growth rates revealed the most significant difference between groups I and II. These parameters are as follows: distance between patella base and side bone, distance between maxillary joint and facial vessel notch, forearm circumference, hand height, distance between the end of nasal facial crest and nasoincisive notch, breast width, metatarsus length, hip length, pelvis length, distance between spinous process of the first sacral vertebra and ischiadic tuber, head length and distance between facial vessel notch and mouth angle. Hucul horse body dimension growth rates in stallions and mares are examples of uniformly retarded motion, in which, within sequential time points, reduction of velocity occurs.

SECONDARY NEURULATION IN HUMAN EMBRYOS

Pytel A, Bruska M, Woźniak W

Department of Anatomy, Poznań University of Medical Sciences, Poznań, Poland

In humans, neurulation occurs in two phases, viz. primary and secondary. During primary neurulation, the ectodermal neural plate is folded and forms the neural tube (termed the primary neural tube). Secondary neurulation involves the formation of the caudal portion of the neural tube from the pluripotent cells within the caudal eminence. These cells form a solid neural cord which then cavitates along its central axis. Secondary neurulation begins with the closure of the posterior neuropore during stage 12 (5th week) and lasts until stage 17–20 (6 and 7 weeks). The site of closure is opposite somites 30/31, which corresponds to future vertebral level S2. During secondary neurulation,

the spinal cord caudal to the S2 level and the terminal filum are formed. The mechanism of secondary neurulation is species specific. There are discrepancies as to the formation of the caudal neural tube in humans. Some investigators claim that the secondary neurulation resembles that of the mouse, others suggest that this process occurs similarly as in chicks.

The purpose of this study was to trace the development of the secondary neural tube in human embryos of developmental stages 13–17 (32 to 41 days).

The study was performed on 10 human embryos, aged between 32 and 41 days after fertilization (stages 13–17). All the embryos were embedded *in toto* in paraffin or paraplast and serial sections were made in the horizontal, sagittal and frontal planes. Sections were stained according to routine histological methods and impregnated with silver salts.

It was found that the solid neural cord in the caudal eminence is continuous with the primary neural tube. No overlapping zone of the primary neural tube with the secondary one was observed. The secondary neural tube develops by cavitation of the neural cord along its central axis. Multiple, isolated cavities coalesce to form a single canal in the upper part of the neural cord. This canal is continuous with the central canal of the primary neural tube. Canalization of the neural cord proceeds in a cranial-to-caudal direction. Within the caudal eminence the somites and tail gut also develop.

BENIGN TUMOURS OF THE LIVER AND ACTIVITY OF CATHEPSIN B, D AND L IN ASSOCIATION WITH OESTROGENIC THERAPY

Radzikowska E[1,2], Łuszczewska-Sierakowska I[3], Madej B[1], Burdan F[1], Mandziuk S[4], Wallner G[2], Dąbrowski A[2], Maciejewski R[1]

[1]*Human Anatomy Department, Medical University of Lublin, Poland*
[2]*Second Surgery Department, Medical University of Lublin, Poland*
[3]*Department of Animal Anatomy, Agricultural University of Lublin, Lublin, Poland*
[4]*Pulmonology, Oncology and Allergology Department, Medical University of Lublin, Lublin, Poland*

Long-term use of oral contraceptives may be responsible for an increased risk of benign hepatic tumours. The usage of oestrogens has had little effect on the risk of toxic processes in parenchymal tissues. Cathepsins are lysosomal enzymes that are used as important indicators and sensitive markers of toxicity. The purpose of this study was to determine the casual link between oestrogen preparations and hepatic cell adenoma or focal nodular hyperplasia as well as to evaluate the influence of oestrogens on the activity of cathepsin B, D and L in rat livers.

The whole experiment was based on an animal experimental model. Oestradiolum benzoicum was administered i.m. for 8 weeks in six different doses: E1 — 0.00075 g/kg of the body weight (n = 15 number of rats) once per week; E1.1 — 0.00075 g/kg b. w. (n = 15), every three days, E2 — 0.0015 g/kg b. w. (n = 15), once per week; E2.1 — 0.0015 g/kg b. w. (n = 15), every three days; E3 — 0.003g/kg b. w. (n=15), once per week; and E3.1 — 0.003 g/kg b. w. (n = 15), every three days. Two control groups were designed: K0- untreated animals (n = 20), K1-the animals received the adequate quantity of oleum pro injectione (n = 20). All the animals were killed by decapitation after 9 weeks of experiment and the livers were delivered by laparotomy. Fragments of organ were assigned for histological and ultrastructural examinations. The activities of free and bound fractions of cathepsin B, D and L were evaluated spectrophotometrically in liver homogenates.

Observed common features were as follows: nodular regenerative hyperplasia, adenomas and peliosis hepatis. Ultrastructural changes — mitochondrial damage, diffusely distributed round spaces with blood fluid inside - were clearly visible in groups of animals that received higher than therapeutic doses of oestrogen. Lysosomal enzyme activity, observed in all experimental groups (hence non-specifically), seems to be secondary to the inflammatory process in the neighbourhood.

Oestrogen therapy can be responsible for changing the characteristics of benign lesions of rat livers. The activity of cathepsin B, D and L taken from livers changed non-specifically over the course of the performed experiment. The observed changes seem to be secondary to the inflammatory process in the liver.

MORPHOLOGY, TOPOGRAPHY AND CYTOARCHITECTONICS OF THE MANDIBULAR GANGLION IN THE DOMESTIC DUCK (*ANAS DOMESTICUS*)

Radzimirska M

Department of Comparative Anatomy, Institute of Biology, Świętokrzyski University, Kielce, Poland

The presented study is the third part of the investigation into head autonomic ganglia in the domestic duck (*Anas domesticus*). The first and second parts, pterygopalatine and ciliary ganglion in the domestic duck, were presented as posters at Anatomical Conferences in Würzburg, October 2001 and in Wien, April 2004. The aim of this research is to supply data about the mandibular ganglion in the domestic duck because this ganglion in birds is the least studied. There are only a few studies about the morphology of this ganglion in hens, Japanese quails and domestic turkeys. The reported investigations were carried out on twenty adult turkeys of both sexes. The animals were killed by decapitation under ether anaesthesia. The mandibula canal was opened with the use of the stereoscope. Two research methods were used: the Koelle-Friedenwald thiocholine method, adapted to macromorphological preparations by Gienc [Gienc J (1977) Zool Pol, 26] and the routine histological research method.

The mandibula was obtained for the histological research. Tissues were fixed with 4% formaline and Carnoy's fixative. The tissues then were dehydrated, embedded in paraffin and cut on a microtome into 4–5 μm thicknesses. The research material was stained with haematoxylin and eosin and with toluidine blue.

The histochemical research revealed that the mandibular ganglion (*ganglion mandibulare*) of the domestic duck is located on the distal part of the tympanic chorda and on the surface on the mandibular nerve as several cell agglomerations (3–6). These agglomerations have a characteristic rosary-like shape. This part of the tympanic chorda lies along the mandibular nerve, the mandibular artery and the internal mandibular vein in a canal formed by a corpus of mandibula and thin bone plate from the medial side. The canal begins in half of the mandibula and ends as a foramen mentale on the apex of the mandibula.

The histological research confirms the presence of agglomerations of the ganglionic cells in the distal part of the tympanic chorda. They formed agglomerations with 6–11 ganglionic neurocytes (9–27 μm in diameter) at the cross-sections.

DEVELOPMENT OF THE MEMBRANOUS PART OF THE INTERVENTRICULAR SEPTUM IN HUMAN EMBRYOS AT STAGES 13 TO 21

Rauhut M, Bruska M

Department of Anatomy, Poznań University of Medical Sciences, Poznań, Poland

Ventricular septal defects are the most common of all heart malformations (25%), and they result from perforation of the interventricular muscular

septum or failure of fusion of the muscular and membranous ventricular septa.

The most serious consequence of these defects is massive left-to-right shunting of blood and pulmonary hypertension. Study of the formation of the particular components of the heart may contribute to a better understanding of congenital malformation of that organ.

The aim of this study was to describe the development of the membranous part of the interventricular septum.

Investigations were performed on human embryos (stages 13 to 21, aged 32 to 50 days) from the Departmental Collection. All embryos were embedded *in toto* in paraplast and serial sections were made in the horizontal, frontal, and sagittal planes. Sections were stained with haematoxylin and eosin, with cresyl violet according to Nissl's method, and were impregnated with silver salts.

In embryos at stage 13, the median musculary ridge as a primordium of the interventricular muscular septum lying in the floor of the ventricle near its apex is observed. In the atrioventricular canal, two endocardial cushions appear which divide this canal into right and left parts. The main part of the outflow tract was formed by the bulbus cordis, which arises from the right ventricle and is divided by two bulbar ridges which continue as ridges of the truncus arteriosus. Fusion of these ridges divides the outflow tract into the aorta and the pulmonary trunk. The bulbar ridges contribute to the formation of the interventricular septum.

At the beginning of the 5th week, the muscular part of the interventricular septum grows toward the fused atrioventricular cushions. The primary interventricular foramen was located between the free edge of the interventricular septum and the fused endocardial cushions. The size of the interventricular foramen decreases during stage 17. The conotruncal septum is continuous with the endocardial cushions.

In embryos at stage 18, the secondary interventricular foramen was closed by the membranous part of the interventricular septum, which is formed by fusion of the conotruncal septum and the endocardial cushions. At stage 19, both parts of the interventricular septum separate the ventricles. On the right side of the interventricular septum, the septal cusp of the tricuspid valve is visible as it attaches to the superior part of the interventricular septum. The membranous part of the interventricular septum does not differ in thickness from the muscular part. After closure of the interventricular foramen and formation of the membranous part of the interventricular septum, the pulmonary trunk communicates with the right ventricle and the aorta arises from the left ventricle.

DISTRIBUTION OF GABAERGIC INNERVATION AND LOCALIZATION OF CART-LIKE IMMUNOREACTIVITY IN THE MAMILLARY BODY OF THE PIG

Robak A[1], Równiak M[1], Bogus-Nowakowska K[1], Kolenkiewicz M[1], Skobowiat C[2], Majewski M[2]

[1]*Department of Comparative Anatomy, Division of Clinical Physiology, University of Warmia and Mazury, Olsztyn, Poland*
[2]*Department of Functional Morphology, Division of Clinical Physiology, University of Warmia and Mazury, Olsztyn, Poland*

The CART (cocaine- and amphetamine-regulated transcript) system appears to have different functions (orexigenic or anorectic) dependent on specific circuits of the brain. CART has been reported to have inimical effects on the gamma-aminobutyric acidergic synaptic inputs into two different populations of adipostat neurons in the hypothalamic paraventricular nucleus in rats. Only limited evidence has previously been available for the presence and distribution of CART neuropeptide and GABA neurotransmitter in the mamillary body of mammals, whereas no reports were available about pigs.

The aim of the study was to gain knowledge about the GABAergic innervation of the mamillary complex nuclei and distribution of CART-like immunoreactivities. The study was carried out on the brains of immature pigs. After perfusion, the hypothalami were dissected and postfixed in the same liquid (4% paraformaldehyde in PBS) and were then cryoprotected in a 30% solution of sucrose. Then they were cut into 10 or 20 μm scraps that were stained with standard immunofluorescence procedures using primary (GAD, CART) and secondary antibodies conjugated with FITC or CY3.

The mamillary body (Mbs) contains the medial and lateral mamillary nuclei (MM, ML) that are surrounded by the supramamillary (SM) and the posterior part of the tuberomamillary (TMp) nuclei. The GAD-ir fibre densities are especially high in the pars posterior of MM. The fibres have various thicknesses and densities, but they form a network covering the whole cross-section of the MMp, which was clearly demarcated from the GAD-negative broad area (capsula mamillaris) surrounding the nucleus. The narrow band or single thick GAD-ir fibres were also observed on the capsula mamillaris. The perimamillary area has abundant GAD-ir fibres, but the highest reactivities have two semilunar cell bands in the dorso-lateral and the ventro-lateral aspects of Mbs (SM and TMp, respectively). These areas were topographically colocalized with the highest CART-ir structures, but no colocalization (fibres and perikarya) of these substances have been seen. On the cross-sections, CART-ir perikarya has been observed along the ventro-lateral side of Mbs and in the lateral aspect of Mbs.

FORMATION OF DORSAL AND VENTRAL VAGAL TRUNKS OF PIGS IN THE PRENATAL PERIOD

Rodek E[1], Pospieszny N[1], Pospieszna J[2], Bąkowska J[1]

[1]*Department of Anatomy and Histology, Faculty of Veterinary Medicine, University of Environmental and Life Sciences, Wrocław, Poland*
[2]*Institute of Basic Electrotechnic and Technology, University of Technology, Wrocław, Poland*

This issue is not precisely presented in available academic literature.

The research was carried out on 197 foetuses of 20 wombs. 100 foetuses were from the left uterine horn (50.5%) and 97 from the right uterine horn (49.5%). In the entire research work there were 105 females (53%) and 92 males (47%). The research material was from one farm with the same conditions. Wbp x pbz sows were inseminated by Duroc and Hampshire boar or by crossbreed with Pietrain. This led to the detailed statistical and morphological analysis and proper analyses of the received results. The age was estimated according to Marrable and we used extracts from farm books. Statistical, macro- and micro-anatomical methods were used; the morphology of the researched nerve was analyzed on account of biokinetic matter.

Near Tracheal bifurcation, the vagal nerves divide into a dorsal and a ventral vagal nerve. The dorsal right vagus joins the dorsal left vagus and the ventral right vagus joins the ventral right vagus forming the dorsal and ventral vagal trunks. Upon vagus nerve division, the ventral left and right vagal nerves are formed. This takes place at the level Th4–Th6. This division is connected with tracheal bifurcation- trachealis division into the main bronchus. Right vagal nerves are weaker than left vagal nerves. The dorsal right vagus nerve is bigger (thicker) than the left dorsal vagus nerve. The dorsal left vagus nerve goes aslant the oesophagus wall and reaches its dorsal part, where it joins the same nerves of the right side creating dorsal vagal trunks. The analyzing branch is mostly double. Taking into consideration skeletotopie, ventral vagus trunks are forming in 4 weeks of pregnancy at the level Th_6 and in the perinatal period it takes place at level Th_8. The location of the ventral vagus trunks on the oesophagus wall are changing too. At the beginning of the prenatal period the vagal trunk is on right-

lateral; in 10-12 weeks of pregnancy it is on the ventral side, and in the perinatal period its topography concerns the left side of the oesophagus. The communicating branch to the dorsal vagal trunk divides from this ventral vagal trunk. The dorsal vagal trunk of the youngest foetus is formed at the level Th_7 and it moves at level Th_{11}. The ventral vagal trunk location on the oesophagus wall: the youngest — 48% are on the right-ventral side, in 10–12 weeks of pregnancy 37% are on the ventral side, and the oldest foetus — 48% on the left-ventral side.

THE INFRAORBITALIS NERVE IN PIG FOETUSES ON THE 110th DAY OF FOETATION

Rozpędek W[1], Pospieszna J[2], Pospieszny N[1]

[1]*Department of Anatomy and Histology, Faculty of Veterinary Medicine, University of Environmental and Life Sciences, Wrocław, Poland*
[2]*Institute of Basic Electrotechnic and Technology, University of Technology, Wrocław, Poland*

The mere occurrence of a specialized organ such as the rostrum is not sufficient and one may even state that it would be inutile, if it were not for the numerous nerve endings on its surface and nerve conduction for which the infraorbitalis nerve is responsible. Carrying out the research concerning this nerve is well-founded because of the scarcity of elaborations about this particular nerve in pigs. One can find more elaborations about this thematic in the postnatal period in different species. In this study, a thorough analysis of the infraorbitalis nerve (*n.infraorbitalis)* was carried out, in respect of the number of major branches and their minor branch lines. The purpose of the study was also to answer the question of whether there are any differences between the left and right side, and if there are any differences in the examined nerves in subjects of different genders.
The research was carried out on six pig foetuses which came from one litter, on the 110th day of foetation. The material was fixated with 5% formaldehyde solution and then it was prepared. During preparation, the method of neurofibrillary syringing with 2–3% acetic acid solution was used, to exposing the neurofibrils in a better way. Detailed photographic documentation was also carried out. It was done by means of a Nikon digital camera. The photographs were then processed using Lucia computer software. The software enabled the precise measurement of the particular branches of the infraorbitalis nerve after anterior scale calibration.
During preparation, we observed that the infraorbitalis nerve meets the dorsal buccal branches and joins with the internal nasal branches and labial maxillary branches. Moreover, the whole nerve is covered with well-developed perineurium, which merges the major branches and their numerous branch lines into one main nerve stem. Barely after removing the perineurium, one is able to see the division of the nerve into major branches, from which come minor branch lines built from single nerve fibrils. As far as the division of the infraorbitalis nerve is concerned, after coming out of the infraorbitalis canal we can observe the following division starting from nose ridge down: external nasal branches, internal nasal branches, labial maxillary branches and palpebral branches. One cannot find distinct differences in the infraorbitalis nerve branch course in subjects of different gender. In addition, the functioning of the infraorbitalis nerve is similar on both sides. The biggest number of nerve branches appear in the external nasal branches and internal nasal branches, which points to their significant role. Their number in the case of external nasal branches amounts to 12–16, and in the case of internal nasal branches, from 12 to 15. The labial maxillary branch is the worst-developed branch line and it consists of nerve fibres numbering 5–9. The total number of nerve branches amounts to between 29 and 40. The total number of nerve branches on the left side fluctuates from 30 to 40, and on the right side from 29 to 35, which indicates that the left side is slightly better nerved.

THE COCAINE- AND AMPHETAMINE-REGULATED TRANSCRIPT (CART) IMMUNOREACTIVITY IN THE AMYGDALA OF PIGS

Równiak M[1], Robak A[1], Bogus-Nowakowska K[1], Najdzion J[1], Wojtkiewicz J[2], Bossowska A[2], Majewski M[2]

[1]*Department of Comparative Anatomy, Division of Clinical Physiology, University of Warmia and Mazury, Olsztyn, Poland*
[2]*Department of Functional Morphology, Division of Clinical Physiology, University of Warmia and Mazury, Olsztyn, Poland*

Cocaine- and amphetamine-regulated transcript (CART) is a brain-enriched mRNA with a protein product(s) that is a candidate brain neurotransmitter. Although some earlier reports indicate that CART peptides are widely distributed in the central and peripheral nervous systems of mammals, there is no detailed data concerning the immunoreactivity of this substance in the mammalian amygdala (CA). In the present study, CART peptide immunoreactivity was investigated in the CA of immature, female pigs by using routine immunofluorescence methods.
The animals were deeply anesthetized and perfused intracardially with 4.0% paraformaldehyde in 0.1 M phosphate buffer. Following perfusion, brains were removed from the skulls and postfixed for 4 h in 4.0% paraformaldehyde, washed twice in 0.1 M phosphate buffer and then stored in 30% sucrose until sectioning. The 20 μm cryostat sections were processed for routine immunofluorescence staining with an antiserum directed against the CART peptide fragment 61–102.
The antiserum adopted in the present study produced robust immunofluorescence staining in all subdivisions of the pig CA and several adjacent forebrain structures. The highest densities of CART peptide positive fibres were evident within the large-celled part of the basolateral nucleus as well as the central and medial nuclei. Moderate to high expression was found within the lateral nucleus and moderate to low levels in the basomedial and cortical nuclei. CART-peptide immunoreactive cell bodies were mostly concentrated in the small-celled parts of the basolateral and basomedial nuclei; however, scattered somata were also present in the other CA subdivisions. Especially high CART peptide staining in the basolateral amygdala (present investigation) and nucleus accumbens (data in the literature) continues to suggest a role in drug-induced reward and reinforcement.

RECOGNITION OF THE GEOMETRICAL FEATURES OF BONE POPULATION USING PRINCIPAL COMPONENT ANALYSIS

Rychlik M, Stankiewicz W

Department of Methods of Machine Design, Poznań University of Technology, Poznań, Poland

Nowadays, many engineering CAx technologies have an application not only in mechanics but also in different disciplines like biomechanics, bioengineering, etc. In this work, the PCA method from fluid mechanics was used to recognize the geometrical features of bone population.
PCA decomposes the population of 3D objects into mean shape and individual features (empirical modes), describing deviations from the mean value. Modes can also represent non-geometrical features, like density, temperature and others. Only the few first modes carry the most information. Therefore, each original object S_i is represented by using K principal components: $S_i = \bar{S} + \sum_{k=1}^{K} a_{ki} \Psi_k$, where Ψ_k is an eigenvector representing the orthogonal mode (the feature computed from the data base) and a_{ki} is the coefficient of the eigenvector.
For numerical experiment, a generic database was created. The database contains 99 lumbar vertebrae. Each vertebra has a different geometry and is described by a Finite Element grid with the same structure (616 nodes,

2000 elements). For this database, Principal Component Analysis was done. The result of this operation is the mean object, eleven modes and coefficients, describing all the important features.
The first five modes include ninety-six percent of the information about the reconstructed geometry (Fig. 1). Modes: twelfth and others contain negligible information (this is only numerical noise) and they are not used for further reconstruction. The first and fourth modes describe the deformation of the vertebral body; the second, third and seventh modes represent the deformation of the spinosus process. Other modes describe the deformation of the transverse process.
The presented method makes possible the recognition of three-dimensional features and the mean shape of the population of biological objects. This method can be used for statistical analysis, e.g. for the creation and visualization of the 3D anthropometry base.

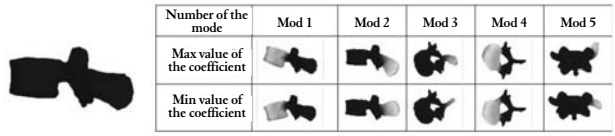

Figure 1. Three-dimensional visualization of mean geometry and first 5 modes

SECRETORY ACTIVITY OF PARAFOLLICULAR CELLS AT DIFFERENT STAGES OF RAT LIFE

Seidel J, Zabel M, Kasprzak A

Chair of Histology and Embryology, University of Medical Sciences, Poznań, Poland

The aim of this study was the expression of selected proteins in the parafollicular cells at different stages of rat life.
The studies were performed on rat thyroids. The thyroids were isolated from male and female rats of Wistar strain aging from 14 days to 2 years. The material was fixed in Bouin's solution or in 4% paraformaldehyde and, then, it was embedded in paraffin. In paraffin sections, the presence of calcitonin, CGRP, somatostatin, synaptophysin and NPY was tested employing the classical ABC immunocytochemical reaction. In situ hybridisation was also performed to detect mRNAs for the calcitonin, CGRP and somatostatin. mRNAs were detected using digoxigenin-labelled oligonucleotide probes.
The immunocytochemical reactions demonstrated that at all age periods of rat life, thyroid parafollicular cells produced calcitonin, CGRP, somatostatin and synaptophysin.
However, the number of cells underwent changes with increasing age of the rats. In young rats (14 days of life), the cells were individually present close to thyroid follicles. With progressing age, the number of cells increased and very frequently, parafollicular cells entwined the follicles. In every case, calcitonin-producing cells were most numerous. CGRP and synaptophysin were present in around 1/2 to 2/3 of the cells which secreted calcitonin. In the case of somatostatin, before the 3rd month of rat life, a positive reaction was noted only in individual parafollicular cells (3 to 5 cells per section) while in older rats, the cell number increased to around 100 positive cells in one-year-old rats. NPY was observed (weak reaction) only in 12 and 18-month-old rats. Hybridocytochemical studies on expression of mRNAs for calcitonin, CGRP and somatostatin showed that most parafollicular cells contained mRNA for calcitonin and CGRP. In the case of somatostatin, however, multiple parafollicular cells produced mRNA for the hormone, but few cells demonstrated the presence of the corresponding protein. Our studies demonstrated that the number of parafollicular cells as well as the hormonal content of cells changed with progressing age of the rats. Increasing age was accompanied by an increase in the number of cells secreting calcitonin, CGRP, synaptophysin and somatostatin. Application of in situ hybridisation permitted the disclosure that a relatively high number of parafollicular cells produced mRNA for somatostatin.

THE MORPHOMETRIC STUDY OF LUNGS DURING HUMAN PRENATAL DEVELOPMENT

Siedlecki Z[1], Cieściński J[1], Szpinda M[1], Lisewski P[1], Wawrzyniak J[2], Wiśniewska J[2]

[1]Department of Normal Anatomy, Nicolaus Copernicus University in Toruń, Collegium Medicum in Bydgoszcz, Bydgoszcz, Poland
[2]Student's Scientific Society of Normal and Clinical Anatomy, Nicolaus Copernicus University in Toruń, Collegium Medicum in Bydgoszcz, Bydgoszcz, Poland

The aim of the study was to analyse the dimensions, development and skeletotopy of foetal lungs during human prenatal life. The study was carried out on 35 human foetuses of both sexes (18 female, 17 male) between the 16th and 25th weeks of intrauterine life. The foetuses were fixed in 10% formalin solution. Foetal age was determined by crown-rump (CR) measurement on the basis of Iffy tables. Using anatomical dissection and statistical analysis, the eight following dimensions of fetal lungs were measured: (1, 2) the longitudinal dimensions of right and left lung; (3, 4) the transverse dimensions of right and left lung; (5, 6) the sagittal dimensions of right and left lung; (7, 8) the longitudinal dimensions of hilus of the right and left lung. For each foetus, the skelototopic distance of the following seven lung parts to ribs was measured: (1, 2) apex of right and left lung; (3, 4) base of the right and left lung; (5, 6) hilus of the right and left lung; (7) the transverse fissure of the right lung. No gender differences were observed ($p > 0.05$). Every measured dimension of the right and left lung correlated statistically significantly with the foetal age ($r = 0.50$, $p < 0.05$), the correlation coefficient was the highest for the longitudinal dimension of the right lung ($r = 0.69$, $p < 0.05$). The size of the hilus of the right lung correlated statistically significantly with the foetal age ($r = 0.44$, $p < 0.05$), and the size of the hilus of left lung was statistically irrelevant. For every foetus, the location of the right and left lung hilus and horizontal transverse fissure of right lung to ribs were correlated with foetal age ($p < 0.05$) and raised during prenatal development.

THE MORPHOMETRIC STUDY OF THE MIDDLE CRANIAL FOSSA IN HUMAN FOETUSES

Siedlecki Z[1], Cieściński J[1], Szpinda M[1], Lisewski P[1], Wiśniewska J[2], Wawrzyniak J[2]

[1]Department of Normal Anatomy, Nicolaus Copernicus University in Toruń, Collegium Medicum in Bydgoszcz, Bydgoszcz, Poland
[2]Student's Scientific Society of Normal and Clinical Anatomy, Nicolaus Copernicus University in Toruń, Collegium Medicum in Bydgoszcz, Bydgoszcz, Poland

The middle cranial fossa contains the temporal lobes of the brain, cavernous sinuses, internal carotid arteries, cranial nerves: III, IV, V, VI and the middle meningeal arteries. It is the site of various pathologies and it is used in neurosurgical intracranial approaches. The aim of the study was to analyse the dimensions and development of the middle cranial fossa during prenatal life. The examinations were carried out on 42 human foetuses of both sexes (22 female, 20 male) between the 16th and 26th weeks of intrauterine fife. The foetuses were fixed in 10% formalin solution. Foetal age was determined by crown-rump (CR) measurement on the basis of Iffy tables. Using anatomical dissection and statistical analysis, the six following dimensions of the middle cranial fossa were measured: (1) anterior transverse dimension; (2) posterior transverse dimension; (3) lateral

longitudinal dimension; (4) medial longitudinal dimension; (5) oblique dimension between the apex of the petrous pyramid and the pterion; (6) oblique dimension between the anterior clinoid process and the base of the petrous pyramid. The following five dimensions of the foetal head were measured: (1) mento-occipital; (2) suboccipitobregmatic; (3) fronto-occipital, (4) bitemporal; (5) biparietal. All six dimensions of the middle cranial fossa increased according to a linear function and correlated with foetal age ($r = 0.8$) and with all five head dimensions ($r = 0.8$). These correlation coefficients were statistically significant ($p < 0.05$). The material examined revealed gender differences of oblique dimension of the middle cranial fossa (5). The length of this dimension was statistically significantly longer in female foetuses ($p < 0.05$).

THE DEVELOPMENT OF THE TENTORIUM OF THE CEREBELLUM DURING HUMAN PRENATAL LIFE

Siedlecki Z[1], Cieściński J[1], Szpinda M[1], Lisewski P[1], Woźniak K[2], Szostak M[2], Stachowicz A[2]

[1]Department of Normal Anatomy, Nicolaus Copernicus University in Toruń, Collegium Medicum in Bydgoszcz, Bydgoszcz, Poland
[2]Student's Scientific Society of Normal and Clinical Anatomy, Nicolaus Copernicus University in Toruń, Collegium Medicum in Bydgoszcz, Bydgoszcz, Poland

The tentorium of the cerebellum develops in the 3rd month of gestation. It departents cranial cavity on supratentorial and infratentorial cavities and is of great clinical relevance to neurology and neurosurgical approaches.
The aim of the study was to analyse the dimensions of the tentorium during prenatal development. The examinations were carried out on 42 human foetuses of both sexes (22 female, 20 male) between the 16th and 26th weeks of intrauterine fife. The foetuses were fixed in a 10% formalin solution. Foetal age was determined by crown-rump (CR) measurement on the basis of Iffy tables. Using anatomical dissection and statistical analysis, the eight following dimensions of the tentorium of the cerebellum were measured: (1, 2) the length of the attachment of the tentorium on right and left side; (3, 4) the surface of the tentorium on right and left side; (5, 6) the longitudinal and transverse dimension of the tentorium; and (7, 8) the longitudinal and transverse dimension of the tentorial incision. The following five dimensions of the foetal head were measured: (1) mento-occipital; (2) suboccipitobregmatic; (3) fronto-occipital; (4) bitemporal; and (5) biparietal. The material examined revealed no gender differences. The size of the tentorium of the cerebellum correlated with the foetal age in foetuses between the 16th and 22nd weeks of gestation ($r = 0.68$, $p < 0.05$). The correlation coefficient between the size of tentorium and foetal age in foetuses between the 23rd and 26th weeks was statistically irrelevant ($p > 0.05$). A statistically significant correlation coefficient was observed between the length of attachment of the tentorium on the right side and the head dimensions ($r = 0.47$, $p < 0.05$) in foetuses between the 23rd and 26th weeks of gestation. The dimensions of tentorial incision were highly correlated with the dimensions of the tentorium in every foetal age ($r = 0.8$, $p < 0.05$).

THE MORPHOMETRIC STUDY OF SELLA TURCICA DURING HUMAN PRENATAL DEVELOPMENT

Siedlecki Z[1], Cieściński J[1], Szpinda M[1], Lisewski P[1], Woźniak K[2], Szostak M[2], Stachowicz A[2]

[1]Department of Normal Anatomy, Nicolaus Copernicus University in Toruń, Collegium Medicum in Bydgoszcz, Bydgoszcz, Poland
[2]Student's Scientific Society of Normal and Clinical Anatomy, Nicolaus Copernicus University in Toruń, Collegium Medicum in Bydgoszcz, Bydgoszcz, Poland

The sella turcica contains the pituitary gland and is the site of many congenital and acquired pathologies. These include empty sella syndrome, cranial fistulas and tumours: pituitary adenomas and craniopharyngiomas. The sella turcica is surrounded by cavernous sinuses with internal carotid arteries. The aim of the study was to examine the dimensions and development of the sella turcica during prenatal life. The examinations were carried out on 42 human foetuses of both sexes (22 female, 20 male) between the 16th and 26th weeks of gestation. Foetal age was determined by crown-rump (CR) measurement on the basis of Iffy tables. For each foetus, the following linear distances were measured: (1) between right and left anterior clinoid process; (2) between right and left posterior clinoid process; (3) between right anterior clinoid process and right posterior clinoid process; (4) between left anterior clinoid process and left posterior clinoid process; (5) between limbus sphenoidale and tuberculum sellae; (6) between tuberculum sellae and dorsum sellae. The following five dimensions of the foetal head were measured: (1) mento-occipital; (2) suboccipitobregmatic; (3) fronto-occpital; (4) bitemporal; and (5) biparietal. For each foetus, the correlation coefficients between the length of every linear distance of sella and every head dimension were calculated. No gender differences were observed ($p > 0.05$). The size of the sella turcica correlated with every head dimension ($r = 0.63$, $p < 0.05$). The correlation coefficient was the highest between the size of the sella turcica and the suboccipitobregmatic dimension of the head ($r = 0.78$, $p < 0.05$). The correlation coefficient between the size of the sella turcica and the crown-rump was statistically irrelevant ($r = 0.22$, $p > 0.05$)

IMMUNOHISTOCHEMICAL PROPERTIES OF PREVERTEBRAL GANGLIA (PVG) NEURONS PROJECTING TO THE PORCINE TESTIS

Sienkiewicz W

Faculty of Veterinary Medicine, Department of Functional Morphology, Division of Animal Anatomy, University of Warmia and Mazury, Olsztyn, Poland

Until now, studies disclosing the immunohistochemical properties of prevertebral ganglia (except caudal mesenteric ganglion) neurons supplying male gonads were performed only on laboratory animals, so this is the first paper dealing with this topic in farm animals.
Three sexually mature boars were used. The animals were anaesthetized and injected with FB into the right testis. Three weeks later the animals were re-anaesthetized and transcardially perfused with 10 litres of 4% buffered paraformaldehyde. The collected ganglia were washed in PB and stored in 18% sucrose solution. The cryostat sections were stained using antisera against TH or DβH, VACHT, NPY, VIP and Gal. Preparations were studied using fluorescent microscope.
FB positive (FB^+) neurons were found in the right and left PVG-s namely: caudal mesenteric ganglia (CaMG), testicular ganglia (TG), aorticorenal (ARG) and adrenal (ADG) ganglia. In this study, only TG-s, ARG-s and ADG-s were taken under consideration. These ganglia contained 11% of all FB^+ neurons. Immunohistochemical staining revealed that 65% of FB^+ neurons contained immunoreactivity to DβH, whereas 4% of FB^+ cells were VACHT-positive. Within the ganglia, a dense network of VACHT-IR nerve fibres was observed. Among FB^+/DBH^+ neurons, 63% contained NPY and 1% stained for Gal. All FB^+/$VACHT^+$ neurons were also VIP^+. Forty-six percent of FB^+ somata contained immunoreactivity to NPY, whereas VIP was found in 7.5% of FB^+ neurons.
In conclusion, three subpopulations of the porcine testis–projecting neurons can be distinguished (from the largest to the smallest) including adrenergic, NANC and cholinergic.

VASCULAR ANATOMY OF THE FORAMEN OF LUSCHKA

Sharifi M, Ciszek B

Department of Anatomy, Centre of Biostructure Research, Medical University of Warsaw, Warsaw, Poland

The lateral aperture of the fourth ventricle (foramen of Luschka) is the pathway of insertion of the electrodes implanted to the floor of the fourth ventricle in the region of the cochlear nuclei. This is one of the methods of restoration of hearing due to the definite destruction of the cochlear nerve. The aim of the study was to describe the course of the main arteries around the foramen of Luschka. This microanatomical study was conducted on the base of 100 cerebellar hemispheres.
In 20% of cases, the anterior inferior cerebellar artery or the posterior inferior cerebellar artery run in the vicinity of the foramen. The mean distance between the main trunk of the anterior inferior cerebellar artery and the foramen of Luschka was 4 mm and the same value for posterior inferior cerebellar artery was 6.5 mm. The region of the foramen of Luschka may by also covered by the loop of tortuous vertebral artery in 15% of cases, predominantly on the left side.

AXOTOMY INDUCED CHANGES IN CHEMICAL CODING OF SYMPATHETIC CHAIN GANGLIA (SChG) NEURONS SUPPLYING THE PORCINE DESCENDING COLON

Skobowiat C, Majewski M

Division of Clinical Physiology, Department of Functional Morphology, University of Warmia and Mazury, Olsztyn, Poland

The aim of the present study was to determine axotomy-induced changes in the chemical coding of colon-projecting SChG neurons in pigs after *nervi colici caudales* transsection.
Five immature pigs were injected with a neuronal tracer, Fast Blue (FB), into the colon descending wall and after three weeks, during repeated laparotomy, *nervi colici caudales* were transsected. Then the lumbar SChG were fixed with 4% paraformaldehyde and 10-μm-thick serial cryostat sections were mounted onto gelatinized glass slides and then processed for double-labelling immunofluorescence using primary antibodies raised in different species. The used antisera included antibodies directed towards dopamine-β-hydroxylase (DβH), neuropeptide Y (NPY), calbindin (CB), galanin (GAL), somatostatin (SOM), Leu^5-enkephalin (LENK) and dynorphin A (DYN-A). Axotomy resulted in a drastic decrease in DβH expression (approx. 40%) and an increase in CB expression (up to 28% in all FB$^+$ cells), in comparison to control animals where these neurons constituted 95% and 2.5%, respectively. Furthermore, axotomy induced *de novo* expression of neurotransmitters, which physiologically were not observed in colon-projecting population, i.e., GAL and SOM (90% and 8% of all FB$^+$ cells, respectively). Virtually all the SOM-IR neurons were simultaneously NPY-positive, but they were DβH-immunonegative. Approximately half of the SOM-IR neurons were GAL-IR, while approx one-fourth of them simultaneously exhibited CB. GAL was found in both the DβH-IR (39%) and DβH-immunonegative neurons (61%). The number of NPY-IR cells remained at the same level as in control animals (approx. 90%). DYN-A- or LENK-IR retrograde labelled perikarya were observed neither in the control, nor in axotomized animals. However, there was a decrease in the density of SOM-, LENK- or DYN-IR nerve fibres surrounding FB$^+$ positive neurons. In contrast, numerous GAL- and/or NPY-IR nerve fibres were observed around clusters of FB$^+$ neurons in axotomized ganglia. Thus, the present data confirmed that neurons of the SChG are involved in neurophysiological regulation of the porcine colon and that they responded to axotomy with changes in their chemical phenotypes.

THE EFFECT OF EXPERIMENTALLY INDUCED INFLAMMATION ON COLON-PROJECTING SYMPATHETIC CHAIN GANGLIA (SChG) NEURONS IN PIGS

Skobowiat C, Majewski M

Division of Clinical Physiology, Department of Functional Morphology, University of Warmia and Mazury, Olsztyn, Poland

The colon is an organ in which ulcerative inflammation frequently occurs in western countries. We tried to determine if a chemically induced inflammation of the colonic wall is able to induce any changes in the chemical coding of the SChG neuron population supplying the colon, because the available data concerned mainly small laboratory animals (rats and guinea pigs) and because the pig is thought to be the best animal model for human bowels. Three immature pigs were injected with a neuronal tracer, Fast Blue (FB), into the colon wall. After three weeks, during repeated laparotomy, the colon wall was injected many times with 4% buffered paraformaldehyde to induce aseptic inflammation. After four days, the bilaterall SChG were collected. 10-μm-thick serial cryostat sections were processed for double labelling immunofluorescence using antibodies against β-hydroxylase dopamine (DβH), neuropeptide Y (NPY), calbindin (CB), galanin (GAL), somatostatin (SOM), Leu^5-enkephalin (LENK), dynorphin A (DYN-A), substance P (SP) and calcitonin gene-related peptide (CGRP).
The experimentally induced colon inflammation lead to an increase only in the number of CB-positive neurons (to approximately 12% of all FB$^+$ cells), which were predominantly catecholaminergic (up to 9%), in comparison to control animals (2.5%). Similar to the control, the expression of DβH and/or NPY remained at the same high level (94% and 87% of all colon-projecting perikarya, respectively). Although we were not able to observe any GAL-, SOM-, LENK-, DYN-A-, SP- or CGRP-IR neurons in the population of retrograde traced cells, there were much more numerous GAL-, SOM-, LENK-, DYN-A-, SP- and CGRP-IR nerve fibres as apposed to FB$^+$ cells. Thus, our study presents data suggesting that aseptic inflammation of the colon is able to induce profound changes in the viscerofugal and/or sensory projections to porcine colon-projecting SChG neurons.

DISTRIBUTION OF TENDINOUS CHORDS IN THE TRICUSPID VALVE OF THE HUMAN HEART

Skwarek M[1], Hreczecha J[2], Dudziak M[3], Jerzemowski J[4], Grzybiak M[3]

[1]*Department of Sports Medicine, Jędrzej Śniadecki Academy of Physical Education and Sport, Gdańsk, Poland*
[2]*Department of Clinical Anatomy, Medical University of Gdańsk, Gdańsk, Poland*
[3]*Noninvasive Cardiovascular Diagnostic Unit, Institute of Cardiology, Medical University of Gdansk, Gdańsk, Poland*
[4]*Department of Anatomy and Anthropology, Jędrzej Śniadecki Academy of Physical Education and Sport, Gdańsk, Gdańsk, Poland*

Tendinous chords of the tricuspid valve are a supreme kind of connection between the papillary muscles and the tricuspid valve. Studies describing the evolutionary line of these connections are well-known. Flexibility of particular leaflets of the tricuspid valve are different, and the tension of the blood stream varies in particular leaflets as well.
The present study was performed in a group of 96 formalin-fixed, adult human hearts ranging from 18 to 90 years without congenital malformations and pathology. The valves were divided into types according to earlier studies. Studies were performed with regard to their type. Tendinous chords, with regard to their position in the leaflet (margin, ventricular surface and commissure), and their ramifications were counted for each main and accessory

leaflet with regards to the type of tricuspid valve. Fields of the surfaces of particular leaflets were measured with a planimeter. The quotient between the number of chords in a particular leaflet and its surface was counted.
The number of tendinous chords decreased in leaflets in particular types of tricuspid valve, but the quotient between chords attaching to margins and ventricular surfaces was similar. The number of chords for the surface of leaflets (measured in mm^2) was similar in particular types of valves for all cusps.
The most differentiated were commissural chords in all types of valves. The quotient between chords attaching margins and ventricular surfaces did not depend on the surfaces of the leaflets.

RADIOLOGICAL STUDIES OF DIRECTIONS OF MINERALISATION PROCESSES IN THE PETROUS PART OF THE TEMPORAL BONE IN HUMAN FOETUSES

Sławiński G, Czerwiński F, Dzięciołowska-Baran E, Teul I, Sulisz T

Department of Anatomy, Pomeranian Medical University, Szczecin, Poland

The aim of this work was the observation of the mineralization of the petrous part of the temporal bone and the determination of the main direction of this process. Temporal bones of 76 foetuses aged between 9–32 weeks of gestational life were separated and divided into four groups depending on their age. X-ray images of each bone in projection on the anterior and posterior surface of the pyramids were performed to determine their structure. Attention was paid to the presence and position of the primary centres of ossification and the direction of the progress of the mineralization process.
Ossification of the petrous part originates from five primary nuclei, which appear between 15 and 20 weeks of gestation. They are located around the vestibular and cochlear cavities. Analysis of RTG images of foetuses after 20 weeks of foetal life allow detailed observation of the mineralization process. Primary nuclei enlarge and fuse. In 23–24 weeks, a characteristic "C" around the vestibule opened in the lateral direction appears on X-ray images. The "C" shaped mineralization process changes into an "O" shape, which surrounds the vestibule and part of the cochlea in the end of the 25th week. After this, the mineralization process develops eccentrically from the centre of the otic capsule (the inside of the "O") to the peripheral parts of the pyramid. Rapid progress of the mineralization is observed in the two older groups. Images of the pyramids of 28-week-old foetuses shows that the process of complete mineralization can be observed around the otic capsule, and advanced mineralization is seen in the remaining parts of the temporal bone, which completely ossifies in postnatal life.

METROLOGY OF SCAPULA IN THE PRENATAL PERIOD

Stankowski J[1], Kędzia A[1], Dudek K[2], Dziewiszek W[3], Koźlik M[1], Krefft M[1], Kobierzycki C[1]

[1]*Department of Normal Anatomy, Medical University of Wrocław, Wrocław, Poland*
[2]*Institute of Machine Design and Operation, Wrocław University of Technology, Wrocław, Poland*
[3]*Department of Pharmacology, Medical University of Wrocław, Wrocław, Poland*

Analysis of available literature revealed a lack of information in bibliography about computerized measurements of scapula. The aim of our research was to rate the metrology of scapula in the prenatal period. The study was performed on 126 scapulas of 63 foetuses — 35 female, 28 male, aged from 4 to 8 months (prenatal period). Foetus age was evaluated on tables of Scammon-Calcins by crown-rump dimension in values from 85 to 235 mm.
The methods included preparation, anthropological methods, measurement using Scion for Windows 98 program and statistics: Shapiro-Wilks test of measured features, T-student test used for sexual dimorphism and symmetry, analysis of speed of growth Z. Measurements were made with 1/100 mm accuracy. Digital photographs were taken with a millimetre scale on them. Measuring techniques were authoritative because the pixels where converted to millimetres on each measured digital photograph. An advantage of this method was the possibility of multiple measurements without devastating the autopsy material. Measurements were made of ossification parts of the scapula and their cartilage parts. Ossification points were clearly marked borders, set parallel to the edge of the scapula. In rating 22 features were used, describing geometry of the ossification and cartilage parts of the scapula. Values of geometric parameters on both left and right sides were compared using T-student test, for dependent variables. The critical level was set as $p < 0.05$. A matrix of correlation was set for all measurements. All features were correlated with age, except for the distance between cavitas glenoidale and processus coracoideus, which proved not to be correlated with age. The biggest growth, 4 mm monthly, was observed in the case of the length of the margo lateralis of the scapula. The distance between the margo medialis and the beginning of the spina scapulae increased at a rate of 3.8 mm per month. A geometric model was created for rating the ossification and cartilage areas of the scapula. The ossification area in the 14th week was equal to 34 mm^2, and in the 28th week — 405 mm^2. The area of cartilage of the scapula in the 14th week was equal to 49.5 mm^2, and in the 28th week was equal to 161 mm^2. In conclusion, we affirmed that the growth of individual features is constant. The growth rate of the studied features was steady with a preserved length-width index. No relevant difference between values of the analyzed parameters on the left and right sides were noticed. In addition, no sexual dimorphism was noticed.

NUCLEAR ABCC2 EXPRESSION IS A NEW UNFAVOURABLE PROGNOSTIC FACTOR IN HUMAN CANCERS OF DIFFERENT ORIGIN

Surowiak P[1, 2]

[1]*Department of Histology and Embryology, University School of Medicine, Wrocław, Poland*
[2]*Lower Silesian Centre of Oncology, Wrocław, Poland*

ABCC2 is commonly localized on apical cell membranes and can confer cisplatin resistance to various cancer cell lines including ovarian carcinoma cells. In our previous study we demonstrated that ABCC2 can be localized in the plasma membrane as well as in the nuclear envelope. Expression in the nuclear envelope was specific for cisplatin-resistant human ovarian carcinoma cell lines, cases of ovarian cancer with the worst prognosis and for stem cells in many healthy human tissues. The aim of the work was to investigate the prognostic value of nuclear ABCC2 expression in cancers of different origin. Until now, we have performed immunohistochemical studies on sections from 69 primary Fallopian tube cancers and from 32 cases of stage IIIB and IV non-small cellular lung cancers. The statistical analysis has shown that the elevated expression of nuclear ABCC2 expression is typical for the Fallopian tube and lung cancers of shorter survival rates. The study has shown that nuclear ABCC2 expression is a new unfavourable prognostic factor. This ABCC2 location is typical not only for drug-resistant cancers, but also for cancer cases of more aggressive behaviour.

AN ATTEMPT AT MAKING MORPHOLOGICAL EVALUATION OF AUTOPSY CORONARY ARTERIES WITH THE AID OF TRANSILLUMINATION AND TEXTURE ANALYSIS — INITIAL REPORT

Syrycki M[1], Mazurek W[2], Biały D[2], Stachurska A[2], Trzaska M[1]

[1]*Department of Normal Anatomy, Medical University of Wrocław, Wrocław, Poland*
[2]*Department of Cardiology, Medical University Wrocław, Wrocław, Poland*

The quantitative estimation of atherosclerotic lesions in autopsy coronary arteries has both a cognitive meaning and a clinical one for building the experience of the operator restoring coronary vessel patency during PCI. Such objective estimation usually takes place in microscopic histopathological examinations. The use of the new method of transillumination permits the evaluation of obtained images in a macroscopic range, regarding what is accustomed to the intervening cardiologist.
The 20 transilluminative images of carefully dissected coronary arteries, received from the autopsy, were obtained by over-exposing them using white light. Equal, multifocal halogen lights (15 Watt/6 Volt) with focusing screens, were used. Studio DC10plus software version 1.06.4 was used for the acquisition of the image. The images were applied from the stereoscopic microscope Olympus SZ40 with a Sony Exwave HD CCD 1/2, type SSCDC50AP camera. The obtained images were prepared for further analysis through to a maximum possible removal of interferences that could have an influence on the intended analysis of their direction-isotropy. Five different methods of context filtration were used on the images. Besides the first order statistical methods of texture estimation such as the average and the standard deviation of threshold levels, the plugin for the program ImageJ under the name GLCM_Texture was used for the analysis of the texture. This plugin makes analysis of the following second-ordered statistic parameters of the texture possible, such as: the second angular moment — ASM, the contrast, the correlation, the inverse differential moment — IDM and the entropy.
The performed observations of parameters of the texture with reference to atherosclerotic lesions, such as: decreasing the image complexity and its local differentiation and increasing the arrangement and hesitations of brightness levels. The mentioned values were correlated with the area and with the thickness of the investigated atherosclerotic lesions. Absolute correlations oscillated near the level of essentiality, which encourages continued investigation of more numerous material.

THE MORPHOLOGY OF NEURONS AND TOPOGRAPHY OF GYRUS PARAHIPPOCAMPALIS IN CHINCHILLAS (*CHINCHILLA BREVICAUDATA*)

Szalak R, Lonc G, Eustachiewicz R, Boratyński Z

Department of Animal Anatomy, Faculty of Veterinary Medicine, Agricultural University of Lublin, Lublin, Poland

The aim of the research was to get to know the structure and topography of gyrus parahippocampalis in chinchilla (chinchilla brevicaudata). The parahippocampal region is a cortical area interposed between the neocortex and the hippocampal formation, which is known to serve a primary function in declarative memory processes.
The examination was carried out on five brains of sexually mature chinchilla brevicaudata. The material of the examination after fixing, dehydrating, embedding in paraffin and cutting was coloured according to Klüver and Barrer's method. The gyrus parahippocampalis, which was the object of examination, is a cortical structure which joins the formation of the hippocampus with the neocortex. It is the rear part of the gyrus fornicatus, which stretches from the splenium of the corpus callosum to the abdomino-medial angle of the brain hemisphere. It is made up of the following cortical structures: area entorhinalis, parasubiculum and presubiculum. The above-mentioned parts of the gyrus parahippocampalis cortex are made up of four layers: marginal, cellular I, cellular II and cellular III.

ANATOMY OF THE FOETAL ACHILLES TENDON

Szaro P, Ciszek B

Department of Anatomy, Centre of Biostructure Research, Medical University of Warsaw, Warsaw, Poland

Our previous investigations on the internal structure of the Achilles tendon in adults revealed that it is composed of four segments with a spiral arrangement. The aim of study was to confirm this structure of Achilles tendon in the foetal period. The study was conducted on 10 foetuses aged 15–26 weeks of foetal life (20 Achilles tendons). Dissection was carried out with microsurgical instruments and a surgical microscope.
The general structure was similar to adult cases. The central core of the tendon was composed of the fibres of the soleus muscle while the fibres from the medial head of the gastrocnemius constitute the posterior layer of the Achilles tendon and lateral border of the tendon; fibres from the lateral head of the gastrocnemius constitute the anterior layer of the Achilles tendon.

ARTHROSCOPIC ANATOMY OF THE PALMAR LIGAMENT OF THE RADIOCARPAL JOINT

Szaro P[1], Witkowski G[1], Kordasiewicz B[2], Krajewski P[3]

[1]*Department of Anatomy, Medical University of Warsaw, Warsaw, Poland*
[2]*Centre for Postgraduate Medical Education, Otwock Orthopaedic Hospital, Otwock, Poland*
[3]*Department of Forensic Medicine, Medical University of Warsaw, Warsaw, Poland*

The palmar ligaments of the capsule of the radiocarpal joint can be obtained during arthroscopy although classical anatomical handbooks do not describe them.
The aim of our study was to describe the topographical relations of the palmar ligament and the triangular fibrocartilage complex. The knowledge of this region is essential to successful treatment.
Twenty cadaveric wrist arthroscopies were preformed within the scope 2.7 mm of outside diameter and an angle of 30 and 70 degrees. The joint was injected with isotonic solution with approximate volume between 10–15 ml. The traction tower was used before introducing the arthroscope. The procedure was conducted via the following portals: 3–4, 4–5, 1–2, 6R and 6U. The wrist arthroscopy was recorded on video. To compare the arthroscopic view with the macroscopic view, arthrotomy was preformed and photographs were taken.
The arthroscopy visualized the following ligaments: the ulnotriquetral, the ulnolunate, the short radiolunate, the radioscapholunate (the Testut ligament), the long radioulnar and the radioscaphocapitate. Moreover, the triangular fibrocartilage complex with the ulnar ligaments, disc, the radioulnar ligaments and the subsheet of the extensor carpi ulnaris were visualized. The procedure requires understanding and knowledge of topographic anatomy.

CORRELATION BETWEEN THE EXPRESSION OF CYCLOOXYGENASE-2 AND MULTIDRUG RESISTANCE TO ANTICANCER DRUGS IN NON-HODGKIN'S LYMPHOMAS

Szczuraszek K[1], Zabel M[1,4], Mazur G[2], Jeleń M[3], Surowiak P[1]

[1]*Department of Histology and Embryology, Medical University of Wrocław, Wrocław, Poland*
[2]*Department of Haematology, Blood Neoplasms and Bone Marrow Transplantation, Medical University of Wrocław, Wrocław, Poland*
[3]*Department of Pathological Anatomy, Medical University of Wrocław, Wrocław, Poland*
[4]*Department of Histology and Embryology, Medical University of Poznań, Poznań, Poland*

Non-Hodgkin's lymphomas (NHL) are a heterogeneous group of disorders characterised by malignant proliferation of lymphoid cells.

Multidrug resistance (MDR) is the most important reason for unsuccessful chemotherapy of malignant lymphomas. One of the best understood and most intensively studied mechanisms of drug resistance is the overexpression of membrane-associated glycoprotein. Cyclooxygenase-2 (COX-2) is an inducible enzyme that plays an important role in inflammation and tumour cell biology. Many studies indicate a positive correlation between MDR1/P-gp expression and Cox-2 expression suggesting that the combination of COX-2 inhibitors with standard chemotherapy may enhance the potential of treatment options for malignant lymphomas.
The aim of this study was to examine the relationship between the expression of COX-2 and MDR associated proteins in a group of primary non-Hodgkin's lymphoma cases. The relation between the expression of proteins and the clinicopathological parameters and survival was also investigated.
Immunohistochemical analysis was performed retrospectively on tissue samples that were taken from 56 previously untreated patients. The expression of COX-2 and MDR proteins was evaluated using monoclonal antibodies anty-COX-2 and anty-MDR proteins. The results were compared to the clinicopathological feathers and survival date of these patients. COX-2 expression was detected in 42 (79%) cases of NHL. Studies have shown that expression of COX-2 was significantly associated with expression of all ABC-transporters ($p < 0.05$). There was no correlation between expression of COX-2 and any clinicopathological parameters ($p > 0.05$). Kruskall-Wallis analysis showed that MRP2 and BCRP expression was significantly associated with the clinical response ($p = 0.0469$ and $p = 0.0285$, respectively). LRP expression was correlated with the clinical stage of the disease ($p = 0.0266$) and serum level of β-microglobulin ($p = 0.014$). Kaplan-Meier analysis showed that cases with higher BCRP expression significantly correlated with shorter progression-free survival ($p = 0.078$). The results demonstrate the relationship between COX-2 and ABC-transporters suggesting that COX-2 inhibitors may prove useful in the prevention of multidrug resistance in response to lymphoma chemotherapy and should be further evaluated.

THE TRIGEMINAL GANGLION IN PIGEONS (*COLUMBA LIVA*)

Szczurkowski A

Department of Comparative Anatomy, Institute of Biology, Świętokrzyski University, Kielce, Poland

The aim of the investigation was the morphology and cellular structure of trigeminal ganglions in pigeons (*Columba liva*).
The reported examinations were carried out on five pigeons of either sex. For histochemical examinations, the material was prepared and studied in situ by the thiocholine method of Koelle-Friedenwald modified by Gienc for morphological investigations. For histological examinations, tissues were cut into sections (3–4 μm) and stained with H–E and cresyl violet methods.
The trigeminal ganglion of the pigeon is a structure connected with two branches of the trigeminal nerve: the ophthalmic branch and the mandible branch. Both parts of the ganglion are distinctly different in their morphology. The part connected with the ophthalmic branch — V_1 forms a thickening of the nerve, which becomes narrow as it approaches the orbital cavity. The second part connected with the mandible branch — V_2 is a regular shape. This part of the ganglion is located in the vicinity of a delicate maxillary branch. Histological investigations allowed observation of the characteristic arrangement of neurocytes of the investigated structure, and on the surface of the ganglion there was only one layer of nerve cells. Neurocytes were dispersed on the whole surface of cross-sections.

DIGITAL-IMAGE ANALYSIS OF THE LEFT COMMON CAROTID ARTERY IN HUMAN FOETUSES

Szpinda M

Department of Normal Anatomy, Nicolaus Copernicus University in Toruń, Ludwig Rydygier Collegium Medicum in Bydgoszcz, Bydgoszcz, Poland

The rate of growth of the left common carotid artery during gestation has not been sufficiently determined. The present study was performed on 128 spontaneously aborted human foetuses aged 15–34 weeks to compile normative data for dimensions of the left common carotid artery at varying gestational ages. Using anatomical dissection, digital image analysis (system of Leica Q Win Pro 16) and statistical analysis (ANOVA, regression analysis), a range of measurements (length, original external diameter, volume) for the left common carotid artery during gestation was examined. No significant differences were found ($p > 0.05$). Growth curves of the best-fit for the plot of each morphometric parameter against gestational age were generated. The length ranged from 14.82 ± 2.22 to 42.84 ± 4.32 mm, according to the linear fashion $y = -9.6918 + 1.5963\ x \pm 3.1706$ ($r = 0.95$; $p < 0.001$). The original external diameter increased from 0.72 ± 0.18 to 3.28 ± 0.40 mm, according to the linear model $y = -1.5228 + 0.1428\ x \pm 0.2749$ ($r = 0.95$; $p < 0.001$). The left common carotid artery-to-aortic root diameter ratio increased from 0.356 ± 0.062 to 0.480 ± 0.101. The left common carotid artery-to-aortic arch diameter ratio increased from 0.447 ± 0.079 to 0.535 ± 0.113. The volume ranged from 6.73 ± 4.06 to 369.30 ± 107.42 mm^3, in accordance with the quadratic function $y = 344.8–41.001\ x + 1.254\ x^2 \pm 46.955$ ($R^2 = 0.87$). The parameters examined have clinical application in the early recognition of arterial abnormalities, especially aortic coarctation.

MORPHOMETRIC STUDY OF THE AORTIC ARCH IN HUMAN FOETUSES

Szpinda M, Flisiński P, Wiśniewski M, Krakowiak-Sarnowska E, Dombek M

Department of Normal Anatomy, Nicolaus Copernicus University in Toruń, Collegium Medicum in Bydgoszcz, Bydgoszcz, Poland

The present study was performed on 128 spontaneously aborted human foetuses aged 15–34 weeks, to establish normal values for aortic arch dimensions at varying gestational ages. Using anatomical dissection, digital-image analysis (system of Leica QWin Pro 16) and statistical analysis (ANOVA, regression analysis) the growth of the length, external diameter, and volume of the aortic arch and the aortic isthmus diameter were examined during gestation. No significant gender differences were found ($p > 0.05$). The aortic arch length ranged from 3.93 ± 0.57 to 15.25 ± 1.98 mm, according to the linear function $y = -6.079 + 0.6370\ x \pm 1.1133$ ($r = 0.96$, $p < 0.001$). The aortic arch diameter ranged from 1.61 ± 0.24 to 6.13 ± 0.49 mm, according to the linear fashion $y = -2.413 + 0.2532\ x \pm 0.3532$ ($r = 0.97$, $p < 0.001$). The aortic isthmus diameter ranged from 0.92 ± 0.24 to 4.99 ± 0.58 mm, in accordance with the linear model $y = -2.4247 + 0.2232\ x \pm 0.3983$ ($r = 0.96$, $p < 0.001$). In foetuses aged 4–6 months the intensive increase of the relative aortic isthmus diameter was observed, and then its stabilization. The thoracic aorta volume ranged from 8.84 ± 2.90 to 453.51 ± 125.54 mm^3, according to the quadratic function $y = 513.4–58.464\ x + 1.704\ x^2 \pm 49.254$ ($R^2 = 0.90$). The normal values for aortic arch growth provided in this study will permit the identification of even minimal changes in aortic arch dimensions at different gestational ages.

HETEROTOPIC BONE FORMATION IN VARIOUS PATHOLOGICAL LESIONS

Szumilo J[1], Burdan F[2], Swatek J[1], Dudka J[1]

[1]*Clinical Pathomorphology Department, Medical University of Lublin, Lublin, Poland*
[2]*Experimental Teratology Unit of the Human Anatomy Department, Medical University of Lublin, Lublin, Poland*

Heterotopic bone formation is a rare phenomenon, occasionally seen in the stroma of both benign and malignant tumours, as well as in some non-neoplastic lesions of many locations. The pathogenesis of the condition is unclear. It has been suggested that bone-producing cells — osteoblasts — derive from mesenchymal precursor cells. Many factors, both systemic (e.g., hormonal, metabolic, genetic) and local (e.g., bone morphogenetic proteins secreted by neoplastic or/and inflammatory cells), may influence this process. The aim of the study was to evaluate the localisation and significance of the heterotopic bone formation in various unrelated pathological lesions. Based on the author's own diagnostic material, such changes were observed in intramuscular cavernous haemangioma, skin compound melanocytic nevus, recurrent adenoid cystic carcinoma of the maxillary sinus, primary rectal adenocarcinoma and postinflammatory lesions in omentum of patients with a history of colorectal adenocarcinoma. In all the cases, heterotopic bone was unexpectedly revealed in routine specimens. It seems that this type of lesion is without any clinical significance; however, it could be sporadically visualized by imaging and brings about some diagnostic difficulties.

RAT LIVER LYMPH NODES AFTER INJECTION OF ANTIGEN INTO INDIVIDUAL LIVER LOBES

Ślusarczyk K, Jarosz R, Pastuszka A

Department of Descriptive and Topographic Anatomy, Zabrze, Medical University of Silesia, Katowice, Poland

Since lymph from rat livers flows in different directions, the question arises - what is the response of different regional lymph node groups?
The material consisted of 30 male Wistar rats.
The methods were injection of antigens (India ink, erythrocytes, LPS or BSA) into individual liver lobes. Examination of regional lymph nodes (histological slices, H-E staining, localization of B and T lymphocytes) was carried out after 1, 4, 7 and 14 days.
In each case, the left mediastinal anterior lymph node responses were taken after 7 days, as well as the hepatic and deep hepatic after administration of antigen into the median left and right or caudate lobes, respectively.
Site antigen administration influences the location of lymph node response.

CEREBRAL ARTERIAL CIRCLE — MORPHOLOGY AND ANATOMIC VARIATIONS

Świątnicki W, Izdebski W, Wolski C, Rotkiewicz A

Department of Radiology and Diagnostic Imaging, University of Łódź, Łódź, Poland

The purpose of this report is to observe the morphology and anatomic variations of the circle of Willis.
Contrast enhanced Multi-Slice Detector Computer Tomography (MDCT) was performed in 89 healthy subjects. The anatomic variants of the anterior and posterior parts of the circle were determined separately. According to its morphology, the cerebral arterial circle was divided into four types. Type A — intact circle, type B — circle with complete anterior circulation and incomplete posterior circulation, type C — circle with incomplete anterior circulation and complete posterior circulation and type D — circle having incomplete anterior and posterior circulation. Moreover, based on ontogenetic development, assessment of the circle component vessels was performed.
Twenty subjects (22.5%) demonstrated a complete anterior part of the circle. Double anterior communicating artery (ACoA) occurred in 3 subjects (3.4%), and 8 subjects (9%) had a median callosal artery branching from the ACoA. The posterior communicating artery (PCoA) on the left was present in 44 subjects (49.4%), mainly in women. Adult configuration was its predominant ontogenetic type (63.6%). Right PCoA occurred in 45 subjects (50.6%), mainly in women. Adult configuration was its predominant ontogenetic type again. Type A, B, C and D were found in 20 (22.5%), 48 (53.9%), 7 (7.9%) and 14 (15.7%) subjects, respectively. No statistically significant differences were found in each type between the different sex groups.

APLASIA OF SINUSES IN HISTORICAL SKULLS

Teul I[1], Lorkiewicz W[2], Zbisławski W[1], Czerwiński F[1], Lorkowski J[3]

[1]*Chair and Department of Human Anatomy, Pomeranian Medical University, Szczecin, Poland*
[2]*Chair of Anthropology, University of Łódź, Łódź, Poland*
[3]*Rehabilitation Centre "Health", Cracow, Poland*

It has always been thought that the skull hides in itself the most amount of information about man's past. For this reason, it was, and still is, the most interesting investigative material.
The frontal sinuses form the part of pneumatic cavities in the mucosa lined bones which open to the nasal cavity. The lack of symmetry in size and shape is actually a rule in the structure of sinuses. Anatomists and clinicians have been discussing this area of the head for centuries. Historical speculations concerning the presence of pneumatic spaces were as variable and numerous as they are today.
The aim of the study was the assessment of frontal sinus aplasia in four series of skulls representing chronologically diverse populations from Poland: Neolithic, early mediaeval, mediaeval and contemporary. Evaluation of the shape and symmetry of the sinuses was performed on the basis of X-rays taken in the a–p projection. Among the four examined groups, sinuses of Neolithic skulls are most variable: they are the smallest, have the simplest morphology and highest incidence of aplasia. Early- and mediaeval skull sinuses resemble, with their morphology and area, contemporary skulls but they still have a high index of aplasia. Obtained results suggest a tendency toward an increase of pneumatisation of the frontal bone in the examined period. Associations between the degree of development of sinuses and craniometric features were also established. Skulls with aplasia show an overall tendency toward smaller dimensions, especially those including breadth (*ft–ft, co–co, eu–eu*). Correlation coefficients between the area of the sinuses and analyzed craniometric traits change with time (relatively stronger in Neolithic series, as well as early mediaeval, lacking in contemporary series) which suggests a change in their importance in the developmental processes of the skull.

VASCULARITY OF THE FOETAL ACETABULAR LABRUM

Topol M[1], Masłoń A[1], Snopkowska D[2]

[1]*Department of Angiology, Chair of Anatomy, Medical University of Łódź, Łódź, Poland*
[2]*Department of Pathology and Clinical Cytopathology, Medical University of Łódź, Łódź, Poland*

The aim of this study is an analysis of the vascularity of the foetal acetabular labrum and its regional differences.

Twenty-three labra taken from 23 fifth to tenth lunar-month-old, formalinized foetuses were used. We divided each labrum into four quadrants, each in the shape of 1/4 of a circle. Next, we took a specimen from each quadrant for histological examination, cutting it perpendicularly to the base of the labrum. Later the specimens were embedded in paraffin, cut into 7 μm sections stained with haematoxylin and eosin and examined with light microscopy at 200× magnification. We divided each specimen into 4 areas: proximal capsular, distal capsular, proximal articular and distal articular, and we counted the number of blood vessels in each area, taking into consideration the foetus age in the further course of research. After analysis of 24 specimens (6 labra), we found better vascularity of the capsular areas. However, we did not find significant differences in vascularity depending on the quadrant of the labrum. The study is in progress.

MORPHOMETRIC ANALYSIS OF AGNOR REGIONS IN NUCLEI OF AGGRESSIVE FIBROMATOSIS (DESMOID TUMOUR) CELLS

Tosik D[1], Kopczyński J[2], Stalińska L[3], Łopaczyńska D[3], Sygut J[2], Sidor M[2], Kulig A[4], Bartel H[1], Ferenc T[3]

[1]*Department of Histology and Tissue Ultrastructure, Medical University of Łódź, Łódź, Poland*
[2]*Department of Neoplasm Pathology, Świętokrzyski Centre of Oncology, Kielce, Poland*
[3]*Department of Biology and Genetics, Medical University of Łódź, Łódź, Poland*
[4]*Department of Clinical Pathology, Institute of Polish Mother's Health Centre, Łódź, Poland*

Aggressive fibromatosis, also called desmoid tumour, is a mesenchymal neoplasm that develops from muscle connective tissue, fasciae and aponeuroses. This neoplasm rarely undergoes histological malignancy and lacks metastatic potential; however, it demonstrates the ability to infiltrate local tissue. Desmoids may occur in extra-abdominal, abdominal or intra-abdominal locations. We checked transcriptional activity and, indirectly, proliferative activity of tumour cells by means of silver staining of nucleolar organizer regions (NOR's) of tumour cells and morphometric analysis of stained nucleoli. Silver staining was performed according to the method of Ploton et al. (Histochem J (1986) 18: 5–14). After staining, three parameters were measured: the area of silver dots within the nucleus and dot and cell numbers. Following morphometric parameters, based on that data, were calculated: mean AgNOR dot number per nucleus (N), mean AgNOR area per nucleus (A) and AgNOR content coefficient (N/A). We have found that morphometric parameters of AgNOR's, in the case of desmoid tumours, had values typical for transcriptionally active cells with height proliferative potential. The differences of AgNOR parameters between tumours from various locations were not observed.

DETERMINATION OF SPERMATOZOA SUBPOPULATION PARAMETERS BY MEANS OF MULTIPLE NORMAL DISTRIBUTION

Warchoł W

Department of Biophysics, Karol Marcinkowski University of Medical Sciences, Poznań, Poland

Correct evaluation of spermatozoa motility parameters is essential for the determination of semen fertilization ability. As different types of motile spermatozoa are present, the outcomes are found to be strongly heterogeneous. This caused WHO to recommend the median value instead of the mean value to present the results. This approach, however, omits information on spermatozoa condition. Although this method has been improved by means of thresholding (elimination of spermatozoa that do not meet clearly defined criteria), it still seems to be statistically incorrect and useless in abnormal cases.

The aim of the study was to develop and verify an alternative method to evaluate heterogeneous distribution of motile spermatozoa parameters, based on maximum likelihood fit of theoretical multiple normal distribution to a selected parameter.

The study was conducted on 10,000 randomly generated data sets simulating three normally distributed subpopulations (N_1: 10–200, $mean_1$: 3–5, STD_1 0.3–1; N_2: 10–200, $mean_2$: 5–10, STD_2 1–3; N_3: 10–200, $mean_3$: 10–35, STD_3 3–10) and on real VSL (Velocity Straight Linear) data obtained from 10 samples of normospermic or oligospermic (I°) human semen. The parameters of the simulated data range were prepared posteriori according to real data outcomes with a very wide margin. The analyzed real data covers from 300 to 700 motile spermatozoa. The analyzed data (both simulated and real) were fitted to four models (1, 2, 3 or 4 normally distributed components) with variable fractions, mean and standard deviations. The maximum likelihood method was used. Determination of the number of components was provided using F-test of improvement of goodness of fit. The measure of fit quality was the sum of the squares of residues of theoretical cumulative distribution and sample cumulative distribution. Additionally, the Kolmogorov-Smirnov statistical test was used to find fit quality estimations.

The analysis of simulated data allows the rejection of one-component model. Thirteen percent of the analyzed cases failed to test the improvement of the three-component model vs. the two-component model. The mean error of estimation varies from 6% (mean for 3rd component) up to 12% (fraction of the 1st and the 2nd components). The four-component model failed to meet the improvement criterion ($p > 0.05$) for all cases. The analysis of real samples shows evidence of three normal components for all cases (F-test of improvement $p < 0.05$). The K-S test was passed ($p > 0.5$) as well. The four component model was rejected due to bad improvement against the three-component model.

CHANGES IN SUBPOPULATIONS OF LYMPHOCYTES LOCALIZED IN THE ILEUM AND ILEAL LYMPH NODES OF PIGLETS DURING THE POSTNATAL PERIOD

Wąsowicz K[1], Winnicka A[2], Podlasz P[1], Kaleczyc J[1], Łakomy M[1]

[1]*Division of Animal Anatomy, Department of Functional Morphology, Faculty of Veterinary Medicine, University of Warmia and Mazury, Olsztyn, Poland*
[2]*Department of Clinical Science, Faculty of Veterinary Medicine, Warsaw Agricultural University, Warsaw, Poland*

The aim of the study was to examine with morphological (immunohistochemistry) and quantitative (flow cytometry) methods, the changes in subpopulations of CD2+, CD5+ and CD21+ lymphocytes in the wall of ileum and in ileo-caecal lymph nodes of newborn, 2-week- and 4-week-old gilts. The pigs were deeply anaesthetized. The animals used for immunohistochemistry were perfused with paraformaldehyde. The animals used for flow cytometry were exsanguinated. From all animals, the terminal part of the ileum and the ileo-caecal lymph nodes were excised. Tissues used for immunohistochemistry were cut with a cryostat and processed for indirect immunofluorescence with antibodies against CD2, CD5 and CD21 antigens. Tissues used for flow cytometry (lymph nodes, ileum) were finely chopped and shaken with PBS to liberate the lymphocytes. The lymphocyte suspensions were incubated with antibodies against the studied lymphocyte antigens. The cells were analyzed using FACScalibur and CellQuest (BD). Immunohistochemical staining revealed that CD2+ and CD5+ lymphocytes were distributed in a similar manner. They were disseminated throughout the lymph nodes and ileal wall except for the middle of the germination centres. CD21+ lymphocytes were located as a sharp area in the germination centres, both in lymph nodes

and the ileal wall. No clear-cut differences in lymphocyte distribution were found between the groups. Flow cytometry revealed that the number of CD2+ lymphocytes in lymph nodes was highest in the 2-week-old animals, while in the ileum the number of cells rose steadily from newborn to 4-week-old gilts. The number of CD5+ cells in lymph nodes was again highest in 2-week-old animals, but in the ileum their number decreased with age. The number of CD21+ lymphocytes in lymph nodes rose with age, while in the ileum their number was highest in 2-week-old animals. The differences were found to be statistically significant. Further studies are aimed at the examination of the relationship between the nervous system and the immune system with morphological methods, as well as with quantitative methods (flow cytometry, ELISA) as regards the CD2, CD21, CD4, CD5, CD8 and TCR gamma/delta lymphocyte subpopulation and nerve fibres containing neuropeptides, such as VIP, GAL, SP, SOM and markers of adrenergic (DBH) and cholinergic (VAChT) nerve fibres.

EARLY DEVELOPMENT OF THE CHORDA TYMPANI

Weglowski M, Łuczewski Ł, Woźniak W

Department of Anatomy, Poznań University of Medical Sciences, Poznań, Poland

The normal facial nerve path through the temporal bone is divided into three segments, viz., labyrinthine, tympanic and mastoid.
The facial nerve is the nerve of the second pharyngeal arch and it develops from the fascio-vestibulocochlear primordium, which appears as a column of cells in close proximity to the placode of the arch in relationship to the rhombomere 4.
The aim of the present study is to trace the early development of the facial nerve with special considerations to the topography of the chorda tympani, which is the first branch of the facial nerve to appear during its development.
The study was made on human embryos from the Collection of the Department of Anatomy of the University of Medical Sciences in Poznań. The specimens were staged according to international criteria and covered stages 13 through 16. They have an estimated postovulatory age of 32 to 37 days. They were sectioned at 5 or 10 μm in the transverse, frontal or sagittal planes and stained mainly with haematoxylin and eosin or protargol silver. In embryos at stage 13, somatic and visceral efferent nuclei and the common afferent tract are seen within the brain stem primordia. The otic vesicle is associated with rhombomere 5 and the fascio-vestibulocochlear ganglion is discerned at the level of rhombomere 4.
In embryos of stage 14, the pontine flexure appears and the fascio-vestibulocochlear ganglion is differentiated into primordium of the geniculate ganglion and the vestibulocochlear ganglion. The facial nerve is in vertical orientation and may be traced in the second pharyngeal arch. There are no branches of the facial nerve.
During stage 15, the facial nerve elongates and its first branch, which is the chorda tympani, arises. It runs horizontally, anteriorly and medially. In addition, the greater petrosal nerve appears.
At stage 16, all segments of the facial nerve become well defined and the chorda tympani joins the mandibular nerve.

CYTOMORPHOLOGY DIAGNOSIS OF THE CONJUNCTIVAL SAC

Wesołowska K, Zieliński A

Department of Cytophysiology, Histology and Embryology, Medical University of Łódź, Łódź, Poland

The diagnosis of allergic conjunctivitis is usually made on the basis of clinical signs. More precise tests are taken exceptionally. Most of all these are biochemical tear examinations. Conjunctival sac cytomorphology diagnosis is performed very rarely but can be very useful in the diagnosis of allergic conjunctival inflammation. It is also used in research on the effectiveness of allergic drugs and model examinations of allergic conjunctival inflammation. A cytological test can be performed using tears, conjunctival scrapings, impression cytology or conjunctival biopsy. This article reviews previous knowledge about the performance and usefulness of conjunctival sac cytomorphology diagnosis in various allergic conjunctivals.

LACRIMAL DUCT EXFOLIATIVE CYTOLOGY OF PEOPLE WITH ALLERGIES, OUT OF THE POLLEN SEASON

Wesołowska K, Zieliński A

Department of Cytophysiology, Histology and Embryology, Medical University of Łódź, Łódź, Poland

In an ocular allergy diagnosis, conjunctival provocation test examinations are only based on existing clinical symptoms. Scientific publications regarding the precision of that test are also limited to the evaluation of clinical symptoms. Cytological examinations are performed occasionally. There are no standards for such examinations. However, these examinations can be very instrumental in recognizing as well as monitoring the treatment of allergic conjunctivitis.
The aim of this research is the accurate estimation of the usefulness of tear fluid cytology diagnosis as well as conjunctival provocation tests in the allergic inflammation of lacrimal ducts.
It will help to describe cytograms for the clinical state of both allergic people and healthy subjects. It is supposed to define whether conjunctival provocation tests are coherent with particular clinical stadiums of disease. It would allow a more accurate diagnosis of this disease.
The examinations were performed on 30 patients with seasonal allergic symptoms, out of the pollen season. Material for exfoliative examination of tear fluid was collected from the inner canthus without touching the ocular surface, in an amount of 2 µl with use of a microcapillary tube. The tear fluid was spread on a glass slide and stained with Giemsa. All identifiable cells on each slide were counted at 600 × magnification using light microscopy.
In the case of most patients, the amount of collected tear fluid was minimal. On the glass slides, epithelial cells (superficial layer and deep layer), neutrophils, lymphocytes and monocytes were observed. The epithelial cells were counted in all preparations. Often these cells appeared in big clusters. This related to cells from the deep part of the epithelium, and sometimes to cells from the superficial part of the epithelium. Cells from the deep part of the epithelium often appeared in the form of a "bare" nucleus. Neutrophils appeared rather rarely; mostly it had a tri-segmental nucleus, although double- and four- segmental nuclei cell were also observed.

MORPHOLOGICAL ASPECTS OF THE CRANIOCERVICAL JUNCTION IN DOGS

Wiełądek A, Kupczyńska M

Department of Morphological Sciences, Faculty of Veterinary Medicine, SGGW, Warsaw, Poland

The aim of the study was to describe the morphology of the craniocervical junction ligaments in dogs with the focus on its influence in the occipital dysplasia.
The research examined cadavers of 20 adult male and female dogs of different breeds, fixed in 10% formaldehyde.
The structures of the atlantooccipital and atlantoaxial articulations, particularly of ligaments, have been examined with great care. The atlantooccipital and atlantoaxial ligaments are a constitutional, multicomponent and multilevel system of ligaments. They should be considered as a functional

integrity. The results of the research indicated that the stability of the craniocervical junction depends not only on well-known ligaments like: apical ligament of dens, alar ligaments, transversal atlantal ligament and lateral atlantal ligaments. In addition, three pairs of ligaments have been described about which no information in literature had been found. Names for them have been proposed: dorsal atlantal ligament, collateral internal cranial atlantal ligament and collateral internal caudal atlantal ligament. The investigations have delivered new information about alar ligaments meaning and its course. It is generally known that binate alar ligaments run from the apex of the dens to the inner surface of the occipital condyles. It has been observed that each of them attaches not only to the apex but also to the lateral side of the dens. This has given the impression of alar ligament duality. The briefer part extends under the transverse atlantal ligament to the atlas. The longer part (apical) runs to the occipital condyles. Both of them are fused with a short bridge. Probably the duality of alar ligaments is a result of its development connection with C_1 and C_2 ossification. The part running to the occipital condyles is developmentally associated with "centrum of proatlas", while the part running to C_1 is associated with "centrum I" of the axis. The accident of the dog with the occipital dysplasia, occipital condyles dysplasia, atlantal dysplasia and hypoplasia of the dens pointed at the roll of the craniocervical junction ligaments in the stability in this region. The apical ligament of the dens and the longer parts of alar ligaments were absent in this accident. The collateral internal cranial atlantal ligaments and the briefer part of alar ligaments running to C_1 were responded for stability in the craniocervical junction in this dog.

DOWNREGULATION OF *PLAGL1* AND *LATS1* GENES IN COLORECTAL ADENOCARCINOMA

Wierzbicki P[1], Adrych K[2], Kartanowicz D[1], Dobrowolski S[3], Stanisławowski M[1], Smoczyński M[2], Śledziński Z[3], Kmieć Z[1]

[1]*Department of Histology and Immunology, Medical University of Gdańsk, Gdańsk, Poland*
[2]*Department of Hepatology and Gastroenterology, Medical University of Gdańsk, Gdańsk, Poland*
[3]*Department of Surgery, Medical University of Gdańsk, Gdańsk, Poland*

PLAGL1 and *LATS1* are tumour suppressor genes located at 6q23–25. *PLAGL1* is responsible for mitotic arrest connected with TP53. Decreased expression of *PLAGL1* was observed in various solid tumours, including breast, ovarian and melanoma cancers. *LATS1* is a serine-threonine kinase associated with the mitotic spindle that is dependent on CDK2/cyclin B. *LATS1* is downregulated in sarcomas, astrocytomas, ovarian and breast cancers.
The aim was to investigate the rate of expression of *PLAGL1* and *LATS1* in colorectal adenocarcinomas (CRC) at mRNA level. Further, the loss of heterozygosity (LOH) at 6q23–25 locus was analyzed to determine the deletion rate of *PLAGL1* and *LATS1* genes in genomic DNA.
Mucosal colonic biopsies were obtained from 57 CRC patients (mean age: 67 ± 10.1; M/F: 40/17; mean age: 66.1 ± 10.9; 68.4 ± 8.1, respectively) and 37 healthy patients (mean age: 52.2 ± 14.7, M/F: 16/21; mean age: 48.4 ± 14; 55.1 ± 14). mRNA content of *PLAGL1* and *LATS1* was determined by Real-Time PCR using SybrGreen fluorophore and iQCycler (BioRad, USA). Quantification of *PLAGL1* and *LATS1* mRNA was done using the ΔCt equation in comparison to transcript levels of three constitutive genes: *ACTB* (β-actin), *RPL32* and *HPRT1*. LOH value at *PLAGL1* and *LATS1* loci was based on D6S310, D6S1704, D6S1654 and D6S1687 microsatellite marker analysis.
Underexpression of *PLAGL1* and *LATS1* genes was found in 45 and 52 of 57 tumour lesions, respectively ($p < 0.005$; Mann's-Witney U test). There was also a statistically significant relationship between expression rates of *PLAGL1* and *LATS1* and UICC/AJCC stage ($p < 0.05$; $p < 0.005$, Kruskal-Wallis ANOVA test); the correlation coefficient was $R^2 = -0.3$ and $R^2 = -0.52$ (Spearman's test). LOH analysis showed allelic deletions in separate markers: D6S310 12/40 (30%), D6S1704 12/49 (24%), D6S1654 10/40 (25%) and D6S1687 9/45 (20%). LOH rate corresponded with the lower expression of *PLAGL1* and *LATS1* genes ($p < 0.05$; Fisher's exact test).
The expression of *PLAGL1* and *LATS1* tumour suppressor genes is severely diminished in colorectal cancer. Further studies are needed to elucidate the significance of the reported findings.

COCAINE AND AMPHETAMINE-REGULATED TRANSCRIPT-IMMUNOREACTIVE (CART-IR) STRUCTURES IN THE PORCINE AUTONOMIC AND SENSORY NERVE SYSTEM

Wojtkiewicz J, Skobowiat C, Gonkowski S, Bossowska A, Burliński P, Majewski M

Division of Clinical Physiology, Department of Functional Morphology, University of Warmia and Mazury, Olsztyn, Poland

The neuropeptide CART has been found to be widely distributed in neurons of many areas of the nerve system, including the brain, pituitary, adrenal medulla and lateral horn of the spinal cord. There is also a growing body of evidence that CART may act as a neurotransmitter or neuromodulator involved in sensory processing and autonomic regulation (Fenwick NM et al. (2006) J. Comp. Neurol.; 495: 422–433;). In the present study, we decided to describe the distribution pattern of CART in the intramural enteric, sensory and autonomic ganglia, as well as in the neurons and nerve fibres of the spinal cord of the female domestic pig. CART-IR was detected in nerve fibres and basket-like terminals surrounding many postganglionic neurons of the superior cervical (SCG), stellate (STG), paravertebral (SChG) and prevertebral ganglia (CSMG, AdG, A-RG, OG, IMG and PCG); however, postganglionic neurons of these ganglia exhibited low or non-detectable levels of CART. In contrast, numerous subsets of afferent DRG neurons at C1-Cq4 levels were CART-IR. Furthermore, CART-IR neurons and nerve fibres were abundant in the submucosal and myenteric plexuses of the oesophagus; however, they were less numerous in the myenteric plexuses of the stomach, duodenum, jejunum, ileum and proximal and distal colon. Moreover, CART-IR neurons were absent from the submucosal plexuses within the lower gastro-intestinal tract. Within the spinal cord, a moderate number of CART-IR neurons were present in the intermediolateral cell column along the thoracosacral neuromeres. The presence of CART-IR SPN in the IML and of CART-IR axons in sympathetic ganglia and the adrenal medulla suggest that CART might be a marker for SPN regulating the activity of cardiovascular postganglionic neurons and noradrenergic chromaffin cells. As may be judged from the pattern of CART-IR neuron distribution, perikarya expressing this peptide may play an important role in regulating intestinal functions, sensory information conveyance, and, on the basis of available literature, this peptide may be involved in some of the neuroprotective processes in autonomic and sensory neurons.

SPIRAL COMPUTED TOMOGRAPHIC STUDY OF THE OSSIFICATION OF THE HUMAN FETAL MAXILLA

Woźniak W[1], Bruska M[1], Piotrowski A[1], Radziemski A[1], Kulczyk T[2], Porowski L[1]

[1]*Department of Anatomy, Poznań University of Medical Sciences, Poznań, Poland*
[2]*Section of Radiology, Department of Biomaterials and Experimental Dentistry, Poznań University of Medical Sciences, Poznań, Poland*

The facial bones have no cartilaginous predecessors and they ossify in connective tissue. Intramembranous ossification is preceded by a fibrocellular proliferation derived from ectomesenchyme, in a matrix forming a membranous skeleton. The maxilla develops within the maxillary process, which derives from the first pharyngeal arch, and ossification of the maxilla

begins slightly later than in the mandible. Discrepancies exist as to the ossification of the maxilla, particularly considering the secondary ossification centres. The aim of the present study is to trace the bony maxilla using spiral computed tomography.
The study was made on 7 human foetuses aged 13, 15, 18 and 21 weeks. Radiological investigations were made with the aid of Picker CT PQ 2000. The thickness of the layer was 1.5 mm.
In the foetus aged 13 weeks, all parts of the maxilla are delineated and ossification is well in progress. The premaxillary element is evident and secondary ossification appears at the margin of the interpremaxillary suture. The ossified body of the maxilla forms the lower part of the orbit and continues into the frontal and zygomatic processes. The alveolar process is evident in the anterior part and the short palatine process is marked. The frontal process is in contact with the lacrimal bone.
In the foetus aged 15 weeks, the ossification is advanced in the alveolar and palatine processes. The short frontal process of the premaxilla fuses with the frontal process of the maxilla. The palatine process is in contact with the nasal septum. The infraorbital foramen is seen as a large hiatus. The lacrimal groove is marked. In further foetal weeks, two frontal processes of the maxilla and premaxilla fuse and the alveolar process lengthens and increases in thickness. The frontal processes are in contact with the nasal part of the frontal bone and with the ethmoidal labyrinth. The anterior nasal spine is differentiated.

DEVELOPMENT OF THE PALATAL PROCESSES OF THE MAXILLA DURING THE HUMAN EMBRYONIC PERIOD

Woźniak W, Fenger-Woźnicka S

Department of Anatomy, Poznań University of Medical Sciences, Poznań, Poland

The palate which separates the oral and nasal cavities develops from different sources as the primary and secondary structures. Cleft lip and cleft palate are frequent congenital anomalies. The primary palate is formed by the premaxillary mesenchyme and maxillary processes which establish continuity with the thick nasal septal prominence during the 6th week. The development of the secondary palate is more complex.
The aim of present study is to trace the palatal processes in staged human embryos from the collection of the Department of Anatomy at the Medical University in Poznań.
Embryos were classified according to 23 developmental stages and were sectioned serially in different planes. Sections were stained according to various histological methods. In some embryos, graphic reconstructions were made.
The palatal processes (shelves) develop on the interal aspect of the maxillary prominences at stage 17 (41 days). They are contiguous with the sides of the tongue and bent into a vertical position on each side of the tongue. With the growth of the face, the mandible and tongue are moved forward and the tongue is in contact with the primary palate.
During stages 18–20 (7th week), the palatal shelves are still in a vertical position. In the last week of the embryonic period (stages 21–23), fusion of the palatal shelves begins at its anterior portion. This fusion continues in the early foetal period. The palatal shelves also fuse with the free border of the nasal septum separating the nasal and oral cavities.

MYOSTATIN (MSTN) AND MYOSTATIN PRECURSOR PROTEIN (MSTN-PP) ARE BOTH INCREASED IN SKELETAL MUSCLES OF PATIENTS WITH TYPE-II FIBRE ATROPHY

Wójcik S, Nogalska A, Engel WK, Askanas V

USC Neuromuscular Center, University of Southern California Keck School of Medicine, Los Angeles, CA, USA

During the tenure of this work Dr. S. Wójcik was on leave from the Department of Anatomy and Neurobiology, Medical University of Gdańsk, Gdańsk, Poland

Preferential atrophy of Type-II muscle fibres occurs in several clinical situations, including cachexia, disuse, glucocorticoid treatment, and remote neoplasia, and sometimes as an aspect of recent-denervation. For the patient, the Type-II atrophy itself might be unfavourable (as a glucocorticoid side effect) or favourable (survivalistic via the muscle-alanine liver-gluconeogenesis pathway in starvation). Following total denervation, guinea-pig Type-II fibres atrophy more rapidly than Type-I fibres (Karpati and Engel, 1968). The cellular mechanisms underlying Type-II fibre atrophy are unclear. Myostatin (MSTN) is a negative regulator of muscle mass and strength. In normal human muscle, Type-II and Type-I fibres appear immunohistochemically to have the same amount of MSTN/MSTN-PP. Our study evaluated a possible role of myostatin in Type-II fibre atrophy in human muscle. MSTN and MSTN-PP were studied by a) immunocytochemistry, b) immunoblots, and c) RT-PCR, in 10 muscle biopsies containing Type-II fibre atrophy and in 10 control-muscle biopsies. We found, as compared to control normal fibres: 1) by immunocytochemistry, MSTN /MSTN-PP was diffusely increased in the atrophic Type-II muscle fibres; 2) by immunoblots, both MSTN and MSTN-PP were increased (2.2 and 3.3 times respectively, $p < 0.05$ and $p < 0.01$); 3) by RT-PCR, MSTN-mRNA was not increased.
In conclusion, our results a) suggest that MSTN and MSTN-PP might play a role in the pathogenesis of Type-II muscle fibre atrophy, b) broaden our previously-described associations of myostatin in human muscle pathology and c) could possibly lead to a clinical prevention when Type-II atrophy is unfavourable, e.g. in glucocorticoid therapy.

MICROANATOMICAL STUDY OF THE INFERIOR VENA CAVA TO THE AZYGOS VEIN COLLATERAL PATHWAY

Wółkiewicz A, Drobniak A, Koleśnik A

Department of Anatomy, Centre of Biostructure Research, Medical University of Warsaw, Warsaw, Poland

Developmental anomalies of the inferior vena cava (IVC), such as its lack of hepatic segment, require development of collateral circulation. In cases of isomeric left atrial appendages with interrupted IVC, the azygos vein (AV) serves as a major route of venous outflow from the abdomen and lower extremities. The anastomosis between IVC and AV is possible thanks to the right ascending lumbar vein (RALV), which becomes the AV in the thorax.
The study aimed to investigate the development and morphology of the anastomosis between RALV and IVC in human foetuses.
Research was carried out on 20 human foetuses of both sexes, aged 14–25 weeks of gestation, obtained from the collection of the Department Of Anatomy, Medical University of Warsaw, Poland. The vascular system was injected with gelatin — India ink solution hot fixed in 4% formaldehyde solution. The foetuses were dissected under magnification of a surgical microscope using microsurgical instruments. The anastomosis between the RALV and IVC was found in 15 foetuses (in 2 cases, double anastomosis). In order to exclude age-dependent variation of vessel size and to assess the importance of the anastomosis, the diameter of anastomosis/diameter of RALV (An/RALV) cranially to the anastomosis relation was calculated and reached 0–0.33 in 6 cases, 0.33–0.66 in 3 cases and 0.66–1 in 6 cases. In five foetuses, RALV arose directly from IVC. The anastomosis was present in most cases, and in 9/20 cases that vessel had a significant diameter. These results can also possibly explain the role of this anastomosis for collateral venous drainage in the case of IVC thrombosis or cases of unintentional catheterization of RALV during implantation of IVC filters.

EXPRESSION OF GENE CODING FOR OPIOID PRECURSORS AND RECEPTORS IN MAMILLARY BODIES OF GILTS

Wylot B[1], Kozdryk M[2], Robak A[2]

[1]*Department of Animal Physiology, University of Warmia and Mazury, Olsztyn, Poland*
[2]*Department of Comparative Anatomy, University of Warmia and Mazury, Olsztyn, Poland*

Endogenous opioid peptides and their receptors are found in all classes of vertebrates and numerous invertebrates. They are localized in distinct structures of the brain and this appears to be strictly connected with their physiological function. However, in the available literature there is a lack of data concerning the presence of opioid systems in the mamillary bodies of gilts. Therefore, the aim of this study was to examine the expression of gene coding for three opioid precursors — proopiomelanocortin (POMC), proenkephalin (PENK) and prodynorphin (PDYN) as well as opioid receptors — μ (MOR), δ (DOR) and κ (KOR), in porcine mamillary bodies.
The mamillary bodies were collected from sexually mature gilts (approx. 100 kg of body weight) in a local slaughterhouse. Total RNA was isolated and a qualitative RT-PCR assay with primers specific for opioid precursors and receptors was performed. PCR products were sequenced to confirm their specificity.
The presence of PENK, PDYN as well as DOR mRNAs was demonstrated in the mamillary bodies of gilts. The data obtained for the MOR gene are ambiguous as multiple PCR products were noted. Expression of POMC and KOR genes in porcine mamillary bodies was not detected.
The results of this study show that expression of gene coding for PENK, PDYN and DOR take place in porcine mamillary bodies. Possibly, several μ-opioid receptor transcripts are synthesized in these structures as a result of alternative splicing. These results may suggest a physiological role of opioid systems in the mamillary bodies of gilts.

THE ANATOMY OF HUMAN AND ANIMAL VENOUS FORAMINA OF THE SKULL

Wysocki J

Clinic of Otolaryngology and Rehabilitation, II Medical Faculty, University Medical School, Warsaw, Poland
Centre of Excellence, Institute of Physiology and Pathology of Hearing, Warsaw, Poland
Department of Vertebrate Morphology, Academy of Podlasie, Siedlce, Poland

In order to investigate if the size of selected human skull foramina with significant venous compartment were significantly correlated with the skull capacity, an anatomical study was undertaken. A total of 100 macerated human skulls, 100 from macaques, 67 from bison, 25 from mongrel dogs, 37 from foxes, 22 from cats, 80 from hares, 14 from rats, 11 from ostriches and 47 from chickens were examined to determine the diameter of the foramina and the skull capacity. Measurements of the surface area of the foramina were made using a computerized digital analysis system.
In animals, many correlations between skull capacity and area of foramina have been proven. In humans, only the size of the hypoglossal canal and jugular foramen were found to correlate significantly with the capacity of the skull. This correlation, together with the considerable size of the hypoglossal canal, indicated its important role in the venous drainage of the brain.
In humans, there was considerable centralization of venous outflow from the brain with 60% of the area of all venous foramina of the skull occupied by jugular foramina. In animals, this concentration varied from 16% in bison to 45% in foxes.
An asymmetry between the right and left jugular foramen was identified, with an average ratio of 1.6 (range between 1 and 3.47); however, in animals, the ratio was less than 1.3. In the case of right-sided domination, the correlation between the skull capacity and the size of both jugular foramina was negative (the larger the cavity of the skull, the less the asymmetry), and in the case of left-sided domination, it was positive. Perhaps the left-sided domination is less advantageous for the haemodynamics of blood outflow as the left brachiocephalic vein is longer and is often compressed by the sternum and aortic arch.

PROPORTIONS OF HUMAN AND ANIMAL LARYNXES IN IMMATURE AND MATURE INDIVIDUALS

Wysocki J[1, 2, 3], Kielska E[3]

[1]*Clinic of Otolaryngology and Rehabilitation, II Medical Faculty, University Medical School, Warsaw, Poland*
[2]*Centre of Excellence, Institute of Physiology and Pathology of Hearing, Warsaw, Poland*
[3]*Department of Vertebrate Morphology, Academy of Podlasie, Siedlce, Poland*

The aim of the present study was to investigate the anticipated changes in structure and proportions of the larynx between immature and mature individuals of humans and animals. It was of special interest to obtain an answer for the question: in sexual dimorphism, are the characteristics of the human larynx observed before sexual maturation, and are they observed in other mammals.
Human material selected for the study was obtained from the Forensic Medicine Department, University Medical School, Warsaw. Animal material was obtained from slaughterhouses, where cows and pigs were routinely sacrificed, so there was no need to obtain permission from the bioethics committee. Twenty-five larynges of infants and adolescents were studied and 20 adult human larynges (10 female and 10 male), 31 larynges of pigs (17 piglets and 14 sows and boars) and 27 larynges of cattle (13 heifers and calves and 14 beeves and bulls). Infants and adolescents were less than twelve years old. The age of the mature humans was: 17–48. The piglets were from 12 to 18 weeks of life. The heifers and calves were from 12 to 16 weeks. The sows and boars as well as the cows and bulls were old breeding animals.
The methods used in the study were based on anatomical preparation, anatomical description and measurements performed with use of a digital camera and computer-aided system MULTISCAN. In statistics Tukey's test and Pearson's linear correlation coefficient were calculated.
It was proved that the dependence of proportions of the larynx on the age of the individual is observed in several of them in humans and pigs but not in cattle. Statistically important differences in proportions of the larynx between sexes were observed in some of them in pigs and in one in cattle. In humans, the proportions of the larynx are not dependent on gender and are almost the same in both genders of one age group. Nevertheless, the basic measured parameters were greater in female specimens. The child's larynx, before maturation, is characterised by greater slenderness in comparison with the adult's larynx, which is due to the overweight of axial dimensions over the horizontal ones.

TOPOGRAPHY AND CONTENT OF THE TYMPANIC CAVITY OF RABBITS

Wysocki J[1, 2], Krasucki KP[3]

[1]*Department of Vertebral Anatomy, University of Podlasie, Siedlce, Poland*
[2]*Department of Otolaryngology and Rehabilitation, Second Faculty of Medicine, University of Medical Sciences, Warsaw, Poland*
[3]*Head and Neck Clinical Anatomy Laboratory, Institute of Physiology and Pathology of Hearing, Warsaw, Poland*

In accessible literature, there is no comprehensive topographic description of the tympanic cavity and temporal bone of the rabbit. This paper is an attempt to fill this gap in the literature.
Twenty-four rabbit (12 rabbits of both genders) temporal bones underwent anatomical preparation in a stereoscopic microscope. Soft material was preserved in 10% acetic formaldehyde. Statistical assessment of the results was performed.
Observations revealed that the tympanic cavity is divided into a few smaller parts, making hollows, among them the epitympanic recess and tympanic sinus.
The epitympanic recess makes a cavity of 3.5 mm in diameter. It is closed by the epiphysis of the jugular process and medial wall of the external auditory canal. From the medial site, it is closed by the prominence of the anterior semicircular canal, and in this region it is adjacent to the subarcuate fossa.
From the inferior site, the recess lies directly over the facial nerve, and there is a prominence of the horizontal semicircular canal in its bottom. The tympanic sinus is limited by the colliculus in the frontal part, the facial nerve canal from upper part and is adjacent to the jugular foramen with the internal cervical vein and IX, X, XI cranial nerves in the inferior and medial parts.
However, the colliculus is a special orientation point in the tympanic cavity in the rabbit temporal bone, and it is visible only after opening the tympanic cavity wide.
From the colliculus, the internal carotid artery, placed in the bony canal, goes to the front part. Mean minimum distance between the cochlear window and the carotid artery canal is 4.34 mm. The easiest way to open the middle ear part in this species is to open the tympanic cavity or to get there from the epitympanic recess side. The malleus has a thin rostralis process and shorter and wicker muscular and horizontal processes. The average malleus length is 5.13 mm. The incus consists of a body and long (average length is 2.54 mm) and short (average length is 1.38 mm) crus. The stapes is very delicate. The average height of the stapes is 1.45 mm.

DISTRIBUTION OF SP-IMMUNOREACTIVE NEURONAL ELEMENTS IN THE PANCREAS OF SHEEP

Zacharko-Siembida A

Department of Animal Anatomy and Histology, Agricultural University of Lublin, Lublin, Poland

The pancreas is known to be controlled by a multisignaling system in which both hormones and autonomic nerves are of key importance. The goal of the present study was to map out the distribution pattern of the ovine pancreatic nerve fibres expressing SP. In order to elucidate the possible involvement of neuropeptides in the small ruminant pancreas activity, the co-expression of CGRP, VIP, GRP and SP was studied with double immunocytochemistry.
Interacinar spaces and interlobular connective tissue were richly innervated by SP-positive, mainly varicose, nerve terminals. Numerous, mainly large, pancreatic arteries and veins were supplied with abundant SP-positive nerve terminals which mostly co-expressed CGRP. Immunoreactivity to SP was also detected in single nerve fibres of the duct system, in scarce nerve terminals reaching the islet border and only exceptionally in those penetrating inside the islet. In small populations of nerve fibres located amongst the acini, around small blood vessels and in several neurons of intrapancreatic ganglia, the co-localization of VIP with SP was observed. None of the GRP-positive nerve terminals showed the presence of SP.
In conclusion, the results of the present study clearly documented that the pancreas of the sheep is supplied with peptidergic nerve fibres in a species-dependent manner. On the basis of the occurrence and frequency of SP, VIP and CGRP (alone or in combination) in pancreatic neuronal elements, it is suggested that SP may act as an important regulator of ovine pancreatic functions (both endocrine and exocrine).

ORGANIZATION OF ACETYLCHOLINE CONTAINING STRUCTURES IN THE CRANIAL MOTOR NUCLEI OF THE RHOMBENCEPHALON OF PIGS

Załęcki M, Całka J, Łakomy M

Department of Functional Morphology, Division of Animal Anatomy, Faculty of Veterinary Medicine, University of Warmia and Mazury, Olsztyn, Poland

We explored the immunoreactivity of choline acetyltransferase (ChAT) in the cranial nerve motor nuclei of pig rhombencephalon to reveal the cholinergic nature of these regions.
Three sexually immature gilts of the Large White Polish race were used for the study. In our experiment we applied ChAT-immunohistochemistry for the visualization of all acetylcholine containing structures. The slides were analyzed under a Zeiss fluorescent microscope.
All studied motor nuclei contained ChAT-positive cell bodies and fibres, but the intensity of staining differed between the nuclei. Furthermore, characteristic ChAT-immunoreactive bouton-like structures, which are known to be synaptic terminals of the cholinergic system, were observed in the borders of all studied regions. The localization of ChAT-positive "boutons" in the neuropil of the examined nuclei and their proximity to stained perikarya allowed us to differentiate two groups of motor nuclei in the rhombencephalon of the pig:
— Nuclei containing ChAT-positive bouton-like structures dispersed in the neuropil, often establishing contact with the stained cell bodies — motor trigeminal, abducent, facial, ambiguous and hypoglossal nuclei.
— Nuclei in which characteristic boutons were dispersed between the ChAT-positive cells but were devoid of any contact with perikarya — dorsal motor nucleus of the vagus nerve.
These results provide new data concerning the central nervous system of swine and could be useful in further experiments on amyotrophic lateral sclerosis (ALS) — the disease that results in progressive degeneration of motoneurons in the brain and spinal cord.

VASCULAR AND NONVASCULAR CONNECTION OF THE PROXIMAL A2 SEGMENTS OF THE ANTERIOR CEREBRAL ARTERIES

Zaremba A[1], Izdebski P[1], Ciszek B[1,2]

[1]*Department of Anatomy Centre of Biostructure Research Medical University of Warsaw, Warsaw, Poland*
[2]*Department of Neurosurgery, Bogdanowicz Pediatric Hospital Warsaw, Warsaw, Poland*

The anterior cerebral arteries of both sides are connected by the anterior communicating artery complex. This configuration of the arterial system presents many different variants. During dissection of the anterior cerebral arteries in the proximal A2 segments, several additional connections, nonvascular (fibrous-like bands) as well as vascular, were observed.
The aim of study was to analyze the number frequency and variability of such vascular and nonvascular connections as elements of junctions between both anterior cerebral arteries.
The study was conducted on 100 specimens by means of microanatomical dissection with the use of a surgical microscope.
Connections of the proximal A2 segments other than anterior communicating arteries were observed in about 30% of cases. In about 20% of cases, it was nonvascular single or multiple connections. In about 10 % of the dissected brains, it was accessory thin vascular connections in front of the anterior communicating artery.
These connections of the proximal A2 segments of the anterior cerebral arteries play an important role during execution of different types of the interhemispheric approach to the sellar/suprasellar region and ventricular system of the brain.

ORGANIZATION OF PROJECTION FROM THE LOWER BRAINSTEM RETICULAR NUCLEI TO THE PYRAMIS AND UVULA IN THE RABBIT CEREBELLUM

Zguczyński L[1], Bukowska D[2], Mierzejewska-Krzyżowska B[1]

[1]*Department of Anatomy, University School of Physical Education, Gorzów, Poland*
[2]*Department of Neurobiology, University School of Physical Education, Poznań, Poland*

The brainstem reticular formation (RF) contains many neuronal aggregations, which project into the cerebellar cortex. In this study, the connections from RF of the medulla and pons to the pyramis and uvula of the caudal vermis in the rabbit were studied using retrograde axonal transport of two fluorescent tracers: Fast Blue (FB) and Diamidino Yellow (DY). As a result of the microinjections of FB into the pyramis and DY into the uvula, labelled neurons were seen in several medullary RF nuclei and the nucleus "k" of pons. These neurons (n = 15,766) are parent for the reticulocerebellar projection. The strongest projections arise from the caudal lateral nucleus (n = 7797), both mangocellular (Lcmc) and parvocellular (Lcpc) pars and the oral lateral nucleus (Lo; n = 3893). A lower number of fibres come from the lateral reticular nucleus (LR; n = 1326) and the gigantocellular nucleus (RGc; n = 1319). In general, medullary RF projection is bilateral with over two-times ipsilateral preponderance, and it is over seven times greater to the pyramis than to the uvula. Projection from the nucleus "k" of pons, mainly subnucleus "k_2", is directed almost solely to the pyramis (n = 1417). Projections from Lcmc to the pyramis originate from the entire nucleus, except for the dorsolateral region, and those to the uvula from two separate neuronal populations, ventromedial and dorsolateral, at the rostral levels. Entire Lcpc sends connections to the pyramis, but its rostral dorsolateral region sends to the uvula. As regards LR, the ventral region of the caudal two-thirds projects to the pyramis, whereas two groups of neurons in the caudal part project to the ipsilateral uvula. In Lo, neurons projecting to the pyramis are present in the ventrolateral region, but those connecting the uvula cluster in the dorsolateral and dorsomedial regions. The central core of the caudal Rgc sends fibres exclusively to the uvula. The data show that the RF nuclei influence the two cerebellar targets to different extents. Projections from the individual RF nuclei are not the same regarding laterality and regions of origin. It probably arises due to the different functions of the pyramis and uvula.

DETERMINING GENDER DIFFERENCES OF THE A2 SEGMENT OF THE ANTERIOR CEREBRAL ARTERY USING 3D INTERACTIVE RECONSTRUCTIONS

Żurada A, Gielecki J, Osman N

Department of Anatomy, Medical University of Silesia, Katowice, Poland

Anatomically, there have been many different variations of the anterior cerebral artery (ACA), as well as many different anomalies noted in both human foetuses and adult populations. This fact has been very intriguing, and thus it was noted that a through analysis of the ACA in three dimensions (3D) should be performed. The A2 segment of the ACA was analyzed according to symmetry, age and gender differences using a new method of 3D interactive virtual reality (IVR) examination that accords for the geometrical, spatial and stereotactic parameters of the vessels.
The analysis of the A2 segments was performed using archived angio-CT files from 115 patients (75 female, 40 male) varying in age from 12 to 78 years.
The A2 segment was identified to be symmetrical in 57% of cases. The mean diameter of the A2 segment was 1.86 mm (1.19–2.84 mm) and it was higher in men (1.98 mm) than in women (1.83 mm). The mean volume was 33.83 mm^3 (4.89–128.81 mm^3) and it was also higher in men (38.84 mm^3) than in women (31.16 mm^3). These gender differences were found to be statistically significant ($p < 0.05$) for both volume and diameter. The mean length of A2 segment was 11.86 mm (3.1–32.31 mm); however, there was no statistically significant difference noted in the length between men (12.17 mm) and women (11.69 mm). The measurements were compared in relation to age but no statistical significance was to be found. Similarly, there were no statistically significant differences noted between the right and left A2 segments according to diameter, length or volume.
It is important to understand various morphometric differences particularly between genders, and when planning neurosurgical and neuroradiological procedures. By constructing blood flow simulations and revascularization procedures, surgeons are able to gain a better understanding of the patient's vascular anatomy.

DIGITAL STEREOSCOPIC ANALYSIS OF THE BASE BRAIN ARTERIAL TRIANGLE

Żurada A, Gielecki J, Osman N

Department of anatomy, Medical University of Silesia, Katowice, Poland

The arterial triangle formed by the main base brain arteries is of clinical importance during neurosurgical procedures. The current anatomical and morphometric descriptions of that arterial pattern are incomplete. This study aimed to analyze the distances between triangulation points of the right and left Internal Carotid Artery (ICA_R and ICA_L) and the basilar artery (BA). The authors anticipate that the triangulation points of the ICA and BA form an arterial triangle.
The analysis of the triangulation points was performed using archived angio-CT files reconstructed by GAIDA (gradual angiographic image data analyzer) software from 115 patients (75 female, 40 male) varying in age from 12 to 78 years.
The arterial triangle area is 189.64 mm^2 (79.35–332.29 mm^2) and it was noted to be higher in men (201.4 mm^2) than in women (183.37 mm^2). These gender differences were found to be statistically significant ($p < 0.05$). The mean ICA_R–ICA_L distance was 30.31 mm (23.35 mm – 40.52 mm), the mean ICA_R–BA was 20.65 mm (14.78 – 27.38 mm) and ICA_L–BA was 19.11 mm (11.32 – 25.74 mm). However, there were no statistically significant gender differences noted between all those distances. It was observed that there was a statistically significant difference ($p < 0.05$) between the mean distances of the ICA_R–BA and ICA_L–BA.
The ICA_R–ICA_L distance increased in relation to age with statistical significance. However, the ICA_R–BA and ICA_L–BA distances decreased in relation to age but no statistical significance was found.
Stereoscopic analysis of the arterial triangle demonstrates that the arteries of the base brain change position during an individual's lifetime. The study provides essential background useful for neuroradiologists and neurosurgeons during neurovascular procedures.

EXPRESSION OF CYCLIN A IN HL-60 AND K-562 LEUKEMIC CELL LINES AFTER INDUCTION OF APOPTOSIS WITH CHOSEN CYTOSTATICS

Żuryń A[1], Grzanka A[1], Stępień A[1], Grzanka D[2]

[1]*Department of Histology and Embryology, Nicolaus Copernicus University in Toruń, Collegium Medicum in Bydgoszcz, Bydgoszcz, Poland*
[2]*Department of Clinical Pathomorphology, Nicolaus Copernicus University in Toruń, Collegium Medicum in Bydgoszcz, Bydgoszcz, Poland*

The aim of this study was to estimate the expression of cyclin A in human leukemic cell lines HL-60 and K-562 after induction of apoptosis with cytostatics - doxorubicin and etoposide. The human promyelocytic leukaemia cell line HL-60 and human erythroleukemic cell line were used in this study.

In order to evaluate the expression of cyclin A in light microscopy, the streptavidin-biotin-peroxidase technique was used. The localization of cyclin A was also estimated using the colloidal gold labelling and immunofluorescence staining methods for electron and confocal microscopy, respectively. Additionally, cytophotometric analysis of the cell cycle was performed. The results showed that together with the increasing doses of doxorubicin and etoposide, in both cell lines, the number of cells with morphological apoptotic features was growing. Their highest percentage was observed after treatment with 200 etoposide and 10 μM doxorubicin. There were statistically significant differences in the mean number of apoptotic cells after treatment with different doxorubicin and etoposide concentrations ($p < 0.01$). There was also a decrease in cyclin A expression in HL-60 and K-562 cell lines treated with the lower doses of doxorubicin and etoposide compared to the control, and an increase after treatment with the highest concentrations. A statistically significant difference was noticed in the mean number of cells with cyclin A expression after treatment with different doxorubicin and etoposide concentrations ($p < 0.01$). Moreover, in both cell lines, the translocation of cyclin A from the nucleus to cytoplasm was observed, together with the increase of cytostatics doses. The results obtained using light and fluorescence microscopy were confirmed by electron and confocal microscopy. The immunocytochemical investigation of cyclin A showed its presence predominantly in the nucleus of non-treated cells and cells treated with lower doses of cytostatics: 0.5 µM doxorubicin and 0.2, 2.0 µM etoposide, whereas in the cells treated with 5, 10 µM doxorubicin and 20, 200 µM etoposide, cyclin A was present mainly in the cytoplasm. The observed translocation of cyclin A from the nucleus to cytoplasm may suggest a change in its function from proliferative to pro-apoptotic.

THE INFLUENCE OF HYDROGEN PEROXIDE ON THE BIOLOGY OF HUMAN SPERMATOZOA

Kotwicka M[1], Jendraszak M[1], Filipiak M[1], Warchoł W[3], Jędrzejczak P[2], Warchoł JB[1]

[1]*Department of Cell Biology, Poznań University of Medical Sciences, Poznań, Poland*

[2]*Department of Infertility and Reproductive Endocrinology, Poznań University of Medical Sciences, Poznań, Poland*

[3]*Department of Biophysics, Poznań University of Medical Sciences, Poznań, Poland*

The reactive oxygen species (ROS) produced in human spermatozoa play the important role in cell signalization. A low concentration of ROS guarantees that spermatozoa to reach the capacity for fertilizing the oocyte. However it is suggested that an increase of ROS concentration, inside as well as outside the cell, influences unfavourably on spermatozoa functions. The aim of the study was to evaluate the relationship between phosphatidylserine membrane translocation, caspase-3 activity, mitochondrial potential and spermatozoa motility and hydrogen peroxide dose.

The study was performed on fresh human spermatozoa. Spermatozoa were incubated for during 30 minutes with H_2O_2 [10, 50 and 100 mM]. In order to demonstrating the PS translocation, the spermatozoa were stained with Annexin-V-FLUOS. The mitochondrial potential was estimated using JC-1 fluorescent probe. To visualize the presence of active caspase-3 the FITC-DEVD-FMK or NucView^{TM}488 Caspase-3 substrates were used. The spermatozoa vitality was examined using propidium iodide (PI). Studies were made using a confocal microscope LSM 510 (Zeiss) and flow cytometer FACSCalibur (BD Biosciences). Selected parameters of spermatozoa motion were analysed by CASA system. The velocity of straight linear (VSL) was studied to extract kinematics subgroups of spermatozoa.

In the semen under examination the living spermatozoa with PS translocation (An-V(+)/PI(–) and active form of caspase-3 mainly localized in mid-pieces were found. Spermatozoa with active caspase-3 but without PS translocation. Three kinematics subgroups were identified: rapid, medium and slow according to VSL values. A positive correlation was found between vital spermatozoa with PS translocation and slow velocity ($r = 0.6$; $p < 0.01$) while a negative correlation was found according to spermatozoa with rapid velocity ($r = –0.7$; $p < 0.01$). H_2O_2 in a concentration of 10 mM caused an increase of VSL value, while in a concentration of 50 and 100 mM significant decrease of the VSL value were observed. More over H_2O_2 caused dose dependent increases in the number of spermatozoa with PS translocation and active form of caspase-3 as well as in the number of spermatozoa with low mitochondrial potential.